Survival of Wisconsin's gray wolves from endangered to harvested, 1980 – 2013

By

Jennifer L. Stenglein

A dissertation submitted in partial fulfillment of

the requirements for the degree of

Doctor of Philosophy

(Wildlife Ecology)

at the

UNIVERSITY OF WISCONSIN – MADISON

2014

Date of final oral examination: 5/1/2014

The dissertation is approved by the following members of the Final Oral Committee:

Timothy R. Van Deelen, Associate Professor, Forest and Wildlife Ecology
David J. Mladenoff, Professor, Forest and Wildlife Ecology
Michael D. Samuel, Associate Professor, Forest and Wildlife Ecology
David Drake, Associate Professor, Forest and Wildlife Ecology
Dennis M. Heisey, Research Biologist, USGS National Wildlife Health Center
Adrian P. Wydeven, Wildlife Biologist, Wisconsin Department of Natural Resources

Abstract

From 1980 – 2013, Wisconsin's recolonized wolf population increased to > 800 wolves. Concurrently, Wisconsin Department of Natural Resources counted wolves, recovered wolf carcasses, and radio-collared and tracked individual wolves until death. With these data, I studied survival of an endangered population during initial reestablishment to recovery and into the first years of harvest.

I used mortality cause assessment from collared and not-collared wolf carcasses to study mortality cause patterns related to demographic, spatial, and temporal trends. Collared wolf carcasses with illegal kill mortality cause were most often yearling wolves in 2003 – 2012 in winter in northeastern Wisconsin compared to other ages, periods, seasons, and regions. Collared wolf carcasses with natural mortality cause were prevalent in 1996 – 2002 in winter in northwestern Wisconsin. Number of not-collared wolf carcasses (without legal kills) predicted wolf population size from 2003 – 2011. Estimating correction constants between collared and not-collared datasets revealed roughly half of not-collared carcasses are unrecovered.

I used radio-collar records of wolves to estimate wolf survival, and built a model based on endpoints. I split the model into a hazard piece which modeled the approximate probability that a wolf reached its endpoint in some month, and a cause-specific endpoint probability. I informed the baseline hazard with auxiliary data from population counts of wolves and partitioned some of the censoring into probable known death causes. I estimated that 15% of dead wolves were misclassified as censored, and average annual survival rate was 74%. On average, human-caused mortality >22% led to population decline.

I built an individual-based spatially-explicit model of wolf recolonization into Wisconsin and Michigan to understand population effects of different harvest scenarios. Without harvest, Wisconsin's wolf population stabilized at 1242 wolves after 50 years and breeding pairs persisted for a mean 1.8 years. In general, harvest increased the proportion of pups in the population and decreased breeding pair tenure. Targeted lethal control was more effective than harvest for reducing the number of wolves near known livestock depredation sites. This model facilitates prediction of population patterns that are simultaneously dependent on complexities associated with life history and spatially structured mortality.

Acknowledgements

This work would not have been possible without support and contributions from many people and organizations. My major advisor, Tim Van Deelen, is about the best person you could know. Tim believed in me from our first phone call and has been an amazing mentor, teacher, cheerleader, and friend all along the way. Tim, I am so grateful for the opportunity to work with you these past 5 years, and I know that we will continue to work together in the future.

As part of my Master's program in Biometry at University of Wisconsin – Madison, I had the great pleasure of meeting and working with Dr. Jun Zhu in the statistics department. Jun has been incredibly supportive and a great teacher. My time with Jun in the Biometry program greatly enriched my graduate school experience. Thank you, also, to the statistics department at UW – Madison for their offering of the Biometry program, and to Murray Clayton for serving on my Biometry oral exam committee in December 2013.

I want to thank my other committee member for their involvement and contributions to this project. David Mladenoff was integral in tying wolf population dynamics to spatial variation. David Drake helped me out in a pinch, and guided my thinking on the social implications of wolves. Mike Samuel provided great edits and was always willing to sit down and talk the larger goals of an analysis and ponder over how to interpret 80 parameters from a multinomial model. Dennis Heisey provided great guidance on the Bayesian analyses and was a driving force in developing my statistical modeling skills. Adrian Wydeven kept me grounded to consider that whatever I was working on could help inform wolf conservation and management.

My exceptional committee certainly challenged me, but I know would not have gotten to this dissertation without all of their input. Many thanks.

The other folks at Wisconsin Department of Natural Resources have been incredible. Jane Wiedenhoeft filled all of my data requests that just kept coming her way over the years. Ron Schultz let me tag along for two lovely weeks of field work in Northern Wisconsin where I learned so much. We would not have the dataset and wolf population that we have without the help of Dick Thiel, Randy Jurewicz, the volunteer carnivore trackers, the biologists and technicians that collect the data, and the pilots that get radio-collared locations. Thank you to Karl Martin and others at Science Services that have become my new colleagues.

Big thanks to Jonathan Gilbert and Great Lakes Indian Fish and Wildlife Commission. Jon saw something interesting in the third chapter of this dissertation and that sparked a great collaboration. I am grateful for Jon's contributions to chapter 3 of this work. A special thanks to Nancy Businga, Julie Langenberg, and Nancy Thomas for all of their work on the wolf necropsies and their other contributions to chapter 1.

Thank you to the Department of Forest and Wildlife Ecology, the Novel Ecosystems IGERT crew, and to fellow grad students, lab mates, and office mates, and especially thanks to Laurie Ballentine, Andrew Norton, Erik Olson, Camille Warbington, Wang Dajun, Li Sheng, Becky Kirby, Matt Reetz, Wynne Moss, BJ Byers, Christine Anhalt, Stephanie Steinhoff, and Dan Storm. Thanks to Kara Gebhardt-Tessman, Stacie Robinson, Christy Jones, Stephanie Clegg, Kate Golden, Carolyn Schmitz, Jenny Chipault and many other good friends that helped me keep a balanced life during my Ph.D. work. Thank you to Kevin and Sue Hennis for the

amazing support and friendship, and to the Roths and Carly Schuna for many wonderful Monday night dinners.

Huge thanks to Mike Gresch, my husband, who I met and married during the course of my Ph.D. work. Mike, you are so fantastic and I am incredibly lucky to have you in my life. Thank you for all of your support and good times that we have already shared these last few years. Thanks to my sister and brother, Amy and Eric Stenglein, and to my parents and younger brothers, David, Anita, Matthew, and Nathan Stenglein. I am looking forward to making more time to spend with all of you.

The sources of funding and support of this work include: U.S. Department of Agriculture Hatch Act Grant, NSF-IGERT award DGE-1144752: Novel ecosystems, rapid change, and no-analog conditions: the future of biodiversity conservation in human-dominated landscapes, the Wisconsin Department of Natural Resources, the USGS National Wildlife Health Institute, and the University of Wisconsin – Madison Department of Forest and Wildlife Ecology.

Table of Contents

List of Tables

List of Figures

List of Appendices

Chapter 1: Elucidating past cause of mortality patterns in a recently delisted, newly harvested wolf population

Abstract

A long-term record from recovered carcasses reflects changes in prominent mortality risks through time and can provide information on population dynamics. We assessed mortality causes for radio-collared wolves (n = 208) and not-collared wolves (n = 668) found dead in Wisconsin from 1979 – 2012 to identify temporal variation and regional differences, correlations with population size, and correspondence between the collared and not-collared datasets. We studied mortality cause differences relative to season, age and sex classes, regions of the state (i.e., wolf harvest zones), and period (1979 – 1995: recovery, 1996 – 2002: early growth, 2003 – 2012: late growth). Seasonally, the collared illegal kills and natural deaths were proportionally higher in winter (October – March) than summer (April – September), whereas vehicle strikes and legal kills were higher in summer than winter. This seasonal disproportionality was more prominent in the late growth period relative to other periods. Spatially, the highest proportions of illegally killed collared wolves occurred in eastern wolf harvest zones where wolves reestablished more slowly and in the central forest region where optimal habitat was isolated by agriculture. Naturally killed collared wolves (e.g., mortality because of disease, intraspecific strife, or starvation) were proportionally highest in western wolf harvest zones where wolves established earlier and existed in higher densities. Annual counts of all not-collared carcasses (excluding those with legal mortality cause) regressed against annual population size explained 69% of the variation and predicted the last pre-harvest population size (winter 2011/2012) within its 95% credible interval. Estimating correction constants between collared and not-collared

datasets revealed that roughly half of the not-collared carcasses on the landscape are not recovered, and most of the carcasses that are not recovered have natural and illegal mortality causes.

Introduction

Gray wolves (*Canis lupus*) in Michigan, Minnesota, and Wisconsin, USA of the Great Lakes region were delisted under the Federal Endangered Species Act and are now subject to legal harvest. Prior to legal harvest, Great Lakes wolves had on average 15% less annual human-caused mortality compared to Alaskan and Canadian wolf populations (Fuller et al. 2003). Presumably, the relatively low annual mortality rates in Great Lakes wolves compared to other wolf populations promoted recovery and led to the reestablishment of Wisconsin and Michigan wolf populations (Van Deelen 2009). However, the mortality patterns in the reestablished Wisconsin wolf population have not been studied thoroughly. The effect of the addition of harvest on other mortality in Wisconsin wolves is unknown, and analyses from North American wolf populations are inconclusive on whether harvest mortality is compensatory to other mortality (Adams et al. 2008, Creel and Rotella 2010, Murray et al. 2010, Gude et al. 2012). Further, harvest could have unknown impacts on Wisconsin's wolves because of disruption in social and pack structure (Brainerd et al. 2008, Rutledge et al. 2010). An understanding of past mortality patterns related to management approaches, age, season, and region could lend insight into the sound implementation of regulated legal harvest in Wisconsin. For example, past mortality patterns could inform wolf harvest zone (WHZ) delineation such that regions with higher and lower mortality from various causes are in different WHZs with different harvest rates. WHZs with lower rates of harvest could protect a core wolf population in areas with less

human-caused mortality. Protecting a core wolf population could guard against harvest effects on wolf social structure, especially because these effects are yet unknown (Rutledge et al. 2010). We provide the first assessment of mortality patterns in the Wisconsin wolf population from > 800 wolf carcasses recovered in 1979 – 2012.

Wildlife carcass data can inform demographic parameters (Lovari et al. 2007, Sidorovich et al. 2007), index population mortality rates (Joly et al. 2009), and help estimate unobserved overall mortality (Huso 2011, Peron et al. 2013) when detection and reporting biases are estimated and incorporated. Estimates of mammal carcass detection bias are uncommon and come primarily from road kill studies where carnivore carcasses are more detectable than other taxa (Santos et al. 2011). Carnivores die from many causes other than by vehicle strikes, and it is more difficult to measure detection bias in these cases (Ciucci et al. 2007). Failure to estimate and include these biases for an opportunistic sample of carcasses leads to potential problems if the sample is extrapolated to infer population-level processes (Ciucci et al. 2007). However, if biases remain proportionally similar through time or if trends are known, a long-term record from recovered carcasses could reflect changes in prominent mortality risks through time.

Carcasses found in different ways can have different sources of bias. Some carcasses are found when animals are live-captured, radio-collared, and tracked with radio-telemetry until they die. These collared carcasses provide accurate estimates of mortality rates when the collared sample is representative of the population and any collared individuals that disappear do not actually die (Pollock et al. 1989, Tsai et al. 1999). Another source of carcasses is the convenience sample of not-collared carcasses that are found on the landscape without the aid of radio-telemetry tracking. The not-collared carcasses likely do not represent the population

mortality rates because of variable carcass detection rates from different mortality causes (Ciucci et al. 2007). For example, road kill carcasses are more detectable than a carcass in remote areas with disease as its mortality cause. Although collared carcasses may reflect more accurately the mortality causes in the population, not-collared carcasses also provide mortality cause information. Not-collared carcasses are often many times more numerous than collared carcasses, and may be the only carcass data available. With a sample of both collared and not-collared carcasses, it is possible to understand the biases in the not-collared carcass dataset with respect to the collared carcass dataset. For the first time, this allows researchers and managers to use a convenience sample of not-collared carcasses to understand population parameters.

We studied mortality cause patterns in the Wisconsin wolf population for three decades prior to the regulated legal harvest. Our purpose was to inform management decisions about the regulated legal harvest from these mortality patterns, and develop methodology to make carcass data useful for managers. Our objectives were to: 1) assess how spatial, temporal, and demographic factors influence patterns of wolf mortality causes, 2) develop an index relating the number of not-collared carcasses to the population size, and 3) quantify the bias in the not-collared carcass sample with respect to the collared carcass sample to estimate detection probability for wolf carcasses, by cause, and provide a correction from the more convenient not-collared sample to the more accurate collared sample.

Methods

Dataset and mortality cause assignment

We examined wolf carcasses in the six wolf harvest zones (WHZs) created for the Wisconsin wolf harvest in 2012 (Fig. 1). The WHZs correspond roughly to habitat differences

that align with wolf population density differences. Generally, Wisconsin has a gradient of more forest, smaller human population densities, and fewer roads in the north (WHZ 1 - 4) to more agriculture, higher human population densities, and more roads in the south (WHZ 6, Fig. 1). WHZ 5 is a forested area in central Wisconsin that supports 4 – 16 wolf packs annually (Thiel et al. 2009).

We defined three periods of wolf recovery to align with population growth rates and management changes in Wisconsin: 1) The recovery period: In 1979 – 1995 the wolf population was federally listed as endangered and there was little population growth (Van Deelen 2009, Wydeven et al. 2009), 2) The early growth period: In 1996 – 2002 the wolf population approached the management goal of 350 wolves (Wydeven et al. 2009), and 3) The late growth period: In 2003 – 2012 Wisconsin used lethal methods to alleviate livestock depredation risk and human safety concerns during three separate delisting periods (Ruid et al. 2009).

We used collared and not-collared wolf carcasses found in October 1979 – March 2012 (Wydeven et al. 2009). Agency biologist with the Wisconsin Department of Natural Resources (WDNR) normally did not radio-collar wolf pups unless they were > 4 months old and weighed > 14 kg (Wydeven et al. 2009). Therefore, our sample of collared pups represents wolves from 4 months to 1 year old. We removed three collared female carcasses because we suspected (n = 1) or determined through genetic analysis (n = 2) that they were wolf-domestic dog hybrids. Our second dataset was the convenience sample of 708 not-collared wolf carcasses. We removed 32 carcasses because we suspected (n = 22) or determined through genetic analysis (n = 10) that they were hybrids, and we removed six carcasses because of missing date or location

information. Of the remaining 668 not-collared carcasses, there were 337 M, 278 F, and 53 for which sex was not determined (due to severe trauma, advanced decomposition, scavenging).

Agency biologists (WDNR, USDA-Wildlife Services, U.S. Fish and Wildlife Service, and Tribal Conservation Departments) assigned a provisional mortality cause for each carcass from field investigation at the recovery site. A necropsy was subsequently conducted for 539 carcasses by USGS National Wildlife Health Center (primarily carcasses retrieved in 1979 – 2007) or WDNR (primarily carcasses retrieved in 2004 – 2012). Necropsy evaluations generally included whole body radiography (specifically to detect evidence of gunshot), inspection for gross pathology, and sometimes histopathology and specific laboratory analyses for evidence of viral, bacterial, parasitic, or toxin associated disease. We used the necropsy results to confirm, improve, or establish the mortality cause. When carcasses were not necropsied, we used the mortality cause recorded in the field (by a wildlife biologist, warden, or manager). If there was doubt about the mortality cause and no follow-up necropsy, we assigned an unknown mortality cause. We determined mortality cause from the necropsy report rather than the field investigation if there was disagreement.

We developed a standard procedure and followed a set of definitions to assign mortality cause to carcasses (Table 1). We used natural-cause categories of: 1) infectious disease, 2) intraspecific strife, or 3) other natural causes. The human-associated mortality causes were: 4) illegal kill, 5) legal kill, 6) vehicle strike, or 7) other human causes. We used a final category of unknown: 8) undetermined or unclear, and 9) trauma from an unknown source. We used the most significant factor that led to death as the mortality cause in situations where a wolf was compromised severely by one cause leading to death by another cause. Examples were a wolf

that died of starvation and hypothermia because of mange (mortality cause = disease), a wolf that was hit by a car but close to death from mange (mortality cause = disease), and a wolf that was euthanized because of severe injury from a vehicle strike (mortality cause = vehicle). In order to be classified an illegal kill in this study, the carcass had to have clear evidence of a bullet wound, trap-related injury, or poisoning leading to death. We did not include carcasses with evidence of being shot sometime in the past as 'illegal kills'.

Patterns in mortality causes

We used a baseline category logit model in a Bayesian framework to relate the observed mortality causes to spatial, temporal, and demographic variables. The mortality cause for carcass r, X_r, was one of K causes where K was the total number of causes: $X_r = \{1, 2, ..., K\}$. Carcasses were indexed by r where $r = 1, 2, ..., R$ and R was the total number of carcasses. We modeled X_r as a categorical random variable:

$$X_r \sim categorical(p_{r1}, p_{r2}, ..., p_{rK})$$

The categorical distribution had parameters p_{rk} which were the probabilities of carcass r having mortality cause k and $\sum_{k=1}^{K} p_{rk} = 1$. Through the logit link, the p_{rk} probabilities were related to a vector of $\mathbf{z}_r$ linear predictors and a vector of $\boldsymbol{\beta}_k$ unknown regression coefficients (log odds ratios):

$$p_{rk} = \frac{e^{\boldsymbol{\beta}_k \mathbf{z}_r}}{\sum_{j=1}^{K} e^{\boldsymbol{\beta}_j \mathbf{z}_r}}$$

We defined mortality cause categories as: $k = 1$) natural (i.e., disease, intraspecific strife, and other natural causes), $k = 2$) illegal kill, $k = 3$) legal kill, $k = 4$) vehicle strike, and $k = 5$) unknown and other (including unknown, other human-caused mortality, other trauma; Table 1). We set natural mortality as the baseline category and the regression coefficients for, $\boldsymbol{\beta}_1$, were constrained to 0. We gave all other regression coefficients normal priors with mean 0 and variance 10,000: $\boldsymbol{\beta}_k \sim normal(0, 100^2)$ where $k = 2, 3, ..., K$.

Our predictor variables, $\mathbf{z}_r$, were age and sex categories (adult male, adult female, yearling, pups), seasons, periods (recovery: 1979 – 1995, early growth: 1996 – 2002, late growth: 2003 – 2012), and WHZ. We defined summer and winter seasons. Summer included all carcasses from 1 April to 30 September and covered denning, birth and rearing of pups, and early movement of the nearly grown pups with the pack (Mech and Boitani 2003). Winter included all carcasses from 1 October to 31 March and covered the main dispersal period, nomadic movement of packs, and mating season (Mech and Boitani 2003). We had a total of 15 variables in 4 categories. We constrained the model so that the intercept corresponded to adult male wolves in late growth period in summer in WHZ 1. Therefore, the length of vector $\mathbf{z}_r$ was 11 (15 predictor variables minus 4 categories) plus 1 for the intercept.

We ran one model where the collared carcasses were the response variable, and one model where the not-collared carcasses were the response variable. We did not run a model with collared carcasses and not-collared carcasses together, because we expected that there were substantial differences in these datasets. We removed observations in WHZ 6 from the collared carcass analysis (n = 5) and observations in WHZ 4 from the not-collared carcass analysis (n = 10) because of lack of observations in these WHZs. We reported the log-odds of the mean

posterior parameter estimates and standard errors for each mortality cause category related to the baseline natural mortality category.

For each model, we ran three Markov chain Monte Carlo (MCMC) chains for 10,000 iterations after discarding the first 10,000 iterations as burn-in in program JAGS (Plummer 2003) through program R (R Developement Core Team 2005) and package 'rjags' (Plummer 2011). We assessed convergence using both univariate potential scale reduction factors ($\hat{R}$; (Gelman and Rubin 1992)), and the multiple potential scale reduction factor ($\hat{R}^a$, where a is the number of parameters; (Brooks and Gelman 1998)). We judged convergence to be satisfactory when upper 97.5% confidence limits of all $\hat{R}$ s and $\hat{R}^a$ were < 1.1. We performed external validation and posterior predictive checking to ensure the inferences from the model made sense and the model was consistent with the data (Appendix A).

Recovered carcass counts as a population size index

To understand whether the number of recovered carcasses could index population size, we used simple linear regression to relate the mean population count to different measures of the number of not-collared carcasses found each year. The response variable was the mean population count, N_i , where $i = 1, 2, ..., n$ years and *n* was the total number of years. The WDNR reports annual winter counts as ranges (lower bound is minimum count), and we used the midpoint of the range in each year as our count, N_i (Wydeven et al. 2009). We modeled N_i as normally distributed around some annual mean, μ_i, and variance, σ^2: $N_i \sim normal(\mu_i, \sigma^2)$. The mean μ_i was linearly related to a predictor, z_i, unknown intercept, α, and regression coefficient, β: $\mu_i = \alpha + \beta z_i$. The variance σ^2 was calculated from the difference in the high and

low count for each year. We assumed that the range in counts each year represented four standard deviations and used the mean of the standard deviations across the years as σ (range rule, [Triola 2010]). We gave the intercept α and coefficient β normal priors centered on mean 0 and variance 10,000, $\alpha \sim normal(0,100^2)$ and $\beta \sim normal(0,100^2)$.

The predictors, z_i, were the number of carcasses found in the previous calendar year (e.g., winter count in 2003/2004 and number of not-collared carcasses in January – December 2003). We used data from January 2003 – December 2010 to fit the model and left out the January – December 2011 carcass data and 2011/2012 winter count for validation. We expected the most recent years of data to represent the wolf population of the future and our interest was in using not-collared carcass counts in the future to predict population size. We used five subsets of annual not-collared carcass counts in five linear regressions. The five configurations of z_i were: 1) all carcasses, 2) illegally killed, 3) naturally killed, 4) vehicle strikes, and 5) all not-collared carcasses minus legally killed ('no legal'). We expected the number of legally killed carcasses to potentially confound the index of not-collared carcasses to population size because the number of legally killed carcasses varied from 0 – 42 wolves and was determined by management status.

We assumed the best index had the highest coefficient of determination ($R^2 = 1 - SS_{residuals}/SS_{total}$) and made the best posterior prediction of the mean population count in 2011/2012 ($N_{2011/2012}$ = 848 [range: 815 – 880]). The best prediction was the posterior that overlapped the 2011/2012 population count and had the smallest variance. To understand how the index performed in 2012/2013 after the addition of harvest mortality, we predicted the 2012/2013 winter count using the best model and the number of not-collared carcasses found in January – December 2012. The observed 2012/2013 winter count was 809 – 834 wolves. We

performed all analyses in program JAGS through the library 'rjags' in program R and followed the Bayesian modeling methods outlined previously.

Correction between collared and not-collared carcass datasets

We used a state space model in a Bayesian framework to relate the observed collared and not-collared adult carcass counts in WHZs 1 – 5 through four unknown variables: 1) year-specific seasonal mortality rate for collared wolves, c_{ij}, 2) cause-specific allocation of seasonal mortality rate for collared wolves, m_{ijk}, 3) yearly cause-specific number of wolves that died each season, n_{ijk}, and 4) cause-specific seasonal detection probability of not-collared carcasses, d_{jk}. We had models for the observed data, models for the unobserved process, and models for the parameters in the form of prior distributions. Years were indexed by *i* where $i = 1,2,...,n$ and *n* was the total number of years. Seasons were indexed by *j* where $j = 1,2$ for summer and winter seasons, as defined previously, and mortality causes were indexed by *k* where $k = 1,2,...,K$ and *K* was the total number of causes.

Our data models were for each of our three observed variables. First, we took the number of collared adult carcasses that were found dead in year *i*, season *j*, from cause *k*, R_{ijk}, to be multinomially-distributed with m_{ijk} proportion of all carcasses in *ij* that were assigned to *k* cause and R_{ij} total collared carcasses:

$$R_{ijk} \sim multinomial(m_{ij1}, m_{ij2}, ..., m_{ijK}, R_{ij}).$$

Second, we took the total collared adult carcass count in year *i*, season *j*, R_{ij}, as a binomial distribution with c_{ij} year-specific seasonal collared adult mortality rate and E_{ij} collared wolves: $R_{ij} \sim binomial(c_{ij}, E_{ij})$.

We let E_{ij} be the number of collared wolves that were actively monitored at the start of period *ij*.

Third, we took the number of not-collared carcasses that were found dead in year *i*, season *j*, from cause *k*, V_{ijk}, to be binomially-distributed with d_{ijk} probability that the carcasses were detected in the not-collared sample and n_{ijk} total carcasses:

$V_{ijk} \sim binomial(d_{ijk}, n_{ijk})$.

Here n_{ijk} was an unobserved latent variable. We used all adult wolves found dead in Wisconsin from April 2003 to March 2012, and $K = 5$ mortality causes, including: 1) natural, 2) illegal kill, 3) legal kill, 4) vehicle strike, and 5) unknown. These categories were defined as in the mortality cause patterns section, above.

We modeled d_{ijk} as distributed normally around mean d_{jk} and variance σ^2:

$d_{ijk} \sim Normal(d_{jk}, \sigma^2)$.

We modeled the number of wolves that died in year *i* season *j* from cause *k*, n_{ijk}, as a latent variable with a binomial distribution with probability parameter, $c_{ij} * m_{ijk}$, and population size N_{ij}:

$n_{ijk} \sim binomial(c_{ij} * m_{ijk}, N_{ij})$

We restricted n_{ijk} to be an integer at least as big as the observed number of carcasses, $R_{ijk} + V_{ijk}$.

The probability parameter, $c_{ij} * m_{ijk}$, was the cause-specific collared adult mortality probability

with c_{ij} as the total collared adult mortality probability (non-cause-specific) and m_{ijk} as the proportion of total collared adult mortality due to cause *k*. The population size, N_{ij}, was drawn from a Poisson distribution with its mean and variance parameter equal to the population count (dataset explained above) in year *i* season *j*, $Nobs_{ij}$:

$$N_{ij} \sim Poisson(Nobs_{ij})$$

We calculated the population count in the winter of each year *i*, $Nobs_{i2}$, as the mean population count in year *i* (e.g., winter population count in 2003/2004 = 373 – 410; $Nobs_{1,2} = 391$). We calculated the population count in the summer of each year *i*, $Nobs_{i1}$, as the mean of the winter population count in the previous winter plus the mean of the pup count in the following winter (e.g., pup count in 2004/2005 = 118 – 192; $Nobs_{2,1} = 391 + 155 = 546$). The number of pups in the winter was not estimated in 2009 – 2012. To calculate the observed population size in these last three summer seasons, we used the average proportion of pups in the population in the previous summers (0.38) to calculate the mean expected number of pups.

We assigned the $m_{ijk}s$ Dirichlet priors centered on a uniform multinomial distribution: $m_{ijk} \sim Dirichlet(\alpha_{ijk}), \alpha_{ijk} = 1/K$, and we assigned c_{ijk} beta priors: $c_{ijk} \sim beta(1,1)$. The d_{jk} priors were assigned beta priors for k = 1, 2, 3, 4, 5: $d_{jk} \sim beta(1,1)$, and the prior on σ to estimate a year effect of detection probability was a uniform: $\sigma \sim uniform(0,100)$. We performed all analyses in program JAGS through library 'rjags' in program R and followed the Bayesian modeling methods outlined previously. We performed an extensive model checking procedure

to ensure the predictions from the model made sense and that the model was consistent with the data (Appendix B).

Results

Dataset and mortality cause assignment

Most deaths in the collared wolves dataset were due to illegal killing (33%) and disease (18%), while most deaths in the not-collared wolves dataset were due to vehicle strikes (39%), legal kills (30%), and illegal kills (18%; Table 2). Deaths due to human causes were at least 50% more common in the not-collared dataset (88%) compared to the collared dataset (57%; Table 2). The collared wolves dataset had greater proportion of adults (79% vs. 55%) and fewer yearlings (11% vs. 20%) and pups (10% vs. 25%) compared to the not-collared dataset.

Necropsies were performed on 70% of the collared carcasses and 62% of the not-collared carcasses. The proportion of carcasses that were necropsied varied by mortality cause and period. Over 80% of the natural mortalities were necropsied, compared to 51% and 63% of the legal and vehicle mortalities, respectively. Of the carcasses that were illegally killed, 70% of them were necropsied. By period in wolf recovery, 60%, 85%, and 56% of the carcasses were necropsied in the recovery, early growth, and late growth periods, respectively.

Of the 443 cases where field and necropsy diagnoses of mortality cause were available, there were 52 cases where the mortality cause suspected in the field was different than the cause determined from necropsy. In most of these cases (65%), an unknown mortality cause from the field was updated with a cause determined from necropsy. In five cases, the mortality cause suspected in the field was not confirmed by necropsy and the cause from necropsy was an unknown mortality cause. In three cases, a mortality cause of vehicle strike from the field was

changed to ‘illegal kill’ (two cases) or ‘intraspecific strife’ (one case) after necropsy. In three cases, a mortality cause of ‘illegal kill’ from the field was changed to ‘vehicle strike’ after necropsy. The remaining seven cases were when the field mortality cause diagnosis was ‘other natural’ and the necropsy determined ‘disease’ or vice versa.

Most carcasses in the collared and not-collared samples were found in the late recovery period (77%). There was discernible annual variability in the proportion of carcasses with each mortality cause, especially in the collared carcass dataset (Fig. 2). In particular, the proportion of collared carcasses that was illegally killed ranged from 6 – 82% per year (Fig. 2). We suspect that the not-collared carcass dataset was not as variable because we were consistently unable to detect some mortality causes (e.g., natural mortality) without the aid of telemetry. The not-collared carcasses had high proportions of mortality causes from legal kills and vehicle strikes, and these causes had the most annual variation in the not-collared carcass dataset (Fig. 2).

Patterns in mortality causes

We obtained satisfactory convergence criteria for both models. All $\hat{R}$ and $\hat{R}^a$ values were < 1.054. The results of the external validation and model checking demonstrated reasonable predictions from the model and that the model was consistent with the data (Appendix A). We focused our interpretation on the results of the collared carcass analysis in early and late recovery. The not-collared carcass analysis demonstrated some different patterns compared to the collared carcass analysis because of the detection probability biases of not-collared carcasses (Fig. 2). The model fitted values can be used to derive odds ratios for any baseline set of covariates (Appendix C, Tables C.1 and C.2).

Collared yearling carcasses had more than five times the odds of an illegal versus natural mortality compared to adults (Appendix C, Table C.1). The mortality cause probability estimates for yearling carcasses were higher for illegal killing and lower for legal killing compared to the other age and sex classes. Otherwise, the adult male, adult female, and pup patterns in mortality causes were similar. In winter compared to summer, collared carcasses were on average 7 – 28 times more likely to have a natural or illegal mortality compared to a vehicle, unknown, or legal mortality (Fig. 3). Vehicle and legal mortalities were more common in summer than in the winter (Fig. 3). In the early growth period compared to the late growth period, collared carcasses were more than three times as likely to have a natural mortality instead of another cause (Appendix C, Table C.1). In the late growth period carcasses had lower natural mortality and higher illegal killing probabilities compared to the early growth period (Fig. 3).

Collared carcasses in WHZ 2 and 4 were five times as likely to have an illegal versus natural mortality in the late growth period compared to carcasses in WHZ 1 (Fig. 3). WHZs 1 and 3 had similar mortality cause probability estimates for different covariate combinations. Also, WHZs 2, 4, and 5 had similar mortality cause probability estimates with the exception of WHZ 5 having higher predicted probability of natural mortality and lower probability of illegal mortality in the early and late growth periods compared to WHZs 2 and 4 (Fig. 3).

Recovered carcass counts as a population size index

We obtained satisfactory convergence criteria for all models with all $\hat{R}$ and $\hat{R}^a$ values < 1.031. The best index to population size based on highest R^2 was the model with the predictor of all not-collared carcasses except legally killed not-collared carcasses (Table 3). The 'no legal' model's 95% prediction interval for the 2011/2012 mean population count overlapped the

observed 2011/2012 mean population count (Fig. 4). All other models explained a smaller proportion of the variation and had 95% prediction intervals that did not overlap the observed 2011/2012 mean population count (Table 3). The prediction of the 2012/2013 winter wolf population count based on observing 42 not-collared 'no legal' carcasses in 2012 was 657 (649 – 664), which underestimated the observed 2012/2013 count of 809 – 834 wolves by a third.

Correction between collared and not-collared carcass datasets

Satisfactory convergence criteria were obtained for both models with all $\hat{R}$ and $\hat{R}^a$ values < 1.011. The results of the external validation and model checking demonstrated that the inferences from the model made sense and the model was consistent with the data (Appendix B).

The average annual mortality rate for collared wolves was 0.09 (standard deviation [SD] = 0.01). On average the mortality rate was two-times higher in winter (Mean = 0.06, SD = 0.01) than summer (Mean = 0.03, SD = 0.01; Appendix D, Table D.1). In winter, 74% of collared wolf mortality was due to natural causes or illegal killing with ten and five times higher natural and illegal mortality, respectively, in winter than summer. Legal mortality was five times higher in summer than winter (Fig. 5).

The estimated population size was always lower than the observed population size, but the 95% credible interval for the estimated population sizes in every season and year overlapped the observed population size (Appendix D, Table D.2). Population size estimates that were biased low led to low estimates of the number of carcasses on the landscape and high estimates for detection probability of those carcasses. Summed across years, the estimated median number of carcasses on the landscape was 1 – 3 times (1 – 19 times, upper bound of 95% credible interval) the number that were observed and this varied by season and mortality cause (Table 4).

The year effect σ^2 for detection probability of not-collared carcasses was 0.15 (SD = 0.04). The mean probability of detecting a wolf carcass was higher and more variable in summer (Mean = 0.56, SD = 0.05) than in winter (Mean = 0.45, SD = 0.04). Additionally, there were differences in detectability by mortality cause (Fig. 6; Appendix D, Table D.1). The highest probability of carcass detection was for legal kills (69 – 78%) and vehicle strikes (73 – 76%). On average, we detected only 39 – 53% of the illegal kill carcasses and 22 – 38% of the carcasses with a natural mortality cause (Fig. 6; Appendix D, Table D.1).

Discussion

In three decades, the Wisconsin wolf population recovered from a handful of endangered wolves to a legally harvested population. We detected spatial and temporal patterns in mortality causes from recovered wolf carcasses that lend insight into wolf population recovery. Wolf recovery was aided by high population growth rates, especially since mid-1990s (Van Deelen 2009). We found that carcasses in 1996 – 2002 compared to other periods were less likely to have a human mortality cause, perhaps promoting population recovery. Since then, wolf carcasses were more likely to have an illegal mortality cause, and especially in the northeastern portion of Wisconsin where there is lower wolf density. Perhaps the best way to mitigate the unknown effects of harvest on wolf social structure is to designate WHZs with lower harvest rates in areas where there is lower human-caused mortality, thereby protecting a core wolf population. Our analysis is the first to provide direction on which existing WHZs have the highest rates of human mortality causes for wolves.

In 2003 – 2012, there were proportionally more collared carcasses that had a legal mortality cause in summer and an illegal mortality cause in winter compared to other periods.

These increases led to a decrease in the natural mortality category rather than another mortality cause, suggesting that an increase in human-caused mortality may compensate for some of the natural mortality (Adams et al. 2008, Creel and Rotella 2010, Murray et al. 2010). In 2012, Wisconsin established its first recreational wolf hunting season and no wolves were found dead from natural causes for the first time since 1995 (Wisconsin Department of Natural Resources 2013). However, the lack of natural caused mortality detection may be partially due to reduced reporting of dead wolves with the federal delisting and start of the hunting season. There were some indications that not all dead wolves were being reported (A. Wydeven pers. comm.). It is too early to fully understand how harvest will compensate for other mortality causes, especially because we did not assess other factors like variable recruitment in this study (Gude et al. 2012). Our baseline analysis of three decades of pre-harvest mortality causes will be useful for understanding the potential for compensation between natural and human-caused mortality sources after more hunting seasons.

Yearling collared wolves were more likely to be illegally killed than killed from another mortality cause regardless of WHZ, recovery period, or season. The effect of illegal killing on population growth may be reduced if yearlings are easier targets for illegal killing than adult and breeding wolves (Brainerd et al. 2008). A high rate of illegal killing on young, non-reproductive wolves might be a contributing factor in the wolf population maintaining high annual growth rates at an average of 12% per year since 2000 concurrent with illegal killing as the most common source of mortality (Van Deelen 2009, Wydeven et al. 2009). Of course, low mortality and high recruitment are the primary determinates to population growth, despite the proportion of some age class that died from a certain mortality cause (Gotelli 1995). Based on tooth

cementum analysis, the age structure of the 2012 Wisconsin wolf harvest was 75% pups and yearlings. Harvest, like illegal killing, may also target young, non-reproductive wolves thereby reducing potentially some of the unknown social structure and population-level effects of hunting on a wolf population (Rutledge et al. 2010).

Mortality patterns differed by WHZ. There was more illegal killing of collared wolves in the eastern WHZs (2 and 4) where wolf density was lower. These areas are preferred wolf habitat (Mladenoff et al. 2009), but the population has increased slowly, suggesting that a higher rate of illegal killing inhibited growth. To the west, WHZs 1 and 3 had high proportions of natural mortality. Wolves have been established in these WHZs longest and wolf densities are highest, and density-dependent mechanisms may be driving natural mortality. WHZs 3, 4, and 5 had the highest proportions of vehicle strikes, presumably because of more agricultural land, more human activity, and higher road density. This suggests that the island wolf habitat in the central forest is nonetheless vulnerable to human-caused mortality. However, pack territory sizes are smaller, wolf density is higher, and pup production is higher compared to the northern forest wolf population in WHZs 1 – 4 (J. Wiedenhoeft pers. comm.). The different distribution of mortality causes in WHZ 5 compared to the other WHZs does not appear to coincide with any reduction in overall numbers or productivity for wolves in WHZ 5.

Mortality patterns differed by season. Illegal kills and deaths from natural causes (intraspecific strife and disease) were common in the winter (October – March), coincident with Wisconsin's hunting season for white-tailed deer and the time when wolf packs are highly mobile (Mech and Boitani 2003). In winter, interpack relations may be contentious because mobility increases the potential for territorial disputes caused by incursions into the territories of

neighboring packs (Mech 1977). Also, low ambient temperatures in winter could exacerbate the effects of mange: hair loss resulting in thermoregulatory problems, and starvation in severe cases (Kreeger 2003). Of illegal kills of collared wolves, 43% occurred in November; the presence of > 600,000 hunters on the landscape during deer gun hunting season in November is clearly a significant factor in the illegal killing of wolves. In summer (April – September), the peak in legal control mortalities corresponds to peak cattle calving season. Cattle are the most common target for livestock depredation by wolves in Wisconsin, and the documented cattle depredations motivate most legal control efforts for wolves (Ruid et al. 2009).

The number of not-collared carcasses (without legal kill mortality cause) was a good predictor of annual population size through 2011, but the addition of the recreational harvest in 2012 may affect this index. The underestimate of the 2012 population size from our index is likely related to the presumed lack of reporting of dead wolves in 2012 (see above). Our index may be inaccurate for estimating population size when given a novel mortality cause, in this case hunting and landowner permits to shoot wolves. However, our success in developing an index for the time period pre-harvest is encouraging. Concerted efforts to locate and report road kills and other wolves found dead in the field appears to provide an inexpensive means for estimating the wolf population. Some adjustments in the index may be needed in the future to account for depredation controls and public harvest.

Managers would like to rely on data from a not-collared carcass sample to estimate population parameters because it is a more convenient, less expensive, and a larger sample compared to collared carcasses. Not-collared carcasses are difficult to detect and are subject to biases linked to mortality cause and season (Jennelle et al. 2007). Therefore, the best

opportunity to understand the underlying mortality cause patterns in the population is through estimating detection probabilities for not-collared carcasses that account for these biases. Our correction factor analysis allowed us to quantify the cause-specific bias in the not-collared sample compared to the collared sample, which renders these data more useful. Vehicle strikes and legal kill mortality causes were the most detectable on the landscape. Estimates of not-collared carcass detections suggest that managers miss half of the not-collared carcasses, and our lowest detection was for not-collared carcasses with a natural mortality cause. We recommend that correction between collared and not-collared carcass datasets is reexamined after a few years of legal harvest because this relationship might change.

Quantifying the fates of collared individuals is, by now, a routine technique for inferring variation in mortality patterns in a population (Heisey and Fuller 1985). Using this technique, researchers assume that the fates of collared individuals represent proportional mortality causes, but collared data can also be vulnerable to potential biases (Heisey and Fuller 1985, Jacques et al. 2011, Liberg et al. 2012). The collared carcass sample was most representative of mortality patterns of adult wolves living in the heavily forested portions of northern and central Wisconsin where most wolves were captured and collared (WHZs 1 – 5). While these areas include the majority of Wisconsin's wolf range, those wolves that moved out of these areas into WHZ 6 were probably not represented as well by the collared sample (Mladenoff et al. 2009), and appear to be exposed to higher rates of vehicle strikes and illegal kill. Further, the collared carcass sample represents only those wolves that were tracked until death. Some collared wolves are lost-to-follow-up and therefore not included in the collared carcass sample. Our collared sample is unbiased when the loss-to-follow-up process is independent of the death process (Klein and

Moeschberger 2003). However, if some wolves are actually killed and their collars are destroyed when they are lost-to-follow-up, then we may have bias in our sample. Our collared carcass sample may underestimate the proportion of illegal killing in the population (Liberg et al. 2012).

The majority of carcasses were necropsied, and without necropsy we would have misidentified mortality cause for 10% of the carcasses. When there was a discrepancy between a field and necropsy mortality cause assessment, the necropsy often provided clarity leading to a known mortality cause. Assigning each wolf a single mortality cause simplified a sometimes complicated pattern of health problems identified at necropsy. We assigned one discrete cause (e.g., vehicle) despite other factors (e.g., mange or healed gunshot trauma) that may have contributed to the death. Though this simplification may mask important details of disease patterns in a wolf population, it was necessary for the temporal, spatial, and population prediction analyses in this study. As long as a system of rules and definitions is used when making mortality cause assessments, the simplified set of mortality cause categories used for these analyses is appropriate (Heisey and Fuller 1985). Necropsy is invaluable for obtaining accurate mortality causes from carcasses, and we recommend continuing to necropsy recovered wolf carcasses.

The reduction of protection under state and federal endangered species laws for the recovered wolf population in Wisconsin has led to rapid and recent initiation of a recreational hunting season. Hunting as an additional cause of mortality will change the distribution of mortality cause, including by season and location, and it appears that some of this will be through compensation (Murray et al. 2010). Our study provides important baseline data that can be compared to similar cause-specific mortality analysis for a hunted wolf population. The

designation of hunting zones is an important consideration because hunting has the potential to greatly disrupt the social structure of wolf packs with subsequent effects on population growth (Brainerd et al. 2008, Rutledge et al. 2010). The long term effects of disrupted pack structure is yet unknown, but decisions to focus harvest of wolves in areas where they are already experiencing high rates of human-caused mortality may protect a core population that is socially intact and stable.

Literature Cited

Adams, L.G., R.O. Stephenson, B.W. Dale, R.T. Ahgook, and D.J. Demma. 2008. Population dynamics and harvest characteristics of wolves in the Central Brooks Range, Alaska. Wildlife Monographs **170**:1-25.

Brainerd, S.M., H. Andren, E.E. Bangs, E.H. Bradley, J.A. Fontaine, W. Hall, Y. Iliopoulos, M.D. Jimenez, E.A. Jozwiak, O. Liberg, C.M. Mack, T.J. Meier, C.C. Niemeyer, H.C. Pedersen, H. Sand, R.N. Schultz, D.W. Smith, P. Wabakken, and A.P. Wydeven. 2008. The effects of breeder loss on wolves. Journal of Wildlife Management **72**:89-98.

Brooks, S., and A. Gelman. 1998. General methods for monitoring convergence of iterative simulations. Journal of Computational and Graphical Statistics **7**:434-455.

Ciucci, P., G. Chapron, V. Guberti, and L. Boitani. 2007. Estimation of mortality parameters from (biased) samples at death: are we getting the basics right in wildlife field studies? A response to Lovari et al. (2007). Journal of Zoology **273**:125-127.

Creel, S., and J. Rotella. 2010. Meta-Analysis of Relationships between Human Offtake, Total Mortality and Population Dynamics of Gray Wolves (Canis lupus). Plos One **5**:e12918.

Fuller, T. K., L. D. Mech, and J. F. Cochrane. 2003. Wolf Population Dynamics. Pages 161 - 191 *in* L. D. Mech and L. Boitani, editors. Wolves: Behavior, Ecology, and Conservation. The University of Chicago Press, Chicago, Illinois.

Gelman, A., and D. B. Rubin. 1992. Inference from iterative simulation using multiple sequences. Statistical science **7**:457-472.

Gotelli, N. J. 1995. A primer of ecology. Sinauer Associates Incorporated.

Gude, J. A., M. S. Mitchell, R. E. Russell, C. A. Sime, E. E. Bangs, L. D. Mech, and R. R. Ream. 2012. Wolf population dynamics in the US Northern Rocky Mountains are affected by recruitment and human-caused mortality. The Journal of Wildlife Management **76**:108-118.

Heisey, D., and T. Fuller. 1985. Evaluation of survival and cause-specific mortality rates using telemetry data. Journal of Wildlife Management **49**:668-674.

Huso, M. 2011. An estimator of wildlife fatality from observed carcasses. Environmetrics **22**:318-329.

Jacques, C., T. Van Deelen, W. Hall, K. Martin, and K. Vercauteren. 2011. Evaluating How Hunters See and React to Telemetry Collars on White-Tailed Deer. Journal of Wildlife Management **75**:221-231.

Jennelle, C., E. Cooch, M. Conroy, and J. Senar. 2007. State-specific detection probabilities and disease prevalence. Ecological Applications **17**:154-167.

Joly, D., D. Heisey, M. Samuel, C. Ribic, N. Thomas, S. Wright, and I. Wrigh. 2009. Estimating cause-specific mortality rates using recovered carcasses. Journal of Wildlife Diseases **45**:122-127.

Klein, J. P., and M. L. Moeschberger. 2003. Survival analysis: statistical methods for censored and truncated data. Springer-Verlag, New York, NY.

Kreeger, T. J. 2003. The internal wolf: physiology, pathology, and pharmacology. Pages 192-217 *in* L. D. Mech and L. Boitani, editors. Wolves: Behavior, Ecology and Conservation. The University of Chicago Press, Chicago and London.

Liberg, O., G. Chapron, P. Wabakken, H. C. Pedersen, N. T. Hobbs, and H. Sand. 2012. Shoot, shovel and shut up: cryptic poaching slows restoration of a large carnivore in Europe. Proceedings of the Royal Society B: Biological Sciences **279**:910-915.

Lovari, S., A. Sforzi, C. Scala, and R. Fico. 2007. Mortality parameters of the wolf in Italy: does the wolf keep himself from the door? Journal of Zoology **272**:117-124.

Mech, L. 1977. Productivity, mortality, and population trends of wolves in northeastern Minnesota. Journal of Mammalogy **58**:559-574.

Mech, L. D., and L. Boitani. 2003. Wolf Social Ecology. Pages 1 - 34 *in* L. D. Mech and L. Boitani, editors. Wolves: Behavior, Ecology, and Conservation. The University of Chicago Press, Chicago, Illinois.

Mladenoff, D. J., M. K. Clayton, S. D. Pratt, T. A. Sickley, and A. P. Wydeven. 2009. Change in occupied wolf habitat in the northern Great Lakes region. Pages 119-138 *in* A. P. Wydeven, T. R. Van Deelen, and E. J. Heske, editors. Recovery of Gray wolves in the Great Lakes region of the United States: An Endangered Species Success Story. Springer, New York, NY, USA.

Murray, D., D. Smith, E. Bangs, C. Mack, J. Oakleaf, J. Fontaine, D. Boyd, M. Jiminez, C. Niemeyer, T. Meier, D. Stahler, J. Holyan, and V. Asher. 2010. Death from

anthropogenic causes is partially compensatory in recovering wolf populations. Biological Conservation **143**:2514-2524.

Peron, G., J. Hines, J. Nichols, W. Kendall, K. Peters, and D. Mizrahi. 2013. Estimation of bird and bat mortality at wind-power farms with superpopulation models. Journal of Applied Ecology **50**:902-911.

Plummer, M. 2003. JAGS: A program for analysis of Bayesian graphical models using Gibbs sampling. Pages 20-22.

Plummer, M. 2011. rjags: Bayesian graphical models using MCMC. R package version 3-5.

Pollock, K., S. Winterstein, C. Bunck, and P. Curtis. 1989. Survival analysis in telemetry studies - The staggered entry design. Journal of Wildlife Management **53**:7-15.

R Developement Core Team. 2005. R: A language and environment for statistical computing. R Foundation for Statistical Computing. Vienna, Austria.

Ruid, D. B., W. J. Paul, B. J. Roell, A. P. Wydeven, R. C. Willging, R. L. Jurewicz, and D. H. Lonsway. 2009. Wolf–human conflicts and management in Minnesota, Wisconsin, and Michigan. Pages 279-295 *in* A. P. Wydeven, T. R. Van Deelen, and E. J. Heske, editors. Recovery of Gray Wolves in the Great Lakes Region of the United States: An Endangered Species Success Story. Springer, New York, NY, USA.

Rutledge, L., B. Patterson, K. Mills, K. Loveless, D. Murray, and B. White. 2010. Protection from harvesting restores the natural social structure of eastern wolf packs. Biological Conservation **143**:332-339.

Santos, S., F. Carvalho, and A. Mira. 2011. How Long Do the Dead Survive on the Road? Carcass Persistence Probability and Implications for Road-Kill Monitoring Surveys. Plos One **6**:e25383.

Sidorovich, V., V. Stolyarov, N. Vorobei, N. Ivanova, and B. Jedrzejewska. 2007. Litter size, sex ratio, and age structure of gray wolves, Canis lupus, in relation to population fluctuations in northern Belarus. Canadian Journal of Zoology **85**:295-300.

Thiel, R. P., W. Hall Jr, E. Heillhecker, and A. P. Wydeven. 2009. A disjunct gray wolf population in Central Wisconsin. Pages 107-117 *in* A. P. Wydeven, T. R. Van Deelen, and E. J. Heske, editors. Recovery of Gray Wolves in the Great Lakes Region of the United States: An Endangered Species Success Story. Springer, New York, NY, USA.

Triola, M. 2010. Elementary Statistics. 11 edition. Pearson Education.

Tsai, K., K. Pollock, and C. Brownie. 1999. Effects of violation of assumptions for survival analysis methods in radiotelemetry studies. Journal of Wildlife Management **63**:1369-1375.

Van Deelen, T. R. 2009. Growth characteristics of a recovering wolf population in the Great Lakes region Pages 139-153 *in* A. P. Wydeven, T. R. Van Deelen, and E. J. Heske, editors. Recovery of Gray Wolves in the Great Lakes Region of the United States: An Endangered Species Success Story. Springer, New York, NY, USA.

Wisconsin Department of Natural Resources. 1998. WISCLAND land cover (WLCGW930).

Wisconsin Department of Natural Resources. 2013. Wisconsin Wolf Season Report 2012.

Wydeven, A. P., J. E. Wiedenhoeft, R. N. Schultz, R. P. Thiel, R. L. Jurewicz, B. E. Kohn, and T. R. Van Deelen. 2009. History, population growth, and management of wolves in Wisconsin. Pages 87-105 *in* A. P. Wydeven, T. R. Van Deelen, and E. J. Heske, editors. Recovery of Gray Wolves in the Great Lakes Region of the United States: An Endangered Species Success Story. Springer, New York, NY, USA.

Table 1. Definitions and examples of nine mortality causes for wolves found dead in Wisconsin, USA from 1979 – 2012.

Mortality cause	Category	Definition	Examples
Disease	Natural	Wolves that died from an infectious disease	Sarcoptic mange; canine distemper; bacterial infection; blastomycosis, pneumonia; canine parvovirus
Illegal	Human	Wolves that were killed illegally by humans	Shooting; trapping (not for research); poisoning; clubbing
Intraspecific strife	Natural	Wolves that were killed by other wolves	
Legal	Human	Wolves that were killed legally by humans	Depredation control (attack of livestock; threat to humans or pets); died during capture for research/monitoring
Other human causes	Human	Wolves that were killed by other human causes or a human cause that could not be identified.	Snowmobile or train collision; unintentionally entrapped by unnatural structures (pail, bear bait log); artillery fire on military base
Other natural causes	Natural	Wolves killed by other natural causes or a natural cause that could not be identified.	Starvation; drowning; stuck in crotch of tree
Other trauma	Unknown	Wolves that died from trauma. The trauma could not be ascribed to a particular source, or even to a human or natural cause category.	
Unknown causes	Unknown	Wolves that were found dead without a clear cause of death.	Severe decomposition or scavenging of a carcass that prevented mortality cause determination; more than one suspected mortality cause
Vehicle	Human	Wolves that were killed by a car, truck, or motorcycle on the road	

Table 2. Mortality cause for collared and not-collared wolf carcasses found in Wisconsin, USA, from 1 October 1979 – 31 March 2012.

			Human-caused				Natural			Unknown	
Dataset	Sex	N	Illegal	Legal	Veh[b]	Other Human	Disease	Intra-Specific	Other Natural	Other Trauma	Unk[c]
Collared	F	112	44	15	10	2	19	11	2	2	7
	M	96	25	11	11	1	18	7	1	3	19
	All	208	69	26	21	3	37	18	3	5	26
Not-collared	F	278	54	91	101	5	8	3	0	1	15
	M	337	62	106	133	3	14	5	1	0	13
	All	668[a]	123	198	258	8	23	10	2	1	45

[a] Total includes some carcasses where sex was not determined.
[b] Veh = vehicle
[c] Unk = unknown

Table 3. A comparison of the mean parameter estimates (and standard deviation), mean coefficients of determination (and standard deviation), and mean 2011/2012 wolf population size prediction (and 95% prediction interval) of linear regressions comparing some count of the number of not-collared wolf carcasses found each year and the minimum population count for wolves in Wisconsin, USA in 2003 – 2010.

Predictor	α	β	R^2	Prediction [a]
All	239.7 (15.2)	5.7 (0.3)	0.203 (0.006)	562 (544 – 581)
Illegal	303.6 (10.8)	28.0 (1.1)	0.408 (0.011)	696 (675 – 716)
Natural	608.0 (11.9)	-16.2 (5.5)	0.034 (0.046)	592 (572 – 612)
Vehicle	171.3 (12.5)	20.3 (0.6)	0.550 (0.004)	883 (858 – 909)
No legal	109.4 (12.9)	13.0 (0.4)	0.692 (0.002)	826 (803 - 849)

[a] The observed 2011/2012 population count was 848 wolves (range: 815 – 880)

Table 4. The total observed and estimated median number of wolf carcasses (and 95% credible intervals [CI]) found in summer and winter of 2003 – 2012 in Wisconsin, USA from five mortality causes.

Mortality	summer			winter		
cause	observed	median	95% CI	observed	median	95% CI
Natural	5	10	5 - 41	31	86	49 - 149
Illegal	20	26	20 - 52	57	113	64 - 203
Legal	94	96	94 - 161	17	18	17 - 23
Vehicle	38	39	38 - 45	33	34	33 - 40
Unknown	27	63	32 - 142	10	44	18 - 96

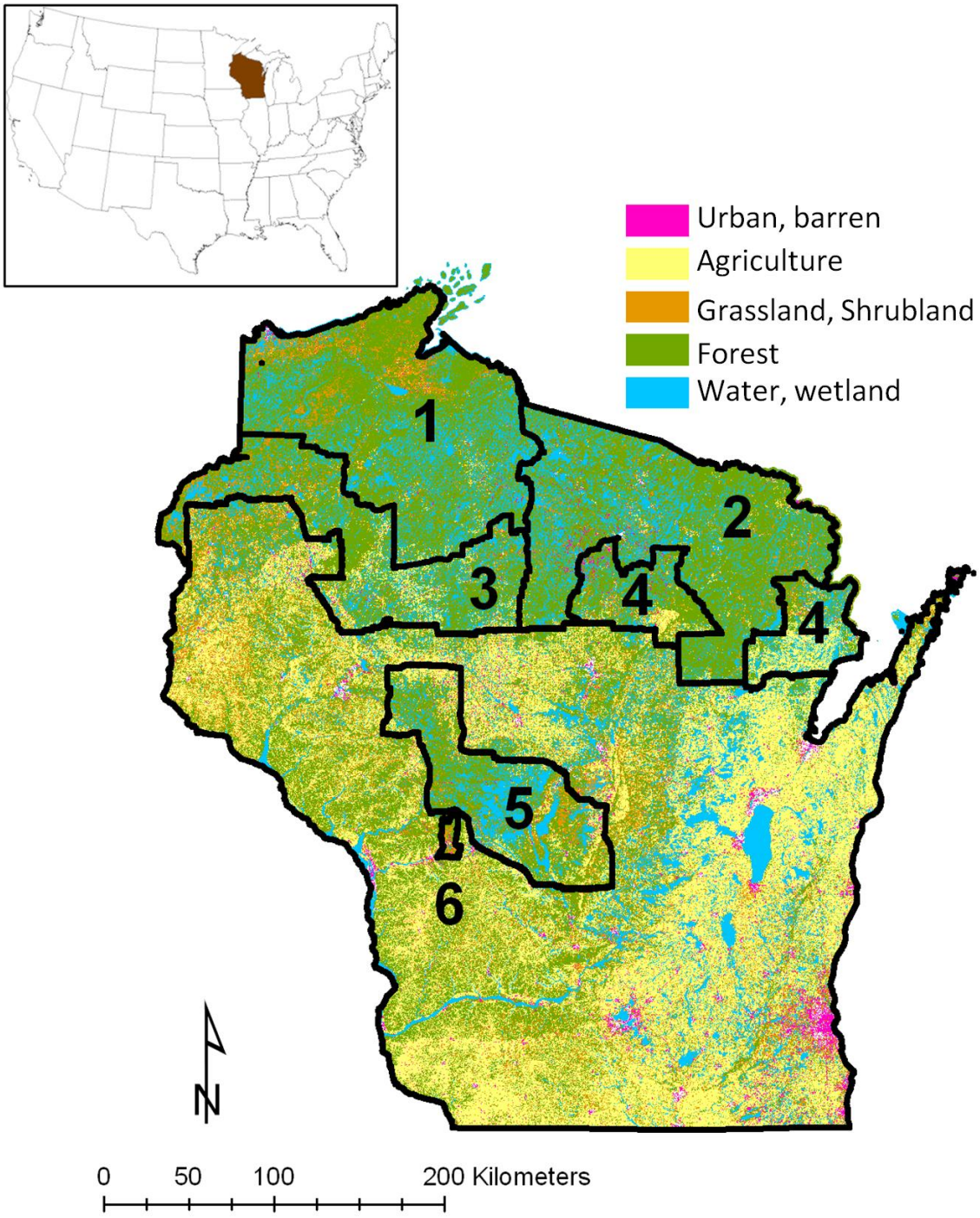

Figure 1. Land cover in Wisconsin, USA, from WISCLAND (Wisconsin Department of Natural Resources 1998), with the six wolf harvest zones created for Wisconsin wolf harvest in 2012.

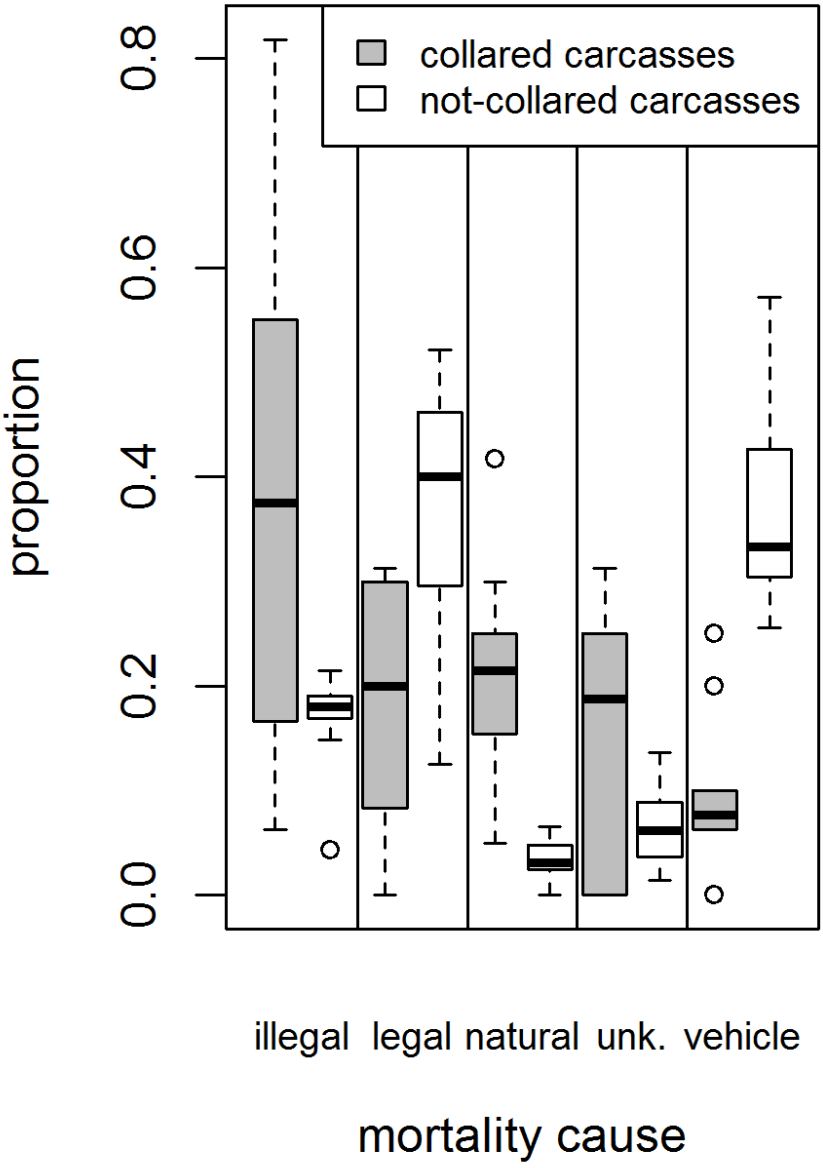

Figure 2. Boxplots of annual proportion of mortality from five causes in collared wolf carcasses and not-collared wolf carcasses in Wisconsin, USA from 2003 – 2012 (unk. = unknown mortality sources).

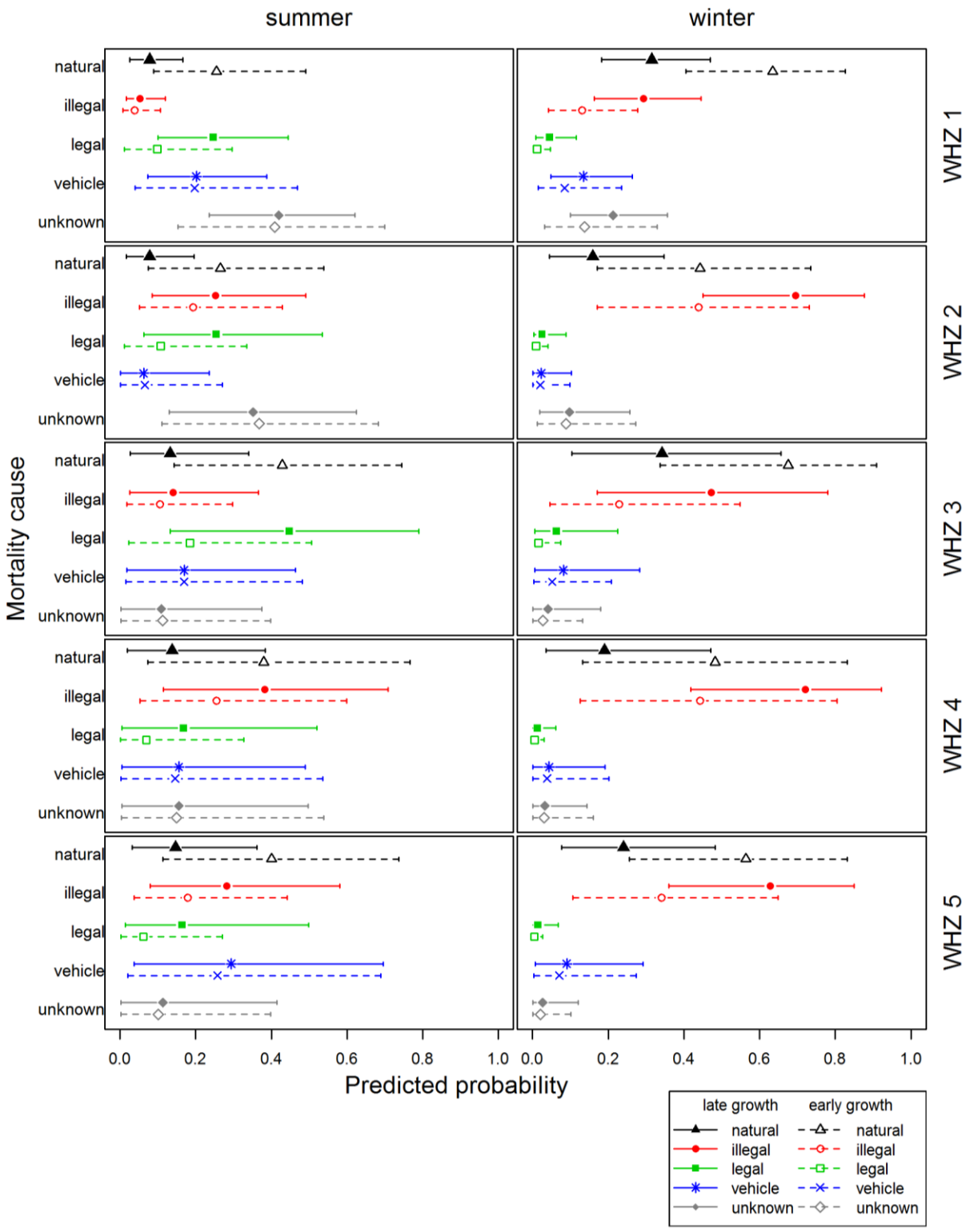

Figure 3. Predicted probabilities for collared adult male carcasses found in Wisconsin, USA in early growth (1996 – 2002) or late growth (2003 – 2012) periods during summer (April – September) or winter (October – March) from five mortality causes.

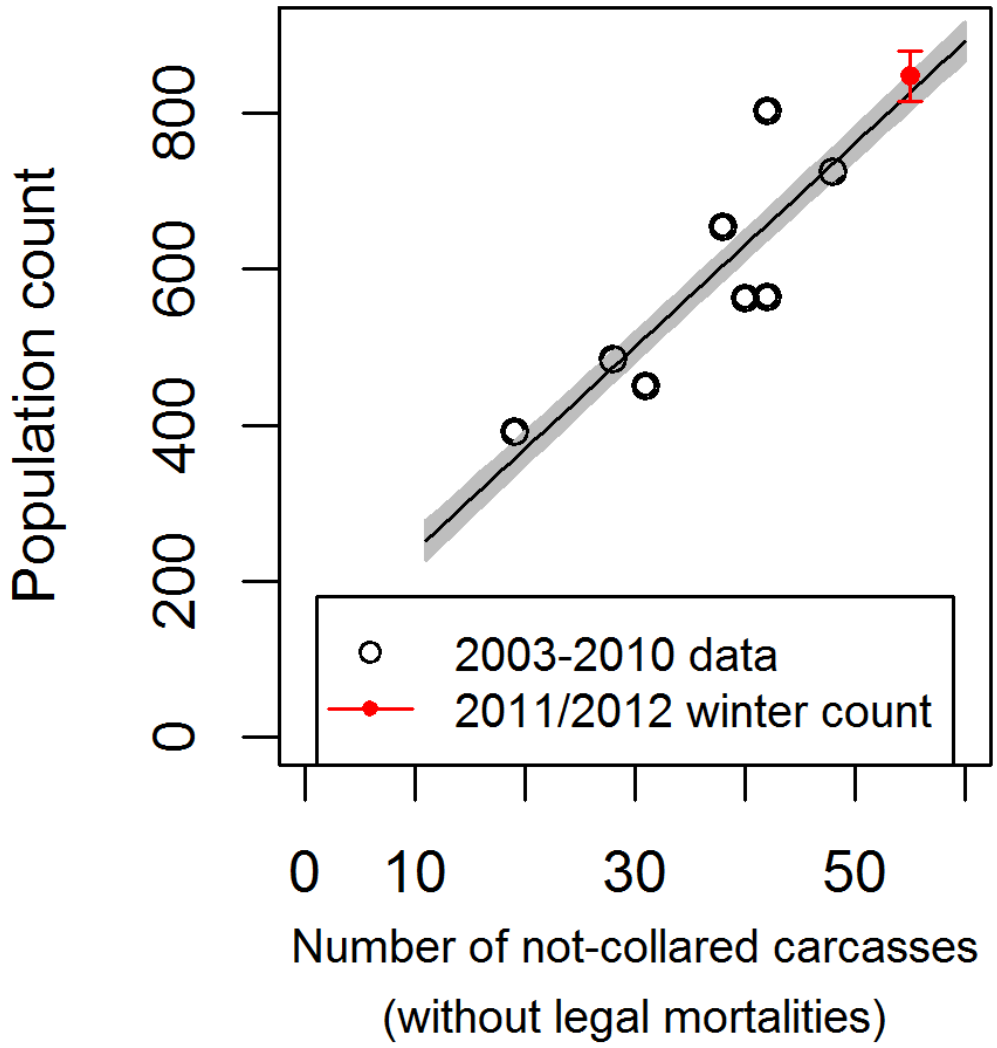

Figure 4. Linear prediction and 95% prediction interval (gray polygon) fit to 2003 – 2010 Wisconsin, USA wolf population counts versus the number of not-collared wolf carcasses found, not including the legal mortalities. The 2011/2012 winter count was left out of the model so that it could be predicted.

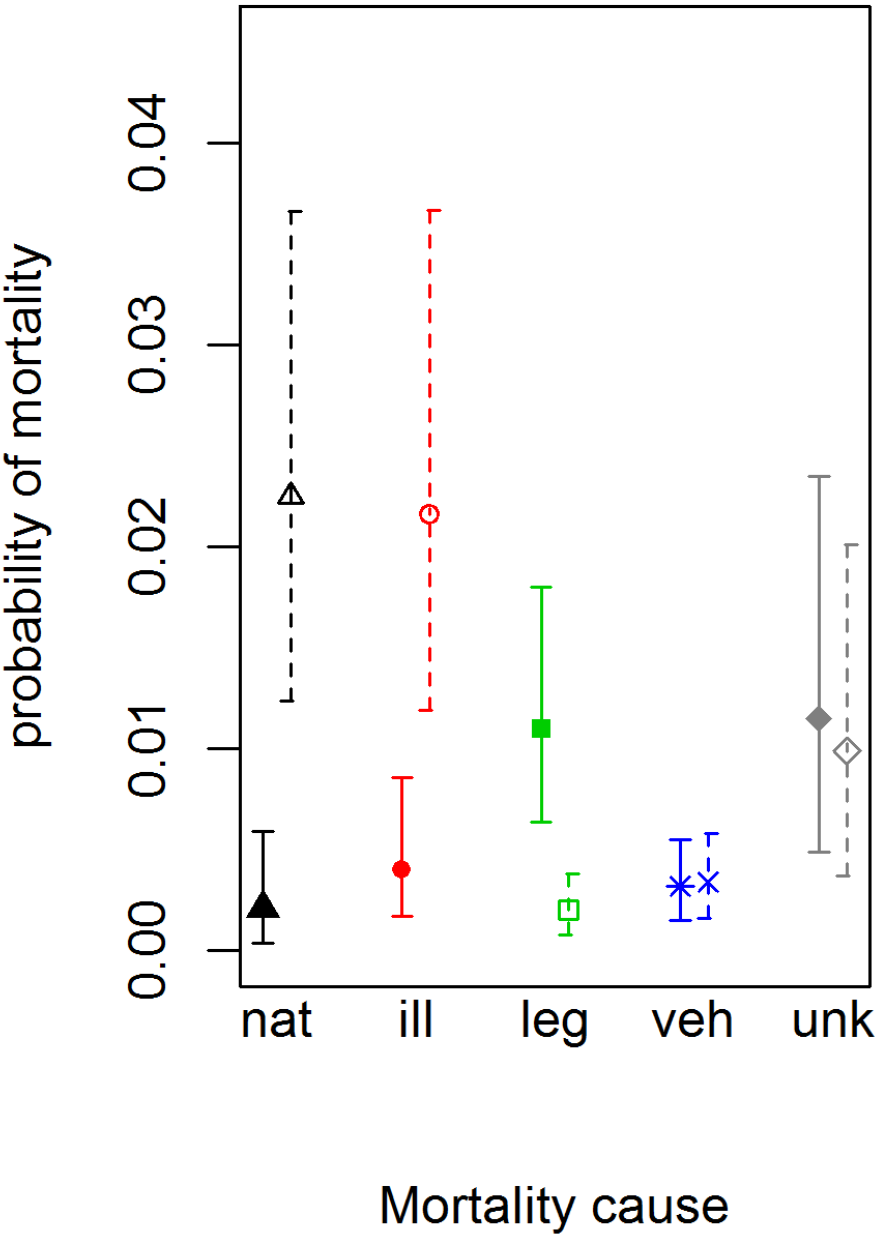

Figure 5. Cause-specific probability of mortality from natural (nat), illegal (ill), legal (leg), vehicle (veh), and unknown (unk) causes for adult collared wolves in wolf harvest zone 1 – 5 of Wisconsin, USA in summer (solid lines) and winter (dashed lines) from 2003 – 2012.

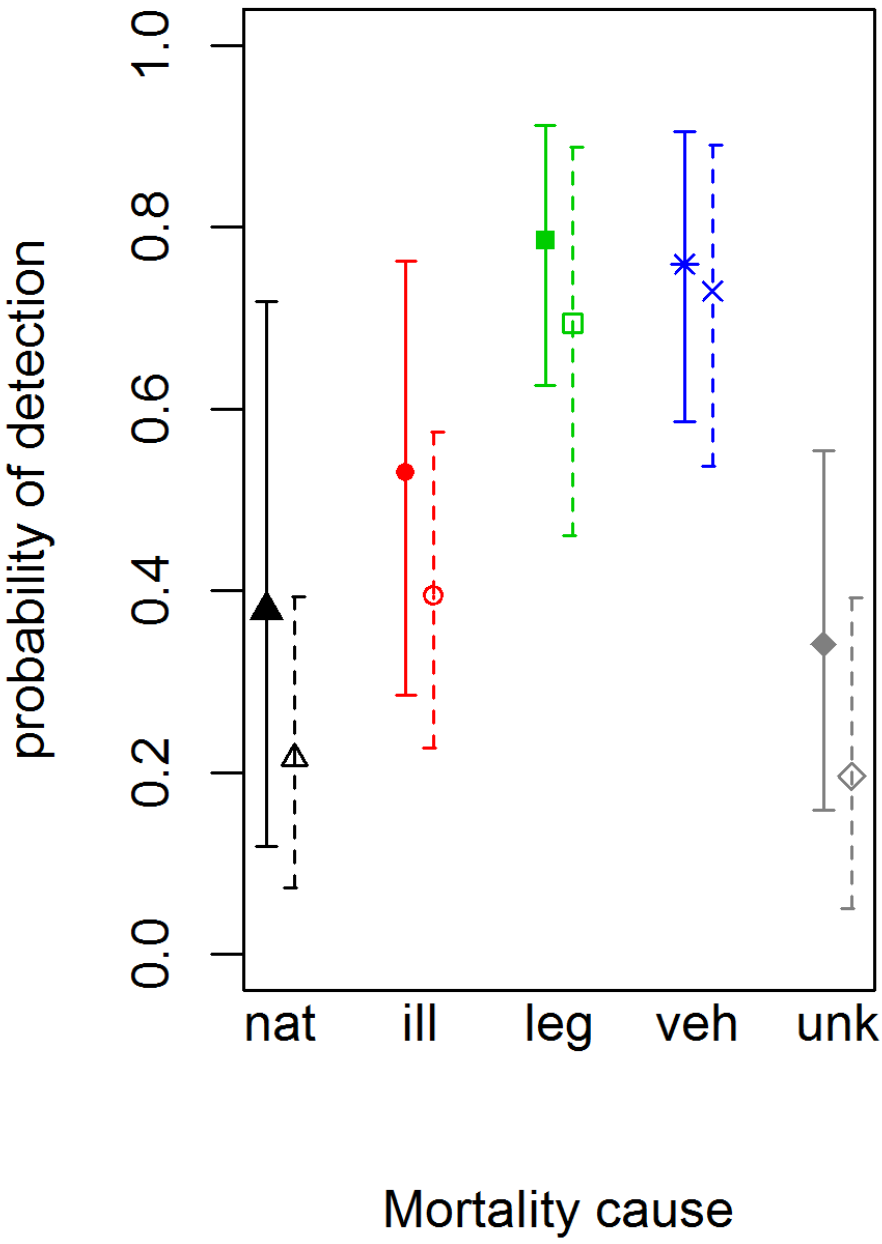

Figure 6. Cause-specific detection probability from natural (nat), illegal (ill), legal (leg), vehicle (veh), and unknown (unk) mortality causes for adult wolf carcasses in wolf harvest zones 1 – 5 of Wisconsin, USA in summer (solid lines) and winter (dashed lines) from 2003 – 2012.

Appendix A. External validation and posterior predictive checking for models of mortality cause patterns

Methods

We implemented an external validation and model checking for each of our models. The validation data that we left out of the model were the 8 collared carcasses and 73 not-collared carcasses found in Wisconsin from 1 April – 30 September 2012 before the first harvest. For each covariate combination represented in the validation data (e.g., adult males in WHZ 1) that had *N* carcasses, where $N > 5$, we predicted the number of carcasses had each mortality cause *k* from the multinomial posterior distribution:

$$X.predict_k \sim multinomial(p_1, p_2, p_3, p_4, p_5, N)$$

We concluded that if the 50% prediction intervals of $X.predict_k$ contained the validation data at least half the time than our model provided reasonable inferences.

For the posterior predictive check, we drew simulated values from the multinomial posterior distributions and observed whether the simulated values matched our observed data. For each covariate combination of the observed data with > 5 carcasses in the collared dataset and > 10 carcasses in the not-collared dataset, we created a histogram of the number of each of 5 mortality causes that were predicted under 1000 draws of the multinomial posterior distribution and plotted 50% and 95% prediction intervals. We compared this distribution to the observed number of carcasses in each mortality cause category. We assumed that the model was consistent with the data if the observed number of carcasses in each mortality cause category were within the middle 50% of the posterior predictive distributions at least half the time.

Results

In the collared carcass model, the external validation was based on 6 adult female carcasses found dead in WHZ 1 (Table A.1). The number of carcasses in each mortality cause from the collared carcass validation data was within the 50% prediction interval in all cases (Fig. A.1). In the not-collared carcass model, the external validation was based on adult males ($N_{WHZ1} = 9, N_{WHZ3} = 12$), adult females ($N_{WHZ1} = 8$), yearlings ($N_{WHZ1} = 6, N_{WHZ3} = 12$), and pups ($N_{WHZ1} = 9$) in WHZs 1 and 3 (Table A.1). The validation data was within the 50% and 95% prediction intervals 60% and 87% of the time, respectively (Fig. A.2). In general for the not-collared carcass model, the validation data was under-predicted for legal mortality cause and over-predicted for vehicle mortality cause (Fig. A.2). The not-collared carcass validation data had 55 out of 56 carcasses with a legal mortality cause which represented a much higher rate of legal killing than was previously seen. Even so, both models predicted the validation data within the 50% prediction interval well over half the time. Therefore, we concluded that the inferences from the model made sense.

The posterior predictive check was based on 10 covariate combinations in the collared carcass dataset (Table A.1). From the predicted distribution for each set of covariates, the observed collared carcass data was within the 50% and 95% prediction intervals 76% and 98% of the time, respectively (Figure A.3). The posterior predictive check was based on 18 covariate combinations in the not-collared carcass dataset (Table A.1). From the predicted distribution for each set of covariates, the observed not-collared carcass data was within the 50% and 95% predicted intervals 82% and 100% of the time, respectively (Figure A.4). The posterior predictive checks demonstrated that the model was consistent with the data a great majority of the time. Therefore, we concluded that the models fit the data well.

Table A.1. Codes for radio-collared and not-collared wolf carcass datasets with different season, period, wolf harvest zone (WHZ), age and sex category, and number of carcasses used for external validation (ev) and posterior predictive checks (pp) in Figures A.1, A.2, A.3, and A.4.

Code	Dataset	Season	Period[1]	WHZ	Age sex category[2]	Number	Type
A	collared	summer	3	1	af	6	ev
B	not-collared	summer	3	1	af	8	ev
C	not-collared	summer	3	1	am	9	ev
D	not-collared	summer	3	1	p	9	ev
E	not-collared	summer	3	1	y	6	ev
F	not-collared	summer	3	3	am	12	ev
G	not-collared	summer	3	3	y	12	ev
1	collared	summer	1	1	am	6	pp
2	collared	summer	3	1	af	11	pp
3	collared	summer	3	1	am	10	pp
4	collared	summer	3	2	am	6	pp
5	collared	winter	1	1	af	7	pp
6	collared	winter	2	1	af	7	pp
7	collared	winter	3	1	af	15	pp
8	collared	winter	3	1	am	24	pp
9	collared	winter	3	2	af	8	pp
10	collared	winter	3	5	af	7	pp
11	not-collared	summer	2	1	p	13	pp
12	not-collared	summer	3	1	af	28	pp
13	not-collared	summer	3	1	am	50	pp
14	not-collared	summer	3	1	p	55	pp
15	not-collared	summer	3	1	y	39	pp
16	not-collared	summer	3	2	p	11	pp
17	not-collared	summer	3	3	am	22	pp
18	not-collared	summer	3	3	p	13	pp
19	not-collared	summer	3	3	y	12	pp
20	not-collared	summer	3	6	af	11	pp
21	not-collared	summer	3	6	am	26	pp
22	not-collared	summer	3	6	y	11	pp
23	not-collared	winter	3	1	af	15	pp
24	not-collared	winter	3	1	am	17	pp
25	not-collared	winter	3	1	p	12	pp
26	not-collared	winter	3	5	am	12	pp
27	not-collared	winter	3	6	af	12	pp
28	not-collared	winter	3	6	am	20	pp

[1] Period of wolf recovery: 1: recovery period in 1979 – 1995, 2: early growth period in 1996 – 2002, and 3: late growth period in 2003 – 2012.

[2] Age and sex categories: af = adult female, am = adult male, y = yearling, p = pup.

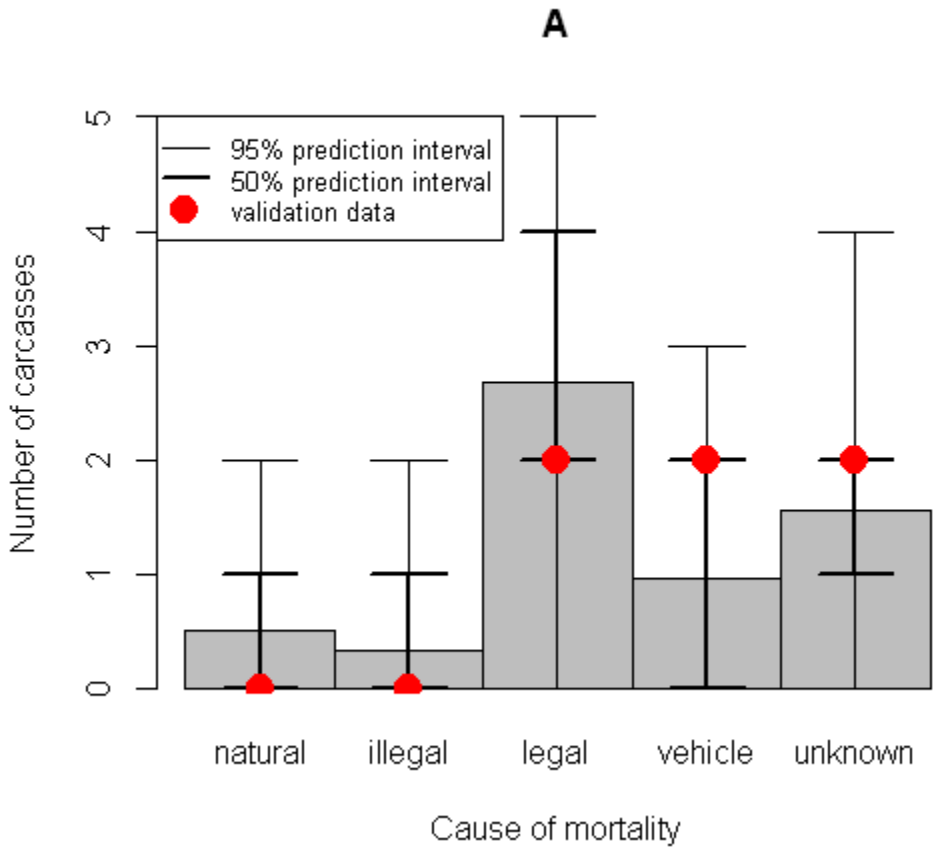

Figure A.1. The mean multinomial model prediction with 50% and 95% prediction intervals of the distribution of mortality causes for six adult female wolf carcasses from wolf harvest zone 1 among five categories with the validation data plotted in red dots. Letter "A" corresponds to specific validation data described in Table A.1.

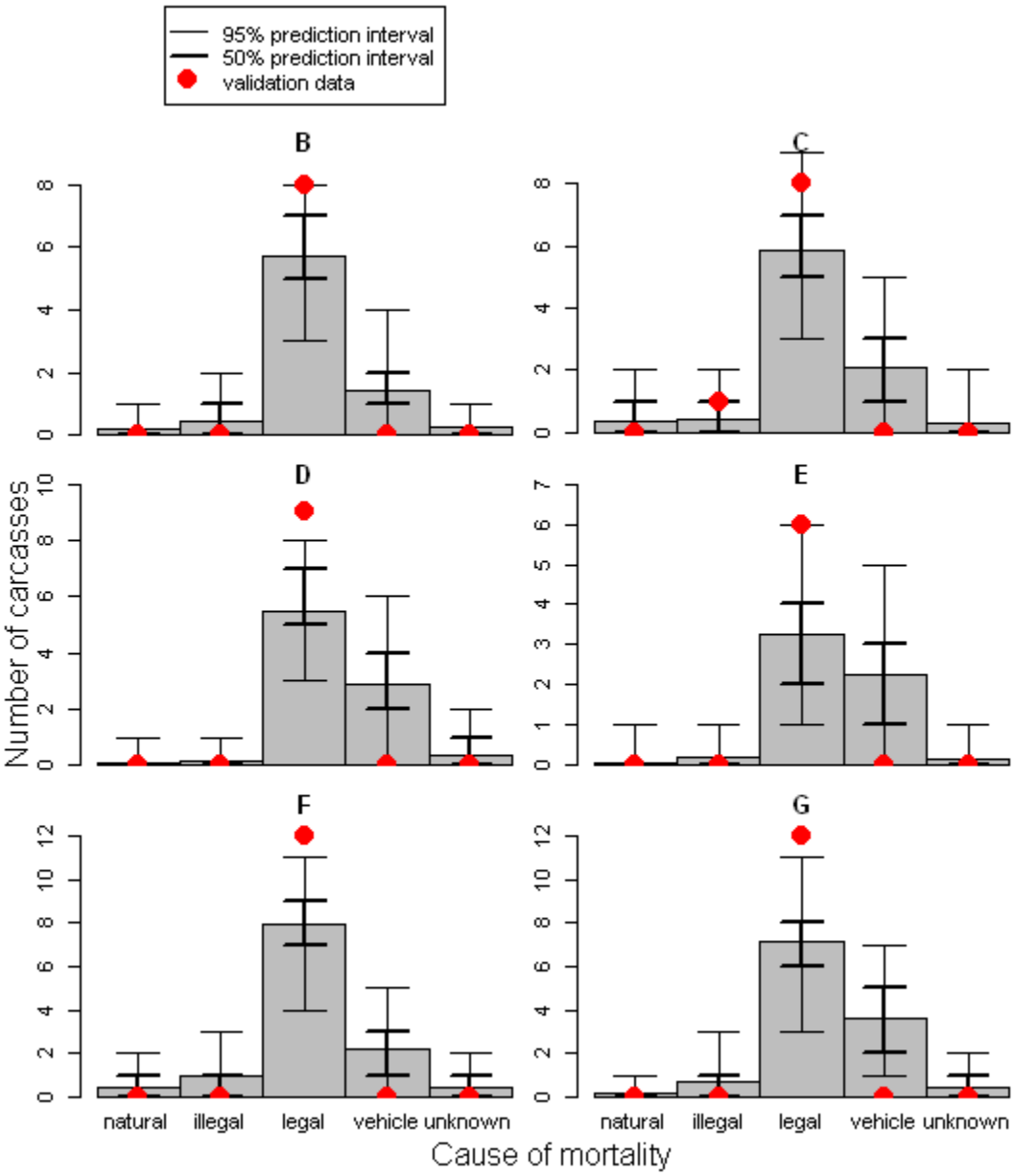

Figure A.2. The mean multinomial model prediction with 50% and 95% prediction intervals of the distribution of mortality causes for different age and sex categories of not-collared wolf carcasses from different wolf harvest zones among five categories with the validation data plotted in red dots. Letters correspond to specific validation data described in Table A.1.

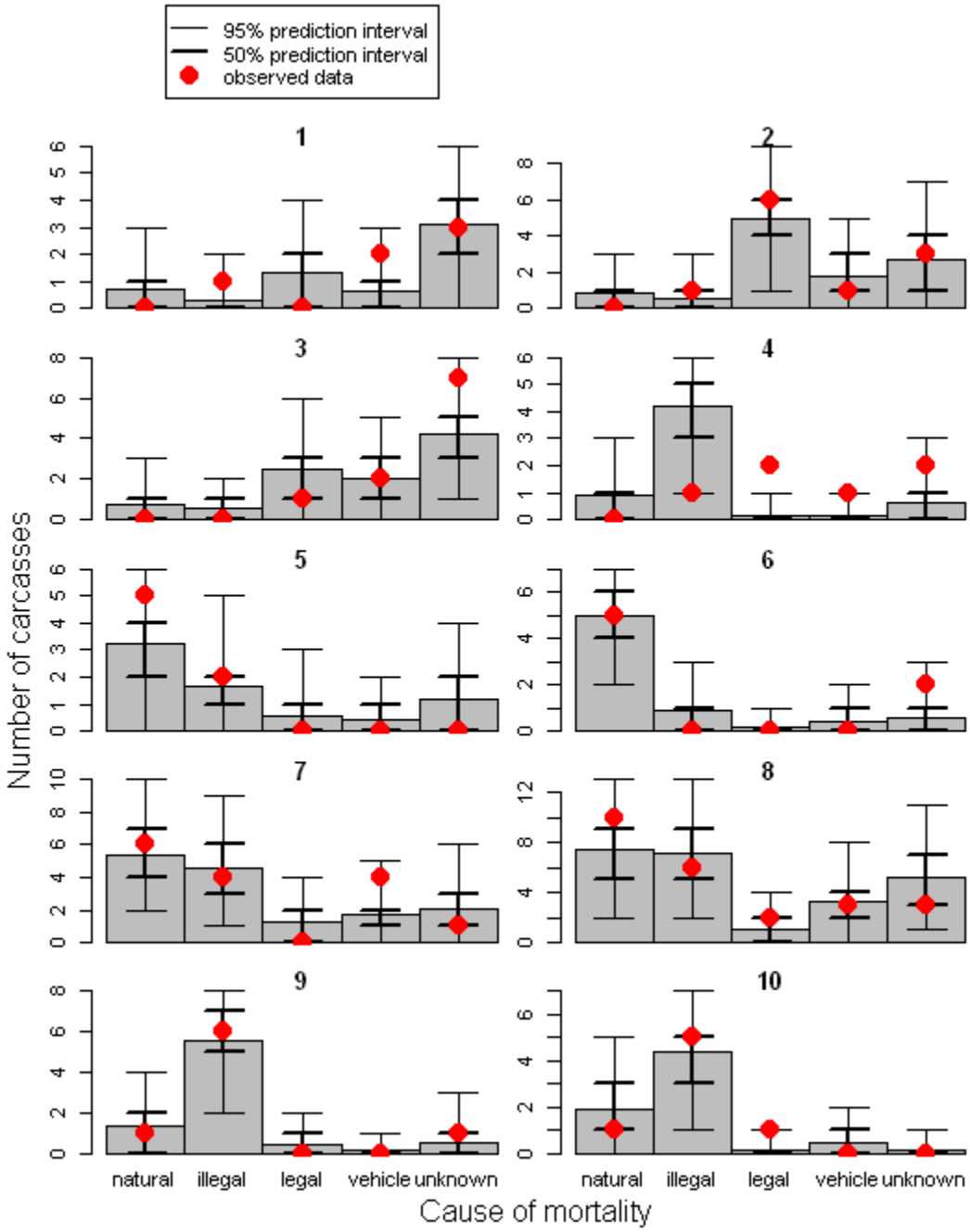

Figure A.3. The mean posterior predictive value (gray bars) with 50% and 95% credible intervals of the distribution of mortality causes for different age and sex categories, season, and recovery period of radio-collared wolf carcasses from different wolf harvest zones among five categories with the observed data plotted in red dots. Numbers correspond to specific validation data described in Table A.1.

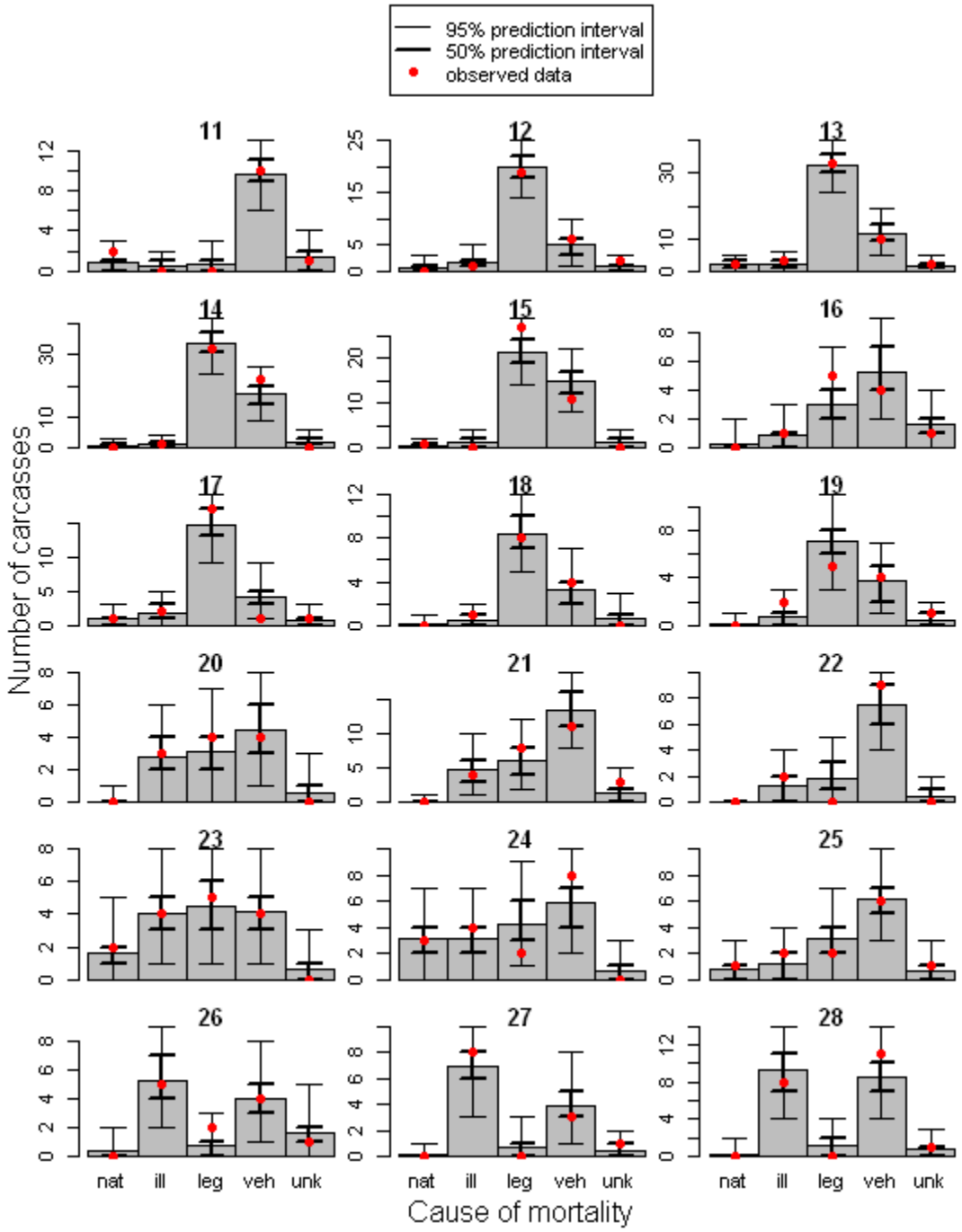

Figure A.4. The mean posterior predictive value (gray bars) with 50% and 95% credible intervals of the distribution of mortality causes for different age and sex categories, season, and recovery period of not-collared wolf carcasses from different wolf harvest zones among five categories with the observed data plotted in red dots. Numbers correspond to specific validation data described in Table A.1.

Appendix B. External validation and posterior predictive checks for correction between collared and not-collared carcasses model

Methods

We implemented an external validation and model checking for our fitted model. The validation data that we left out of the model were the adult not-collared carcasses and the collared carcasses found in Wisconsin from 1 April 2012 – 30 September 2012. We predicted four quantities: 1) the predicted population size in the summer 2012, $N.predict$ 2) the predicted number of adult carcasses on the landscape in summer 2012 from *k* causes, $n.predict_k$ 3) the number of adult not-collared carcasses found dead from mortality cause *k*, $\mathrm{V}.predict_k$, and 4) the number of adult collared carcasses found dead from mortality cause *k*, $R.predict_k$. For $\mathrm{V}.predict_k$, we used the posterior for the average summer probability of collared adult mortality from *k* causes, $c_{\bullet 1k}$, the posterior for the summer adult carcass detection probability for *k* causes, d_{1k}, and the summer 2012 observed population size, $Nobs = 1152$:

$$V.predict_k \sim binomial(d_{1k}, n.predict_k)$$
$$n.predict_k \sim binomial(c_{\bullet 1k}, N.predict)$$
$$N.predict \sim Poisson(Nobs)$$

For $R.predict_k$ we used the posterior for the average yearly cause-specific allocation of collared seasonal mortality rate, $m_{\bullet 1k}$, and the observed number of collared adult carcasses found in the summer of 2012, $R = 9$:

$$R.predict_k \sim multinomial(m_{\bullet 1,1}, m_{\bullet 1,2}, m_{\bullet 1,3}, m_{\bullet 1,4}, m_{\bullet 1,5}, R)$$

We concluded that if the 50% intervals of $V.predict_k$ and $R.predict_k$ contained the observed values at least half the time than our model provided reasonable inferences.

For the posterior predictive check, we drew simulated values from the posterior distributions and observed whether the simulated values matched our observed data. Our observed data were the total number of not-collared adult carcasses, $V_{jk} = \sum_{i=1}^{n} V_{ijk}$, and the total number of collared adult carcasses, R_{jk}, found during the study period in season *j* from mortality cause *k*. For each of 1000 draws from the posteriors, $V.draw_{ijk} \sim binomial(d_{jk}, n_{ijk})$ and $R.draw_{ijk} \sim multinomial(m_{ij1}, m_{ij2}, ..., m_{ijK}, R_{ij})$, we summed the number of adult not-collared carcasses and collared carcasses in season *j* due to mortality cause *k* to get $V.draw_{jk} = \sum_{i=1}^{n} V.draw_{ijk}$ and $R.draw_{jk} = \sum_{i=1}^{n} R.draw_{ijk}$. We created histograms of $V.draw_{jk}$ and $R.draw_{jk}$ and plotted the observed data, V_{jk} and R_{jk}. We assumed that the model was consistent with the data if the observed number of carcasses in each mortality cause category and season were within the middle 50% of the posterior predictive distributions at least half the time.

Results

Our external validation showed that the 50% and 95% prediction intervals overlapped the observed data 80% and 90% of the time, respectively (Fig. B.1). Therefore, we concluded that the inferences from the model were generally making sense. The greatest discrepancy in the external validation was that the number of not-collared carcasses that were legally killed was 3 times higher than the mean posterior prediction (Fig. B.1). On average, the proportion of known carcasses that were legally killed in the population in the proceeding summers was 0.013 (sd =

0.007) compared to a proportion of 0.026 known carcasses that were legally killed in summer 2012. The 50% prediction interval for the predicted population size in the summer 2012, $N.predict$ = 1129 – 1175, contained the observed population size, $Nobs = 1152$.

The posterior predictive check demonstrated that the 50% posterior intervals for $V.draw_{jk}$ and $R.draw_{jk}$ overlapped the observed data 100% of the time (Fig. B.2). The posterior predictive checks demonstrated that the model was consistent with the data and we concluded that the model fit the data well.

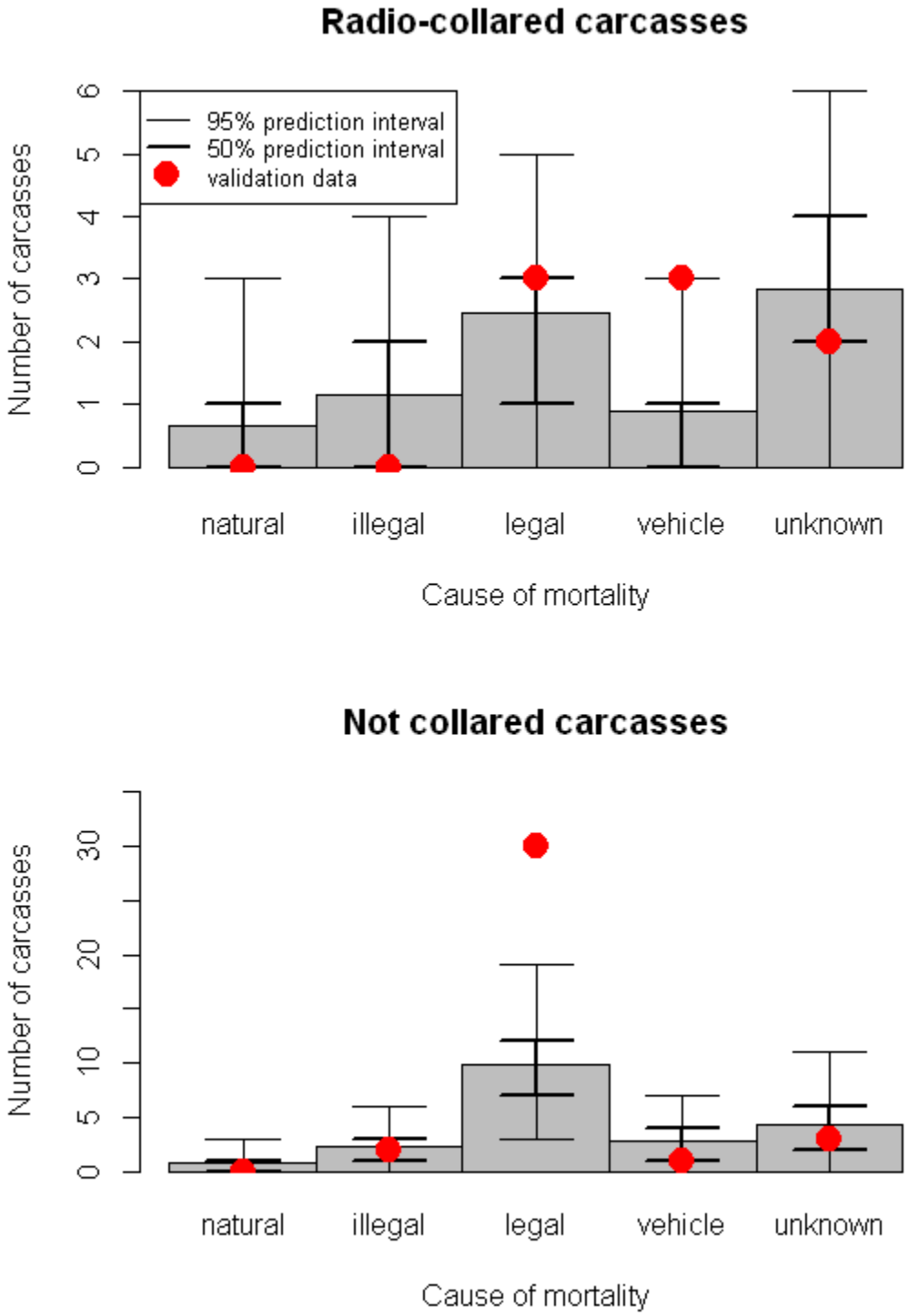

Figure B.1. The mean model prediction with 50% and 95% prediction intervals of the distribution of mortality causes for radio-collared ($R.predict_k$) and not-collared ($V.predict_k$) wolf carcasses found in Wisconsin, USA in the summer of 2012 with the validation data plotted in red dots.

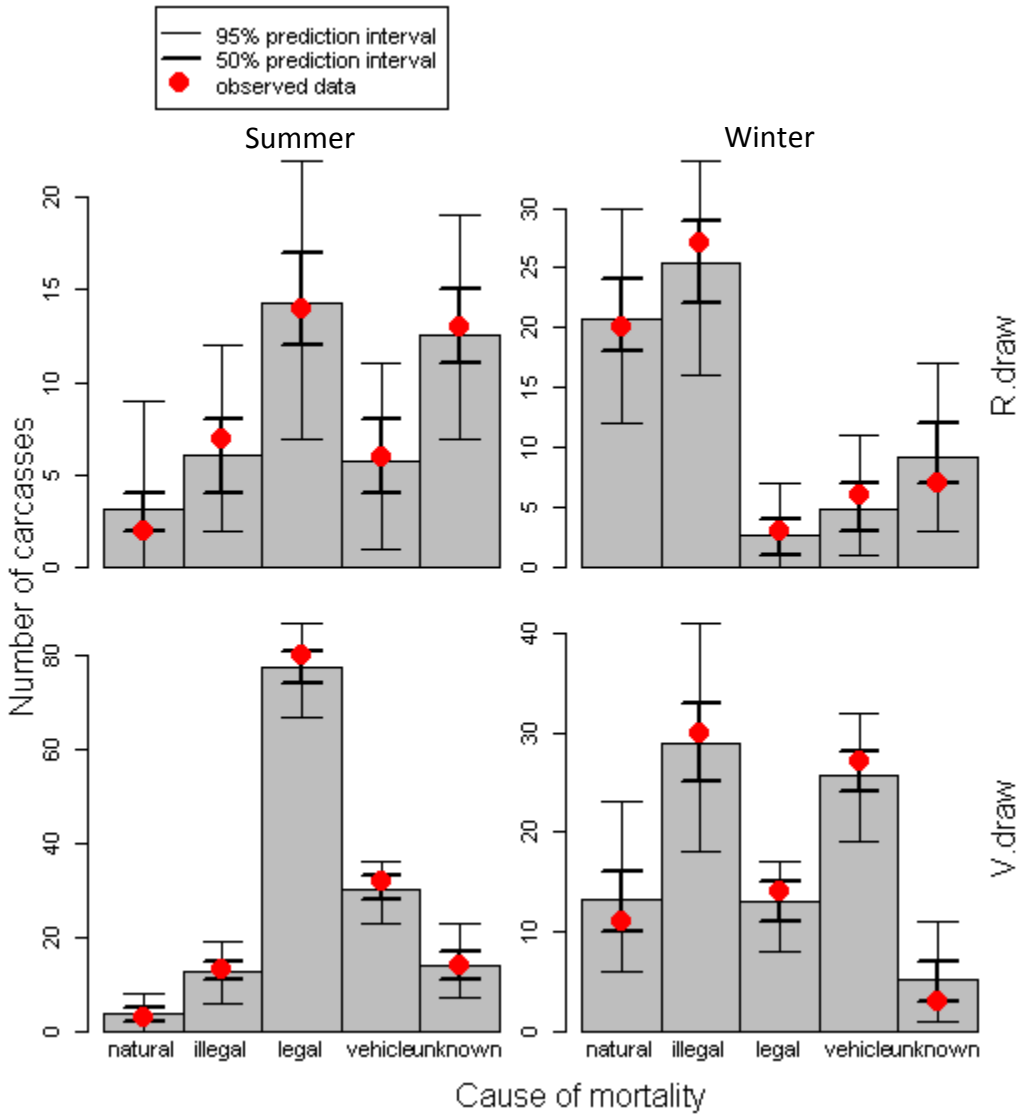

Figure B.2. The mean posterior predictive value (gray bars) with 50% and 95% credible intervals of the distribution of mortality causes for radio-collared carcasses (*R.draw*) and not-collared carcasses (*V.draw*) in Wisconsin, USA with the observed data plotted in red dots.

Appendix C. Additional tables and a worked example of an odds and odds ratio interpretation from the patterns in mortality causes multinomial analysis.

Worked example of an odds and odds ratio interpretation from Table C.1

Tables C.1 and C.2 give the model results in terms of log odds. In order to get an odds interpretation, it is necessary to exponentiate the log odds. For example, the log odds are 1.694 for a collared yearling carcass to have an illegal versus natural mortality cause determination (Table C.1). The odds of a collared yearling wolf carcass having an illegal versus natural mortality cause determination is exp(1.694) = 5.441. Said another way, for a yearling collared carcass the estimated odds that its mortality cause was illegal kill instead of natural mortality was 5.441.

Odds ratios are another way to interpret these data. An odds ratio is the ratio of two odds. We calculate the odds that a collared adult male wolf carcass and a collared adult female wolf carcass had mortality cause determinations of illegal versus natural mortality as exp(0) = 1 and exp(-0.123) = 0.884, respectively (Table C.1). Therefore, the odds ratios of yearlings to adult males is 5.441/1 = 5.441 and yearlings to adult females is 5.441/0.884 = 6.153. Overall, we can say that the odds were > 5 times for collared yearling carcasses to have an illegal versus natural mortality cause determination compared to adults.

Table C.1. Mean posterior parameter estimates (and standard deviations) from a multinomial model of the probability of five mortality causes for radio-collared wolves in Wisconsin, USA from 1979 – 2012 based on the variables of season, period, age and sex, and wolf harvest zone (WHZ). Baseline covariate values were: Season = summer, Period = late growth, Age and sex = adult male, WHZ = 1.

		season	period		age and sex			wolf harvest zone (WHZ)			
Logit[1]	Inter-cept	winter	Recov-ery	early growth	adult female	yearling	pup	WHZ 2	WHZ 3	WHZ 4	WHZ 5
$\log\left(p_I/p_N\right)$	-0.37 (0.58)	0.31 (0.51)	-0.58 (0.64)	**-1.61 (0.51)**	-0.12 (0.49)	**1.69 (0.71)**	-0.39 (0.76)	**1.66 (0.60)**	0.41 (0.72)	**1.59 (0.84)**	1.10 (0.62)
$\log\left(p_L/p_N\right)$	1.20 (0.65)	**-3.32 (0.71)**	-0.54 (0.91)	**-2.34 (0.86)**	0.61 (0.67)	**-80.56[2] (60.27)**	0.14 (1.04)	0.06 (0.86)	0.12 (0.95)	-1.18 (1.58)	-1.24 (1.12)
$\log\left(p_V/p_N\right)$	1.01 (0.65)	**-1.91 (0.64)**	-1.21 (1.02)	-1.33 (0.75)	-0.36 (0.65)	0.26 (0.98)	**-81.29[2] (59.56)**	-1.56 (1.425)	-0.86 (1.04)	-1.11 (1.56)	-0.32 (1.02)
$\log\left(p_U/p_N\right)$	**1.78 (0.57)**	**-2.18 (0.57)**	-0.12 (0.70)	**-1.26 (0.66)**	-0.60 (0.57)	-2.20 (1.47)	-0.48 (0.88)	-0.15 (0.75)	-2.35 (1.44)	-1.85 (1.56)	**-2.43 (1.44)**

Bold type indicates that the 95% credible interval does not overlap 0.

[1] Mortality causes: N = natural, I = illegal kill, L = legal kill, V = vehicle strike, and U = unknown.

[2] Very low posterior estimates were because there were no observed carcasses in these categories.

Table C.2. Mean posterior parameter estimates (and standard deviations) from a multinomial model of the probability of five mortality causes for not-collared wolves in Wisconsin, USA from 1979 – 2012 based on the variables of season, period, age and sex, and wolf harvest zone (WHZ). Baseline covariate values were: Season = summer, Period = late growth, Age and sex = adult male, WHZ = 1.

		season	period		age and sex			wolf harvest zone (WHZ)			
Logit[1]	Inter-cept	winter	recov-ery	early growth	adult female	yearling	pup	WHZ 2	WHZ 3	WHZ 5	WHZ 6
$\log\left(p_I/p_N\right)$	0.21 (0.56)	-0.13 (0.47)	0.30 (1.00)	**-1.04 (0.48)**	0.83 (0.55)	0.89 (0.75)	0.35 (0.64)	0.82 (0.61)	0.70 (0.69)	**3.26 (1.24)**	**3.92 (1.41)**
$\log\left(p_L/p_N\right)$	**2.99 (0.48)**	**-2.58 (0.47)**	**-81.03[2] (58.72)**	**-4.46 (0.90)**	0.64 (0.56)	1.06 (0.73)	1.01 (0.59)	**-1.34 (0.68)**	0.18 (0.62)	0.99 (1.28)	1.42 (1.43)
$\log\left(p_V/p_N\right)$	**1.95 (0.49)**	**-1.22 (0.43)**	-0.45 (1.00)	-0.78 (0.44)	0.25 (0.54)	**1.71 (0.70)**	**1.39 (0.56)**	-0.09 (0.57)	-0.13 (0.62)	**2.36 (1.23)**	**3.23 (1.40)**
$\log\left(p_U/p_N\right)$	-1.04 (0.60)	**-1.36 (0.53)**	0.53 (1.13)	-0.57 (0.55)	0.51 (0.66)	1.10 (0.83)	1.24 (0.66)	0.86 (0.69)	0.17 (0.84)	**3.62 (1.30)**	**2.88 (1.50)**

Bold type indicates that the 95% credible interval does not overlap 0.

[1] Mortality causes: N = natural, I = illegal kill, L = legal kill, V = vehicle strike, and U = unknown.

[2] Very low posterior estimates were because there were no observed carcasses in this category.

Appendix D. Supplemental material for the correction between collared and not-collared carcass datasets analysis

Table D.1. Mean posterior parameter estimates (and standard deviations) from a state-space model relating observed collared wolf carcasses and not-collared wolf carcasses found in Wisconsin, USA in 2003 – 2012 to estimate seasonal and cause-specific probabilities of mortality for collared wolves (*p*), the allocation of the mortality rate (*m*), and the probabilities for detection of wolf carcasses (*c*).

		Mortality cause				
Parameter	Season	Natural	Illegal	Legal	Vehicle	Unknown
p	summer	0.0021 (0.0014)	0.0040 (0.0017)	0.0110 (0.0029)	0.0032 (0.0011)	0.0115 (0.0050)
p	winter	0.0225 (0.0063)	0.0216 (0.0065)	0.0020 (0.0008)	0.0034 (0.0011)	0.0099 (0.0043)
m	summer	0.0802 (0.0419)	0.1453 (0.0437)	0.3123 (0.0560)	0.1128 (0.0357)	0.3495 (0.0607)
m	winter	0.3704 (0.0572)	0.3664 (0.0512)	0.0398 (0.0169)	0.0664 (0.0215)	0.1570 (0.0489)
c	summer	0.3788 (0.1592)	0.5302 (0.1245)	0.7849 (0.0727)	0.7593 (0.0818)	0.3413 (0.1023)
c	winter	0.2159 (0.0816)	0.3946 (0.0890)	0.6944 (0.1096)	0.7293 (0.0897)	0.1959 (0.0887)

Table D.2. The observed mean population size (Nobs) and range and estimated median (N) population size and 95% credible interval of the Wisconsin wolf population size in summer and winter from 2003 – 2011.

Year	Summer Nobs	Range	Summer N	95%	Winter Nobs	Range	Winter N	95%
2003	472	440 - 503	450	407 - 493	391	373 - 410	365	319 - 407
2004	546	491 - 602	514	468 - 561	450	435 - 465	427	381 - 471
2005	637	586 - 687	612	563 - 663	486	467 - 504	451	393 - 500
2006	676	615 - 736	648	596 -701	565	546 - 583	534	487 - 582
2007	742	684 - 799	691	607 - 751	563	549 - 576	519	455 - 573
2008	789	728 - 848	742	684 - 799	655	637 - 673	614	555 - 669
2009	905	887 - 923	879	820 - 939	726	704 - 747	679	621 - 735
2010	1003	981 - 1024	974	903 - 1040	803	782 - 824	758	690 - 818
2011	1109	1088 - 1130	1067	982 - 1138	834	815 - 880	758	649 - 835

Chapter 2: Survival of a recolonized and harvested wolf population in Wisconsin from 1980 – 2013

Abstract

Wisconsin's gray wolf (*Canis lupus*) population increased from 20 to > 800 wolves (1980 – 2013) and has recovered from endangered status under the U.S. Endangered Species Act to become a legally harvested species. Wisconsin's Department of Natural Resources is developing new policies for wolf harvest and management. During this important decision-making process for wolves, we provide critical information on cause-specific mortality and its relation to time and habitat quality. Appropriate analysis of cause-specific mortality requires first estimating cause-specific hazards, from which the cause-specific mortality, or "cumulative incidence function", is obtained. In our case, this was complicated by the fact that some deaths were likely to be incorrectly classified as censoring, violating the usual survival analysis requirement that censoring is noninformative and not statistically associated with mortality risk. This novel approach to survival analysis models endpoints (last radio-telemetry location) for 499 radio-collared wolves in two parts. First, we modeled cause-specific probabilities that an endpoint was due to a particular cause given that an endpoint occurred. Known death causes made up 45% of events and the rest were censored. Second, we modeled monthly hazards as smooth functions of time to estimate approximate probability of a wolf reaching its endpoint in some month. We suspected that some wolves that died but were not found were misclassified as censored wolves, and we used auxiliary data from annual population and pup estimates to inform this misclassification. We estimated that 15% of deaths were recorded as censored wolves. During winter, monthly hazards were double that of summer, and better habitat quality decreased hazards. There was substantial inter-annual variation in survival and cause-specific mortality

rates with some years having 10 times more illegal mortality or natural mortality compared to other years. We estimated 74% annual survival for average habitat quality, and 76% annual survival for a 10% increase in habitat quality. On average, 1 out of 10 wolves was illegally killed, and the rates of illegal killing have decreased since 2011. Mortality instead of recruitment appears to be regulating wolf population growth, and on average > 22% annual human-cause mortality leads to a negative population growth. Natural and human-caused mortality appears to be additive when human-caused mortality is < 15% annually, and there may be some compensation for higher mortality rates. Annual survival has been declining since 2008 and human-caused mortality rates have been > 22% in most years since 2008.

Introduction

Recovery occurred for < 2% of species listed as endangered under the U.S. Endangered Species Act (ESA) since 1974 (Taylor et al. 2005). In 2012, gray wolves (*Canis lupus*) in the Western Great Lakes transitioned through delisting under ESA to a hunted species under state law. For any delisted species, the U.S. Fish and Wildlife Service requires a 5-year post-delisting monitoring period during which ESA's emergency listing rule can relist the species to ensure species' well-being (Refsnider 2009). Removal of ESA protections for wolves is controversial, and people disagree about whether wolves have recovered sufficiently over a significant portion of their range (Bruskotter and Enzler 2009, Bruskotter et al. 2013). Currently, wolves are two years into the post-delisting monitoring period and Wisconsin's Department of Natural Resources (WDNR) is developing a new plan for wolf management that may include a population goal and harvest policy. Here, we provide critical information to inform conservation: an analysis of temporal patterns and habitat influences in wolf mortality in Wisconsin from recolonization (circa 1980) through the first years of harvest.

Recolonization of wolves in Wisconsin began in the late 1970s with five packs establishing territories in forested habitat of northwestern Wisconsin adjacent to occupied wolf territory in Minnesota by 1980 (Wydeven et al. 2009). A decade later, ten packs were established in Wisconsin with some pack territories expanding into the forested north-central regions of the state. Five years later in 1995, the wolf population increased to > 80 wolves in 21 packs and extended their range into a somewhat insular area of forest in central Wisconsin (Thiel et al. 2009). Colonization of the central forest region coincided with increasing wolf population growth and wolves began moving into the upper peninsula of Michigan (Beyer et al. 2009). During these first fifteen years of recolonization, wolf packs established territories in areas with relatively few roads (< 0.45 km roads / sq km; Mladenoff et al. 1995). Wolf packs continued to establish territories in areas of low road density into 1997 when 150 wolves occurred in 35 packs (Mladenoff et al. 1999). Wolf numbers continued to increase at a rate of 30% per year and reached > 800 wolves in 213 packs in 2012, however the growth rate has decreased as wolf numbers increased, suggesting a density-dependent mechanism arising from saturation of the best habitat (Mladenoff et al. 2009, Van Deelen 2009). A final assessment of habitat use based on wolf pack locations in 2006 – 2007 found that when more packs were on the landscape, the best predictors of pack location were lack of agriculture and lack of roads (Mladenoff et al. 2009).

In Wisconsin's wolf range, social tolerance for wolves decreased during a time of frequent policy shifts and increasing wolf numbers. Three times during 2003 – 2011 Wisconsin's wolves were federally listed and subsequently delisted from the ESA, and the state of Wisconsin was denied and approved, respectively, to use lethal methods to control problem wolves each time (Refsnider 2009, Olson 2013). Since 2003, years when wolves were listed

under the ESA during summer associated with increased probability of a wolf in Wisconsin dying from illegal killing, and people living in wolf range reported an increased fear of wolves and an inclination to illegally kill a wolf (Olson 2013, Treves et al. 2013). Hence, changes in policy likely affected the overall survival for wolves as well.

Through extensive radio-collaring, tracking, observations, and territory mapping, WDNR has maintained accurate and consistent counts and distribution estimates of wolves and wolf packs during the >30 years of wolf reestablishment. WDNR has radio-telemetry records on ~ 500 individual wolves. Radio-telemetry data can provide time-to-event information needed to estimate survival when individuals are tracked until death (Heisey and Fuller 1985, Pollock et al. 1989). Incomplete radio-telemetry records occur when individuals are not tracked until death, and these cases require careful statistical approaches (Klein and Moeschberger 2003). In a survival analysis, we observe each individual until death (or the event of interest) or loss-to-follow-up. The loss-to-follow-up event we call censoring, and a critical assumption in survival analysis is statistical independence between censoring times and death times (Klein and Moeschberger 2003). The assumption of independent censoring is rarely tested, but violating this assumption could bias survival estimates high if some censoring events are actually misclassified deaths (Leung et al. 1997, Tsai et al. 1999).

In wildlife population studies, assumptions of independent censoring in survival analysis may not always be valid particularly for species whose life spans exceed the battery life of telemetry transmitters. With gray wolves, a significant portion of the wolves are not tracked until death, and loss-to-follow-up could occur because the study ended, the wolf slipped out of its collar, the wolf's collar failed because of battery life or technology failure, the wolf dispersed out of the study area, or the wolf was illegally killed and its collar was destroyed. Clearly, the

latter reason for the loss-to-follow-up is not independent of death and misclassification would bias survival rates if any of these mortality events were considered censoring events. Also, dispersal probably associates with increased hazard and would be another violation of the independent censoring assumption. Integrated models for wolves in Scandinavia and Wisconsin that incorporate count data with radio-telemetry data suggest discrepancies between the data sources that indicate non-independent censoring (Liberg et al. 2012, Stenglein et al. in review). However, effects of non-independent censoring have not been modeled explicitly in telemetry-based survival analysis. In the case of a recolonized and newly harvested wolf population in Wisconsin, accounting for non-independent censoring will improve the survival estimate and may suggest a more accurate rate of illegal killing than has previously been documented.

Here, we analyze cause-specific mortality for radio-collared wolves in Wisconsin from 1980 – 2013 and the associated variation relative to age class, season, time, and habitat quality. Our objectives were to: 1) estimate cause-specific probabilities of endpoints with respect to time, 2) estimate the overall and cause-specific hazards of endpoints with respect to time, 3) evaluate importance of selected risk factors on mortality hazards while accommodating the effects of misclassification, and 4) estimate the rate of non-independent censoring in the radio-telemetry data.

Methods

Study area and datasets

Our study area was north and central Wisconsin, USA, during 1980 – 2013. Northern Wisconsin forests are dominated by sugar maple (*Acer saccharum*) and other deciduous species on the dominant mesic glacial till plains, with aspen-birch (*Populus* spp.- *Betula papyrifera*) and pine (*Pinus* spp) on sandy glacial outwash. Conifer swamps of species such as fir (*Abies*

balsamea), spruce (*Picea* spp) and cedar (*Thuja occidentalis*) with some deciduous species are common. The sandy central Wisconsin forest is dominated by oak (*Quercus* spp) and pines. Most forested areas are in northern Wisconsin (i.e. northern forest region), but a smaller isolated portion of forest makes up the central forest region. The latter region is surrounded by agriculture. Cultivated crops, hay, and pasture land are interspersed throughout Wisconsin, but most agriculture occurs in central and southern Wisconsin (see Fig. 1 in Chapter 1). Wolves primarily occupy the northern forest region (wolf harvest zones [WHZs] 1, 2, 3, and 4) and the central forest region (WHZ 5) of Wisconsin (Fig. 1B).

We used two sources of wolf data provided by WDNR. First, the radio-collared wolf dataset consisted of > 40,000 weekly locations of 499 wolves. Wolves were generally only radio-collared if they were ≥ 4 months old (Wydeven et al. 2009). We summarized these data by month and kept only the last record in each month for each wolf, resulting in 9,811 monthly location records (Fig. 1A). For each location we compiled data for month, year, age class (adult [≥ 24 months] or non-adult), season (summer: April – September, winter: October – March), habitat quality (Fig. 1B; Mladenoff et al. 2009), and whether it was an endpoint (i.e., the last record for an individual). If the location was an endpoint, we also recorded cause of endpoint consisting of: 1) loss-to-follow-up from unknown causes (*unknown censoring*, hereafter), 2) surviving until the end of the study or loss-to-follow-up during the study and then found dead sometime after its endpoint (*known censoring*, hereafter), 3) dead because of illegal killing (*illegal kill*, hereafter), 4) dead because of human causes other than illegal killing, including vehicle collision, lethal control action, and harvest (*other human mortality*, hereafter), and 5) dead because of other causes, including disease, intraspecific strife, and unknown causes (*other death*, hereafter).

Habitat quality was extracted from a raster surface of wolf pack habitat probability (Fig. 1B from plate 5 in Mladenoff et al. 2009) for each location with Spatial Analyst tools in ArcMap (Version 10; Environmental Systems Research Institute 2009). We used Mladenoff et al.'s (2009) most recent wolf habitat model from wolf pack locations in 2007 – 2008. Their analysis showed that wolf packs were using locations with lower road density and lower amounts of agriculture than randomly generated pack territories (Mladenoff et al. 2009). Mladenoff's habitat probability model did not use the same data that we use in our analysis and was generated on the basis of pack territory mapping. Therefore, using the wolf pack habitat probability model as a predictor for individual wolf endpoints events is novel and appropriate.

The second source of data was annual population counts and corresponding annual numbers of pups estimated in Wisconsin from 1980 – 2013. Each winter, WDNR biologists counted wolves and estimated the number of new recruits from observation of changes in wolf pack sizes and from howl surveys during the previous summer. Annual winter population counts derived from snow-tracking by volunteers and agency personnel, direct observation, photos from wildlife cameras, and by aerial counts in packs containing radio-collared individuals (Wydeven et al. 2009). Annual winter counts (for population size and number of new recruits) were reported as ranges (lower bound is the minimum count) in WDNR annual reports, and we used the midpoint in each year as our count. We used the population count model of Stenglein et al. (*unpublished*) to estimate annual survival rates (Appendix A).

Statistical analysis and modeling

Our goal was to estimate the cause-specific mortality, and to understand the factors affecting the cause-specific mortality over space and through time. Our approach differs from most survival analysis that models an event of interest (often death) and assumes that the other

endpoints are non-informative and hence are censored from the analysis (Klein and Moeschberger 2003). The likelihood for a survival model can be written as the product of component likelihoods for each record, whether it is a censored observation, an observation from an individual that just entered the study, or a death observation (Heisey and Fuller 1985). Under the assumption of independent censoring and death times, the censoring contribution to the likelihood can be factored from the death contribution, allowing the death contribution to be maximized independently of the censoring contribution (Klein and Moeschberger 2003). This assumption is essentially equivalent to an assumption of additive mortality where hazards for mortality and for censoring are completely additive and unassociated (Heisey and Patterson 2006). This also leads to the appearance that censored data can be essentially ignored. Although this result is analytically convenient, it is inappropriate to assume independent censoring without testing that assumption.

One case in which censoring events can be statistically informative is if some mortality endpoints get misclassified as censored endpoints. But death does not need to occur at the exact time of censoring for censoring to be informative; the censoring event only needs to be statistically associated with an increased risk of mortality. An example of this is if the animal disperses out of radio-tracking range, and the act of dispersing increases the animal's mortality hazard. Both of these cases, direct misclassification and elevated mortality risk, can be modeled as misclassified mortalities, although in the latter case, the misclassification probability is serving as a proxy for the elevated risk associated with the informative censoring event and does not exactly depict the misclassification mechanism.

Here, we modeled all endpoints because we could not be confident about the assumption of independent censoring for endpoints that did not end in death (Chapter 1, Stenglein et al.,

unpublished). By incorporating auxiliary data, we estimated the probability that a death was misclassified as an *unknown censoring* event, which allowed us to obtain a misclassification-adjusted mortality hazard. We describe our model in three parts: 1) the cause-specific endpoint probability, 2) the hazard function, and 3) the misclassification effect. We used a hierarchical Bayesian modeling approach to analyze the endpoints for radio-collared wolves.

Cause-specific endpoint probabilities

We used a multinomial logit model to relate cause-specific endpoints to covariates, including a smooth function for time. For each observed endpoint, c_m, with $m = 1, 2, \dots, M$ and M is the total number of endpoints (equal to the number of individuals), we modeled cause-specific probabilities that the enpoint m was observed to be due to cause j, p^*_{mj}, where $j = 1, \dots, J$ and J is the number of causes, as categorical and $\sum_{j=1}^{J} p^*_{mj} = 1$:

$$c_m \sim categorical\left(p^*_{m,1}, p^*_{m,2}, \dots, p^*_{m,J}\right)$$

We refer to p^*_{mj} as the error-prone classification probabilities because these are the probabilities that we observed and they likely are biased by misclassification. We used auxiliary data to adjust these error-prone probabilities for misclassification errors. We related the observed cause-specific probabilities p^*_{mj} to the true cause-specific probabilities p_{ml} through a misclassification parameter Φ_{lj} informed by auxiliary data (see misclassification section): $p^*_{mj} = \sum_{l=1}^{L} (\Phi_{lj} \times p_{ml})$. We defined parameter Φ_{lj} as the probability that an individual that actually experienced the endpoint l was observed and classified as endpoint j; these parameters generalize the ideas of test sensitivity and specificity (Appendix B).

Through the logit link, we related the accurate probabilities $p_{m,l}$ to the linear predictor $D_{mr}\alpha_{rl} + Y_{mk}a_{kl}$. The D_{mr} were covariate data and came from an $M \; x \; R$ matrix design $\boldsymbol{D}$ with row $\boldsymbol{D}_m = (D_{m,1}, D_{m,2}, \dots, D_{m,R})$, and the α_{rl} was an $R \; x \; L$ matrix $\boldsymbol{\alpha}$ of regression

coefficients (log odds ratios) with $r = 1, 2, \ldots R$ and R number of regression coefficients. The $Y_{mk}a_{kl}$ portion of the linear predictor for observation m is a smooth function of time and was incorporated into the cause-specific endpoint probabilities by means of a low-rank thin-plate spline (Ruppert et al. 2003; Appendix C):

$$p_{ml} = \frac{e^{\varepsilon_{ml}}}{\sum_{l=1}^{L} e^{\varepsilon_{ml}}}$$

$$\varepsilon_{ml} = D_{mr}\alpha_{rl} + Y_{mk}a_{kl}$$

We include some detail about the linear predictor to eventually clarify how the auxiliary data inform the true cause-specific probabilities p_{ml}. The linear predictor had $r + k$ terms for each endpoint cause l. In our case, we had four covariates plus an intercept ($r = 5$) and we used 20 knots in the spline ($k = 20$). We keep discussion of the spline in Appendix C and keep the spline term $Y_{mk}a_{kl}$ together for simplicity. The linear predictor for cause l was: $D_{m,1}\alpha_{1,l} + D_{m,2}\alpha_{2,l} + D_{m,3}\alpha_{3,l} + D_{m,4}\alpha_{4,l} + D_{m,5}\alpha_{5,l} + Y_{mk}a_{kl}$. For an endpoint m, $D_{m,1}$ was 1 for the intercept, $D_{m,2}$ was the time of the event as part of the time spline, $D_{m,3}$ was an indicator variable for non-adults, $D_{m,4}$ was an indicator variable for winter, and $D_{m,5}$ was the habitat quality value. We defined the reference category as adult wolves in summer with average habitat quality and this category had all regression coefficients equal to 0. We used *unknown censoring* as a constraint and set $\alpha_{r,1} = 0$, for $r = 1, 2, 3, 4, 5$. We put a normal prior on each of the α_{rl}s for $l = 2, 3, 4, 5$ with mean equal to 0 and standard deviation equal to 100: $\alpha_{rl} \sim normal(0, 100^2)$

Hazard function

We modeled the endpoint cumulative monthly hazard using discrete time proportional hazards, or a complementary log-log (cloglog) model to relate radio-collared relocation observations to covariates, including a smooth function of time. If the log cumulative monthly

hazard is h, the monthly event-free probability is e^{-e^h}, and the monthly event probability is $1 - e^{-e^h}$. The likelihood contribution for a single wolf is the product of these terms over the span of months during which the wolf was monitored. The resulting product has the same appearance as arises from a same-length series of independent Bernoulli trials modeled with the cloglog link (the conditional independence of survival data gives rise to this appearance; Heisey et al. 2007). Thus we modeled the monthly relocations of radio-collared wolves, $y_i = \{0, 1\}$, for $i = 1, \ldots, N$ and N is the total number of observations, as independent Bernoulli random variables with μ_i probability of an endpoint for relocation. Then, through the cloglog link, we related the μ_i probability to a linear predictor, $\gamma + \omega_g + X_{iq}\beta_q + Z_{ik}b_k$, for $q = 1, 2, \ldots, Q$ and Q is the total number of predictor variables, and we transformed μ_i into the hazard.

$$y_i \sim Bernoulli(\mu_i)$$

$$\text{cloglog}(\mu_i) = \gamma + \omega_g + X_{iq}\beta_q + Z_{ik}b_k$$

$$h_i = -\log(1 - \mu_i)$$

We let γ be the grand mean, and defined a vague, normal prior with mean equal to 0 and SD equal to 100: $\gamma \sim Normal(0, 100^2)$. The ω_gs were the increments for each year g from the grand mean γ, and we also defined normal priors on the ω_gs with mean equal to 0 and SD equal to 100: $\omega_g \sim Normal(0, 100^2)$, for $g = 2, 3, \ldots, G$. We set $\omega_1 = 0$ as a constraint and to establish a meaningful baseline. Together, the $\gamma + \omega_g$ term can be thought of as a year-specific intercept. The X_{iq} terms are data that come from a potentially time-varying covariate (risk factor) matrix $\boldsymbol{X}$ with dimensions $N \; x \; Q$, and row $\boldsymbol{X}_i = (X_{i,1}, X_{i,2}, \ldots, X_{iQ})$. The β_q terms are from the vector $\boldsymbol{\beta}$ of regression coefficients where $\boldsymbol{\beta} = (\beta_1, \beta_2, \ldots, \beta_Q)^{\mathrm{T}}$. We put a normal, vague prior on each of the β_qs with mean equal to 0 and standard deviation equal to 100:

$\beta_q \sim normal(0, 100^2)$. The $Z_{ik}b_k$ portion of the linear predictor for observation i is a smooth function of time and was incorporated into the hazard function by means of a low-rank thin-plate spline (Appendix C). Written out for observation i and keeping the spline portion together, the linear predictor was: $\gamma + \omega_{g[year[i]]} + X_{i,1}\beta_1 + X_{i,2}\beta_2 + X_{i,3}\beta_3 + X_{i,4}\beta_4 + Z_{ik}b_k$. The index for $\omega_{g[year[i]]}$ denotes that the year increment corresponds the year of observation i, $X_{i,1}$ was the time of the event as part of the time spline, $X_{i,2}$ was an indicator variable for non-adults, $X_{i,3}$ was an indicator variable for winter, and $X_{i,4}$ was habitat quality value for observation i.

We now use slightly different generalized notation to accommodate the same time scale for the cause-specific endpoint probabilities and the hazard function. For month t where $t = 1, 2, \ldots, T$ and T is the total number of months, we modeled the cause-specific endpoint monthly hazard, $h(t)_l$, as the product of the overall hazard, $h(t)$, and the cause-specific probability that the endpoint was due to cause l given that there was an endpoint, $p(t)_l$:

$$h(t)_l = p(t)_l * h(t)$$

Misclassification

To handle informative censoring, we took a misclassification approach, where some of the observed *unknown censoring* may have actually been a mortality event. We defined the known mortality portion of the monthly hazard as the baseline hazard times the sum of the baseline cause-specific probabilities that the endpoint was due to a known mortality cause l. Our total baseline hazard included the year-specific intercept, the time spline, and the average season effect, so that the baseline hazard $h(t)_{1:5}$ was:

$$\text{cloglog}(\mu(t)_0) = \gamma + \omega_g + \beta_1 * t + \frac{\beta_3}{2} + Z(t)_k b_k$$

$$h(t)_{1:5} = -\log(1 - \mu(t)_0)$$

Our baseline cause-specific probabilities for cause l, $p(t)_{0,l}$, included the intercept, the time spline, and the average season effect:

$$\varepsilon(t)_{0,l} = \alpha_{1,l} + \alpha(t)_{2,l} * t + \frac{\alpha_{4,l}}{2} + Y(t)_k a_{kl}$$

$$p(t)_{0,l} = \frac{e^{\varepsilon(t)_{0,l}}}{\sum_{l=1}^{L} e^{\varepsilon(t)_{0,l}}}$$

We included the average season effect in the baseline hazard and the baseline cause-specific probabilities because we knew that there could be large seasonal differences for the hazard and the probabilities (Chapter 1). If we chose to use just summer or just winter as the baseline informed by our auxiliary data, than we could have biased our misclassification into representing too large or too small of a correction.

For the misclassification, we were interested in the known mortality portion of the monthly hazard which was mortality causes $l = 3, 4, 5$ for *illegal kill*, *other human mortality*, and *other death* causes respectively, so we wrote this as:

$$h(t)_{3:5} = \sum_{l=3}^{5} p(t)_{0,l} \times h(t)_{1:5}$$

and defined $h(t)_{3:5}$ as the overall mortality hazard. Here, the $p(t)_{0,l}$s are the misclassification-adjusted endpoint probabilities. To drive this misclassification-adjustment, we incorporated auxiliary data, $h(t)_{aux}$ (Appendix A), to allow for the possibility that some of the mortality endpoint probabilities ($p(t)_3, p(t)_4, p(t)_5$) might have been misclassified as censoring instead of mortality. In essence, $h(t)_{aux}$ served as a prior for the overall mortality hazard $h(t)_{3:5}$. In survival analysis, log hazards tend to converge to normality more rapidly than hazards or finite mortality estimates. Therefore, we modeled log of the auxiliary hazard as normally distributed with mean equal to log of the overall mortality hazard and standard deviation equal to log of the

measurement error from the auxiliary data: $\log(h(t)_{aux}) \sim Normal(\log(h(t)_{3:5}), \log(\sigma_{aux})^2)$. Through this distribution, the auxiliary data informed the baseline hazard $h(t)_{1:5}$ and the $\sum_{l=3}^{5} p(t)_l$ term for the cause-specific probabilities that the endpoint was due to a known mortality cause. This meant that the baseline monthly hazard $h(t)_{1:5}$ could change by year depending on the auxiliary data.

We took a generalized sensitivity and specificity approach and defined a misclassification $L \times J$ square matrix $\mathbf{\Phi}$ where row l represented the true cause of an endpoint for L total endpoint causes, and column j represented the observed cause for J total endpoint causes and $L = J$ (Walter and Irwig 1988). The entry Φ_{lj} was the conditional probability that given the actual endpoint was from cause l, it was classified as an event from cause j, and $\sum_{j=1}^{J} \Phi_{lj} = 1$. Where there was no misclassification for cause l, then $\Phi_{lj} = 1$ when $l = j$. We assumed that an animal which truly experienced censoring was never misclassified as having died, hence $\Phi_{1,1} = \Phi_{2,2} = 1$. We limited our inference to $\Phi_{3,1}, \Phi_{4,1}, \Phi_{5,1}$, and $\Phi_{3,3}, \Phi_{4,4}, \Phi_{5,5}$because we were interested in whether endpoints that were actually known mortality were misclassified and observed as *unknown censoring* events. For such a misclassification event, we did not have the information in our dataset to inform which known mortality cause $l = 3, 4,$ or 5 was misclassified as *unknown censoring*. Therefore, we set a single misclassification parameter φ to represent the proportion of any mortality that was observed and classified as *unknown censoring*, and we set up our misclassification matrix as:

$$\mathbf{\Phi} = \begin{bmatrix} 1 & 0 & 0 & 0 & 0 \\ 0 & 1 & 0 & 0 & 0 \\ \varphi & 0 & 1-\varphi & 0 & 0 \\ \varphi & 0 & 0 & 1-\varphi & 0 \\ \varphi & 0 & 0 & 0 & 1-\varphi \end{bmatrix}$$

We assigned φ a uniform prior: $\varphi \sim Uniform(0,1)$. The probability $1-\varphi$ was the probability that a mortality event was classified correctly (Appendix B); it generalizes the idea of a true positive from diagnostic testing theory.

Details of model runs and derived parameters

We ran the cause-specific endpoint probabilities portion of the model alone without auxiliary data (unaugmented model) to visualize the patterns in the event probabilities over time from the radio-collared data. We compared the unaugmented model to the augmented model to visualize how the event probabilities changed in the presence of auxiliary data. Also, we ran the hazard portion of the model alone without auxiliary data to visualize the hazard over time from the raw radio-collared data. We used this run of the model and plotted it with the auxiliary data to see whether there appeared to be a discrepancy between the hazard from the radio-collared data and the hazard from the auxiliary data. Finally, we ran the augmented model which included the cause-specific endpoint probabilities portion, the hazard portion, and the misclassification portion informed by auxiliary data.

We derived the overall mortality hazard $h(t)_{3:5}$ for different age class and season combinations and for different values of habitat quality. From the overall mortality hazard, we estimated annual survival rates S_g for different values of the parameters:

$S_g = \exp(-\sum_{t=1+(g-1)*12}^{12+(g-1)*12} h(t)_{g,3:5})$ where $g = 1, 2, \dots, 33$ to represent annual survival from 1981 – 2013. We did not calculate annual survival in 1980 because the first records did not start until May 1980 and the data for that year were very sparse.

To get cause-specific mortality rates for *illegal kills*, *other human mortality*, and *other deaths*, we were careful to obey the "conservation of mortality" principle (Heisey and Patterson 2006). We calculated survival for each month of each year g, $S(t)_g$, and we defined M_{gl} as the

mortality rate in year g from cause l as the proportion of the survival that was due to cause l: $M_{gl} = \sum_{t=1+(g-1)*12}^{12+(g-1)*12}(h(t)_{gl} \times S(t)_g)$.

We estimated survival rates for adults and non-adults in summer and winter for average habitat quality, a 10% increase in average habitat quality, a 10% decrease in average habitat quality, and for each habitat quality class from Mladenoff et al. (2009). We used the midpoint from the range in each probability class (e.g., for the lowest probability class, the probability is 0 – 0.1 and we used 0.05 as the habitat quality value for this class). Then, we found the average habitat quality for each wolf harvest zone (WHZ) and we calculated the average annual survival rates based on this value by WHZ. In each case, we averaged the annual survival rates to get an average annual survival rate for each combination of adults and non-adults in summer and winter: $S = \sum_{g=1}^{33} S_g/33$. Finally, we calculated a weighted average of this average annual survival rate by age class and season by taking into account the number of radio-collared wolves in each of the age class and season categories. We calculated all of these derived parameters within the model so that we could get distributions from all of them.

We ran the three models with a Gibbs sampler in Program JAGS (Plummer 2003) with library 'rjags' (Plummer 2011) in program R (R developement Core Team 2013). We ran one chain and discarded the first 10,000 iterations as burn-in. Then, we sampled the posteriors for an additional 10,000 iterations.

Results

Without auxiliary data, 16% of endpoints were due to *known censoring*, and 16%, 10%, and 19% were due to *illegal kills*, *other human mortality*, and *other death*, respectively (Table 1). *Other deaths* ($N = 94$) were primarily natural mortality from disease ($N = 40$) and intraspecific strife ($N = 17$). *Unknown censoring* was the most common cause for endpoint (39%) and was more

prevalent in non-adults compared to adults (Fig. 2). Proportion of *illegal kills* was highest during 1980 – 1985 in winter, and proportion of *known censoring* was highest in 2013 because of endpoints occurring at the end of the study (Fig. 2).

The endpoint monthly hazard for average habitat quality without auxiliary data and without the year effects ω_g ranged from 0.022 – 0.240, with an average monthly discrete hazard of 0.063 (Fig. 3). The endpoint monthly hazard was highest in 1980 – 1992, and again in 2013 because of *known censored* wolves that survived until the end of the study (Fig. 3). The monthly hazard for an endpoint was twice as high in winter as in summer, and was similar in non-adults compared to adults (Fig. 3).

Without auxiliary data, average endpoint overall mortality hazard (i.e., the hazard from the known mortality causes of *illegal kills*, *other human mortality*, and *other death*) ranged from 0.018 – 0.084, with an average overall mortality hazard of 0.024 (Fig. 4). Auxiliary information from the count model estimated overall mortality hazards that ranged from 0.006 – 0.049, with an average monthly overall mortality hazard of 0.025 (Appendix A). Overall, average overall mortality hazards from the radio-collared model were low compared to overall mortality hazards from the population count model (auxiliary data), and especially during the mid-1980s and most years since 1997 (Fig. 4). The average monthly overall mortality hazard for the radio-collared data translated into an average annual survival rate of 0.750 ($e^{-(0.024*12)}$). We estimated an average annual survival rate of 0.741 from the auxiliary information ($e^{-(0.025*12)}$). Therefore, on average, there was ~1% more annual mortality represented in the auxiliary data than from the radio-collared data. We expected that the auxiliary data would inform the misclassification model to support a positive estimate of φ to show that some mortality was misclassified as *unknown censoring*.

In the augmented model, mean $\varphi = 0.145$ (SD = 0.067), which meant that on average 14.5% of the radio-collared adult wolves that were actually dead were misclassified as *unknown censoring* events. Incorporating the misclassification predictably shifted the cause-specific endpoint probabilities to have slightly higher probabilities for the known mortality causes (i.e., *illegal kill*, *other human mortality*, *other death*) and a lower probability for *unknown censoring* (Fig. 2). We could not attribute a separate proportion of the misclassified mortality to each of the known mortality causes, and instead each of the known mortality causes increased proportionally to other known mortality causes.

Cause-specific endpoint probabilities differed by age class, season, and habitat quality values but few of the odds ratios were different from 0 (Table 2). Adult wolves in summer had ten times the odds that an endpoint was due to *unknown censoring* versus *illegal kill*. Non-adult wolves had three times higher odds of *unknown censoring* compared to *other human mortality*. In winter, adult wolves were three times more likely to have an endpoint from *illegal kill* and half as likely to have an event from *other human mortality* versus *unknown censoring* (Table 2). An increase in habitat quality increased the odds than an endpoint was from *unknown censoring* versus *other human mortality* (Table 2). For mortality causes, an increase in habitat quality increased the odds that an endpoint was due to *other death* (i.e., primarily natural mortality) versus *illegal kill* and *other human mortality*. Also, increase in habitat quality increased the odds that an endpoint was due to *illegal kill* versus *other human mortality* (Table 2).

Patterns in cause-specific endpoint probabilities also changed over time (Fig. 2). *Illegal kills* were higher in winter than summer (Fig. 2). The highest proportion of *illegal kills* was in the first few years of recovery, and then the proportion of *illegal kills* decreased in the late 1980s to early 1990s. The proportion of *illegal kills* increased again in 2006 – 2011 (Fig. 2).

Proportion of *other human mortality* was highest in summer, and higher in adults than non-adult wolves. Proportion of *other human mortality* was highest in the early 1990s and since 2008. *Other deaths*, which was mainly natural mortality, was higher in adults than non-adults and equivalent across seasons. The highest proportion of *other death* was in the mid-1980s and in the early 2000s (Fig. 2).

After incorporating auxiliary data, monthly hazard for average habitat quality ranged from 0.008 – 0.237 with an average monthly hazard of 0.056. The monthly hazard was lowest for adults during summer (Mean = 0.034). Season had a larger effect on monthly hazard than age class (Table 3). In winter, monthly hazard was double that in summer ($e^{0.70} = 2.01$), and the probability that there was a higher hazard in winter than summer was 100% (proportion of posterior distribution > 0). Monthly hazard for yearlings and pups was 21% higher than for adults ($e^{0.19} = 1.21$), and the probability of a higher hazard in yearlings and pups than in adults was 96.5%. A 10% increase in habitat quality decreased monthly hazard by 9% ($e^{-0.94/10} = 0.91$; Table 3).

Cause-specific hazards varied through time and for different age class and season combinations (Fig. 5). Cause-specific hazards are meaningful alone and can be used to estimate monthly and annual cause-specific mortality and censoring rates. The largest hazard overall was due to *unknown censoring* and young wolves had a higher *unknown censoring* hazard (Fig. 5). For *illegal kill* and *other death* the winter hazards were more than double the summer hazards. Adult and non-adult wolves had very similar hazards from *unknown censoring*, *illegal kill*, and *other human mortality* (Fig. 5). Adult wolves had double the hazard from *other death* compared to non-adult wolves. Probability of mortality from *illegal killing* was highest in the early 1980s and has increased again since 2000 (Fig. 6). Probability of *other human mortality* has increased

since the mid-1990s. Probability of *other death* mortality (mostly natural mortality) peaked in the early 1980s and again in the early 2000s. Since the mid-2000s probability of *other death* has been on the decline (Fig. 6). On average, we estimated natural mortality as < 12% (range: 3 – 26%) per year (the *other death* category also contains unknown mortality), with natural mortality occurring in winter twice that of summer (Fig. 6). On average, we estimated that mortality due to *illegal killing* was 10% annually (range: 2 – 25%) with four times the amount of *illegal killing* in winter than summer. On average, we estimated mortality due to *other human causes* was 5% annually (range: 1 – 12%) with little difference by season (Fig. 6).

We estimated the overall average annual survival rate for average habitat quality for radio-collared wolves in Wisconsin as 0.740 (SD = 0.013). Average annual survival for adult wolves was 0.738 with 16% higher survival in summer (0.838) than in winter (0.673). Average annual survival for non-adults was < 1% lower than adult survival (Fig. 6). A 10% increase in habitat quality increased average annual survival by 2.1% (Mean = 0.761, SD = 0.013).

Estimated average annual survival for average habitat quality classes from Mladenoff et al. (2009) ranged from 0.503 (SD = 0.065) for the 0 – 0.1 habitat probability class to 0.771 (SD = 0.015) for the 0.95 – 1 habitat probability class (Fig. 7). Overall, annual survival was lowest in the early 1980s just as wolves were beginning to recolonize. The highest survival years were in the mid-1990s as the wolf population was entering a sustained growth phase. Since the mid-1990s survival has been slowly decreasing in a pattern that is consistent with density-dependent survival (Fig. 7). Using the average habitat quality value by WHZ, the estimated average annual survival was very similar and highest in WHZs 1 and 2 (Fig. 8). Compared to WHZs 1 and 2 we estimated 5% lower survival in WHZ 3 and 9% lower survival in WHZs 4 and 5 (Fig. 8). WHZ 6 had the lowest estimated annual survival of any WHZ (Mean = 0.500, SD = 0.066).

Discussion

Our survival analysis for radio-collared wolves from 1980 – 2013 quantified the cause-specific hazards that radio-collared wolves experienced, the relationship between survival and habitat quality, and an estimate for misclassified dead wolves. We found that radio-collared wolves in Wisconsin had average annual survival of 74% and there were large differences in survival by season, year, and for different locations in Wisconsin.

Our survival estimates are very similar to previous estimates of wolf survival in Wisconsin generated at different points in time with the same radio-telemetry data. For 1986 – 1991, Wydeven et al. (1995) estimated average annual survival as 82% while the wolf population was starting to expand. On average, our analysis estimated annual survival of 82.8% during this same period. During 1979 – 2003, Wydeven et al. (2009) estimated average annual survival as 75% for adults and yearlings, and our estimated average annual survival for 1981 – 2003 was 75.6% (we did not estimate survival prior to 1981). Correspondence between previous estimates of survival and estimates of survival with a different approach suggests that our novel approach to survival analysis is reasonable.

We took a novel approach to estimating wolf survival by modeling the endpoints without assuming independent censoring. To model the endpoints it was necessary to split the model into a portion for the cause-specific probabilities of different events and a portion for the overall endpoint hazard. This framework has many benefits. First, it allowed us to include auxiliary information and to estimate an amount of misclassified death events. In more typical approaches to survival analysis we would have assumed that all the radio-collared wolves that were lost to follow-up were not dead at the time of last observation and we would have over-estimated the annual survival. Second, it is possible to include separate covariates in each portion of the

model, and the covariates are estimated independently for each portion. We might assume that different circumstances would affect whether an endpoint having occurred (hazard) relative to the discrete cause associated with the event (cause-specific probability). Finally, the split model allowed us to incorporate a time spline separately for the hazard and the endpoint probabilities. This time spline was easy to integrate and was very informative for visualizing how the hazard, the endpoint probabilities, and the cause-specific hazards changed over the three decades of wolf recovery.

Higher hazards for wolves in winter than summer were mostly due to higher illegal killing during winter. This phenomenon likely relates to the fact that the winter period overlaps with Wisconsin's big game hunting seasons when people are afield with weapons, and the enhanced visibility of wolves during winter because of snow cover and reduced vegetative cover. This finding corresponded to our analysis of wolf carcasses where we found that carcasses with illegal kill and natural mortality causes were more common in winter than summer (Chapter 1). However, in our survival analysis we did not detect higher other human-caused mortality in summer than winter contrary to the findings in the analysis from wolf carcasses (Chapter 1).

The negligible difference in survival rates for adults compared to yearlings and pups (> 4 months old) is corroborated by similar findings (Wydeven et al. 2009). The unknown censoring hazard rate was higher for yearlings and pups than adults. Our auxiliary information informed the adult censoring rate, and assumed the same correction factor for adults, yearlings, and pups. There may be higher rates of non-independent censoring in yearlings and pups that we were not able to detect in this analysis. Our sample of yearlings and pups was small (22%) compared to the number of radio-collared adults and we are more confident about our inferences from radio-collared adults.

Incorporating average habitat quality for WHZs, enabled us to estimate annual survival rates by WHZ. WHZs 1 and 2 had higher estimated annual survival rates than the other WHZs because of the higher average habitat quality values in these northernmost WHZs (Mladenoff et al. 2009). We estimated the annual survival rate in WHZ 5 as 10% lower than the survival in WHZs 1 and 2. However, wolves in the central forest region (WHZ 5) appear to be doing well. There were only 12 wolves in 4 packs in the central forest region in 1994 – 1995 and in 2011 – 2012 the WDNR estimated 127 wolves in 32 packs in the central forest region. The central forest region does have higher road density and higher amounts of agriculture than the northern forest region, hence the lower average habitat quality value from WHZ 5.

Habitat quality had a substantial effect on annual wolf survival. To estimate habitat quality, Mladenoff et al. (1995, 1999, 2009) fit a logistic model of actual wolf pack territories and randomly-generated non-pack territories explained by environmental variables summarized within territories. An increase in habitat quality decreased the probability that a radio-collared wolf would experience its last radio-collared location and decreased the probability that its last location was a death location from human causes. Therefore, radio-collared wolves were relatively more likely to die from natural mortality and be censored in areas with a higher habitat quality. This suggests source-sink dynamics (Pulliam and Danielson 1991) because many of the reasons for censoring (dispersal, survival beyond the life of the collar, survival to the end of the study) are likely to be associated with wolves living in established high quality territories where mortality risks are smaller and the probability of living beyond the battery life of a telemetry collar is higher.

We provide the first estimate of non-independent censoring for radio-collared wolves in Wisconsin. We estimate that there were 33 (95% credible interval: 5 – 63) more radio-collared

wolves that died in 1980 – 2013 than were detected. Our correction factor only decreased the average annual survival rate by 1%, even though there was evidence of 19% missing mortality in some years. We estimated a single correction factor across all years even though there were notable differences for different periods in wolf recovery (Stenglein et al., *in review*). In 1980 – 1995 when the wolf population was just beginning to establish, there was on average 4% missing survival in the radio-collar data compared to the count data. Therefore, in these first 15 years, our discrepancy was in the opposite direction than we would have expected, and the negative discrepancy in these years shrank the overall correction factor close to 0. In 1996 – 2002 while the wolf population was increasing, we needed 3% more mortality in the radio-collared data to explain the growth rate, and since 2003, we estimate 4% missing mortality on average. This time of more missing mortality was also when we began to see increases in annual illegal killing rates for wolves. We suggest that the illegal killing rate could be 4% higher than we estimated. The period 2003 – 2013 was a time of political change for wolves and frustration with the process (Olson 2013). Social science indicates that people living in wolf range increased their willingness to illegally kill a wolf during this time period (Browne-Nunez et al. 2012, Treves et al. 2013).

On average, we estimated 15% annual human-caused mortality mostly due to illegal killing (68%). Inter-annual variation was high and some years had > 10 times more human-caused mortality compared to others, and on average 1 out of 10 wolves died from illegal killing. Average rate of annual human-caused mortality in our study is comparable to rates in wolf populations in northeastern Alberta (15%; Fuller and Keith 1980) and northwestern Minnesota (17%; Fritts and Mech 1981). Similarly, we estimated average natural mortality rates of roughly 12% per year and these also varied by a factor of 10 across years. Our average rate of natural-

caused mortality is comparable to wolf populations in south-central Alaska (9%; Ballard et al. 1987) and northwestern Minnesota (11%; Fritts and Mech 1981).

Highest rates of illegal killing occurred during the earliest years of wolf recovery (1981 – 1984) and also coincided with the highest natural mortality rates compared to other years. Therefore, it is no surprise that the wolf population periodically experienced negative population growth during those years and sustained population increase did not occur until after 1986 (Stenglein et al., *unpublished data*). Perhaps more surprising is that the rate of illegal killing drastically declined until 2005, and there have been especially high rates of illegal killing since 2010. Since 2010, the wolf population has also had its highest rates of other human caused mortality (> 10% of the population per year) for total human-caused mortality rates in excess of 25% per year. These high rates of other human mortality from vehicle collisions and lethal control actions correspond to a time when there were > 800 wolves and high quality habitat was largely saturated (Mladenoff et al. 2009, Wydeven et al. 2009). Also, since 2008, there has been a steady decrease in average annual survival. Hence, increased mortality from human causes appears to be a driver of annual growth rates that are decelerating in density dependent fashion (Van Deelen 2009). This could be an example of density dependence in survival if increasing illegal killings are an expression for reduced human tolerance of an increasing wolf population (Olson 2013) and increased rates of other human mortality are an outcome of more wolves being pushed into more marginal (higher human presence) areas where they are more likely to encounter heavily trafficked roads and livestock.

The degree to which human-caused mortality, natural mortality, and their interacting effects (e.g. additive, compensatory, super-additive) control annual growth in wolf populations is controversial (Fuller et al. 2003, Adams et al. 2008, Creel and Rotella 2010, Gude et al. 2012),

and different ecological contexts may preclude identification of a general principle from meta-analyses of trends from wolf populations across North America (Gude et al. 2012). This is further complicated by the fact that different analytical approaches can yield contradictory conclusions (Appendix D). Our analysis using various analytical approaches (Appendix D) suggests that human-caused mortality is an important driver of population trend in Wisconsin. Recruitment is evidently not a compensatory mechanism (Gude et al. 2012) and variation in natural mortality is evidently incomplete as a compensatory mechanism and may in fact be additive or super-additive (Creel and Rotella 2010). There was strong additivity of natural mortality to annual human-caused mortality rates up to 15% (Appendix D). This pattern is quite different than the evidence for compensation in human-caused mortality rates < 29% from other North American wolf populations (Adams et al. 2008).

The relationship between per capita growth and annual human-caused mortality demonstrates that the Wisconsin wolf population would stabilize at 22% annual human-caused mortality, and this is the same rate found by Fuller et al. (2003) from 19 North American wolf populations (Appendix D). However, we have seen years of negative population growth when the annual mortality rate was as low as 19%. In years of modern harvest, we estimated from our analysis that the wolf population has had 29% and 28% annual mortality in 2012 and 2013, with a 1% and 19% decrease in the wolf population size, respectively. The average annual human-caused mortality rate in the years prior to harvest was 14% (range: 3 – 26%), so we estimate a harvest rate of roughly 8% to maintain a stable wolf population, assuming simple additivity.

Literature Cited

Adams, L., R. Stephenson, B. Dale, R. Ahgook, and D. Demma. 2008. Population dynamics and harvest characteristics of wolves in the Central Brooks Range, Alaska. Wildlife Monographs 170:1-25.

Altman, D. G., and J. M. Bland. 1994. Diagnostic tests 1: sensitivity and specificity. BMJ: British Medical Journal 308:1552.

Ballard, W. B., J. S. Whitman, and C. L. Gardner. 1987. Ecology of an exploited wolf population in south-central Alaska. Wildlife Monographs 98:3-54.

Beyer, D. E., Jr., R. O. Peterson, J. A. Vucetich, and J. H. Hammill. 2009. Wolf population changes in Michigan. Pages 65-85 in A. P. Wydeven, T. R. Van Deelen, and E. J. Heske, editors. Recovery of Gray Wolves in the Great Lakes Region of the United States: An Endangered Species Success Story. Springer.

Browne-Nunez, C., A. Treves, and D. MacFarland. 2012. Influence of official lethal control on illegal take, social tolerance, and subsequent depredations? The case of Wisconsin gray wolves (Canis lupus). . Available from http://www.nelson.wisc.edu/people/treves/wolves/wolfhuman.php. Accessed on 5 August 2012.

Bruskotter, J. T., and S. A. Enzler. 2009. Narrowing the definition of endangered species: implications of the US Government's interpretation of the phrase "A Significant Portion of its Range" under the endangered species act of 1973. Human Dimensions of Wildlife 14:73-88.

Bruskotter, J. T., J. A. Vucetich, S. Enzler, A. Treves, and M. P. Nelson. 2013. Removing protections for wolves and the future of the US Endangered Species Act (1973). Conservation Letters.

Crainiceanu, C. M., D. Ruppert, and M. P. Wand. 2007. Bayesian Analysis for Penalized Spline Regression Using Win BUGS.

Creel, S., and J. Rotella. 2010. Meta-Analysis of Relationships between Human Offtake, Total Mortality and Population Dynamics of Gray Wolves (Canis lupus). PLOS One 5:e12918.

Environmental Systems Research Institute. 2009. ArcGIS Desktop. Environmental Systems Research Institute, Redlands, CA.

Fritts, S. H., and L. D. Mech. 1981. Dynamics, movements, and feeding ecology of a newly protected wolf population in northwestern Minnesota. Wildlife Monographs 80:3-79.

Fuller, T. K., and L. B. Keith. 1980. Wolf population dynamics and prey relationships in northeastern Alberta. The Journal of Wildlife Management 44:583-602.

Fuller, T. K., L. D. Mech, and J. F. Cochrane. 2003. Wolf Population Dynamics. Pages 161 - 191 in L. D. Mech and L. Boitani, editors. Wolves: Behavior, Ecology, and Conservation. The University of Chicago Press, Chicago, Illinois.

Gotelli, N. J. 1995. A primer of ecology. Sinauer Associates Incorporated.

Gude, J. A., M. S. Mitchell, R. E. Russell, C. A. Sime, E. E. Bangs, L. D. Mech, and R. R. Ream. 2012. Wolf population dynamics in the US Northern Rocky Mountains are affected by recruitment and human- caused mortality. The Journal of Wildlife Management 76:108-118.

Heisey, D., and T. Fuller. 1985. Evaluation of survival and cause-specific mortality rates using telemetry data. Journal of Wildlife Management 49:668-674.

Heisey, D. M., and B. R. Patterson. 2006. A review of methods to estimate cause-specific mortality in presence of competing risks. Journal of Wildlife Management 70:1544-1555.

Heisey, D. M., T. L. Shaffer, and G. C. White. 2007. The ABCs of nest survival: theory and application from a biostatistical perspective. Studies in Avian Biology:13-33.

Klein, J. P., and M. L. Moeschberger. 2003. Survival analysis: statistical methods for censored and truncated data. Springer-Verlag, New York, NY.

Lebreton, J. D. 2005. Dynamical and statistical models for exploited populations. Australian & New Zealand Journal of Statistics 47:49-63.

Leung, K.-M., R. M. Elashoff, and A. A. Afifi. 1997. Censoring issues in survival analysis. Annual review of public health 18:83-104.

Liberg, O., G. Chapron, P. Wabakken, H. C. Pedersen, N. T. Hobbs, and H. Sand. 2012. Shoot, shovel and shut up: cryptic poaching slows restoration of a large carnivore in Europe. Proceedings of the Royal Society B: Biological Sciences 279:910-915.

Mech, L. 1977. Productivity, mortality, and population trends of wolves in northeastern Minnesota. Journal of Mammalogy 58:559-574.

Mech, L. D. 2001. Managing Minnesota's recovered wolves. Wildlife Society Bulletin 29:70-77.

Mech, L. D., L. G. Adams, T. J. Meier, J. W. Burch, and B. W. Dale. 1998. The Wolves of Denali. University of Minnesota Press, Minneapolis, Minnesota.

Mladenoff, D., T. Sickley, R. Haight, and A. Wydeven. 1995. A regional landscape analysis and prediction of favorable gray wolf habitat in the norther Great Lakes region. Conservation Biology 9:279-294.

Mladenoff, D., T. Sickley, and A. Wydeven. 1999. Predicting gray wolf landscape recolonization: Logistic regression models vs. new field data. Ecological Applications 9:37-44.

Mladenoff, D. J., M. K. Clayton, S. D. Pratt, T. A. Sickley, and A. P. Wydeven. 2009. Change in occupied wolf habitat in the northern Great Lakes region. Pages 119-138 in A. P. Wydeven, T. R. Van Deelen, and E. J. Heske, editors. Recovery of Gray wolves in the Great Lakes region of the United States: An Endangered Species Success Story. Springer, New York, NY, USA.

Olson, E. R. 2013. As a wolf: A Wisconsin case-study of wolf-human conflict and predator-prey ecology. Doctoral Dissertation. University of Wisconsin - Madison, Madison, WI.

Plummer, M. 2003. JAGS: A program for analysis of Bayesian graphical models using Gibbs sampling. Pages 20-22.

Plummer, M. 2011. rjags: Bayesian graphical models using MCMC. R package version 3-5.

Pollock, K., S. Winterstein, C. Bunck, and P. Curtis. 1989. Survival analysis in telemetry studies - The staggered entry design. Journal of Wildlife Management 53:7-15.

Pulliam, H. R., and B. J. Danielson. 1991. Sources, sinks, and habitat selection: a landscape perspective on population dynamics. American Naturalist:S50-S66.

R developement Core Team. 2013. R: A language and environment for statistical computing. R Foundation for Statistical Computing, Vienna, Austria.

Refsnider, R. L. 2009. The role of the endangered species act in midwest wolf recovery. Pages 311-329 in A. P. Wydeven, T. R. Van Deelen, and E. J. Heske, editors. Recovery of Gray Wolves in the Great Lakes Region of the United States: An Endangered Species Success Story. Springer.

Ruppert, D., M. P. Wand, and R. J. Carroll. 2003. Semiparametric regression. Cambridge University Press.

Spencer, J. S., W. B. Smith, J. T. Hahn, and G. K. Raile. 1988. Wisconsin's fourth forest inventory, 1983. Resource Bulletin NC-107. St. Paul, MN: U.S. Dept. of Agriculture, Forest Service, North Central Forest Experiment Station.

Speybroeck, N., B. Devleesschauwer, L. Joseph, and D. Berkvens. 2013. Misclassification errors in prevalence estimation: Bayesian handling with care. Int J Public Health 58:791-795.

Taylor, M. F. J., K. F. Suckling, and J. J. Rachlinski. 2005. The effectiveness of the Endangered Species Act: a quantitative analysis. BioScience 55:360-367.

Thiel, R. P., W. Hall Jr, E. Heillhecker, and A. P. Wydeven. 2009. A disjunct gray wolf population in Central Wisconsin. Pages 107-117 in A. P. Wydeven, T. R. Van Deelen, and E. J. Heske, editors. Recovery of Gray Wolves in the Great Lakes Region of the United States: An Endangered Species Success Story. Springer, New York, NY, USA.

Treves, A., L. Naughton-Treves, and V. Shelley. 2013. Longitudinal Analysis of Attitudes Toward Wolves. Conservation Biology 27:315-323.

Triola, M. 2010. Elementary Statistics. 11 edition. Pearson Education.

Tsai, K., K. Pollock, and C. Brownie. 1999. Effects of violation of assumptions for survival analysis methods in radiotelemetry studies. Journal of Wildlife Management 63:1369-1375.

Van Deelen, T. R. 2009. Growth characteristics of a recovering wolf population in the Great Lakes region Pages 139-153 in A. P. Wydeven, T. R. Van Deelen, and E. J. Heske, editors. Recovery of Gray Wolves in the Great Lakes Region of the United States: An Endangered Species Success Story. Springer, New York, NY, USA.

Vucetich, J. A., and R. O. Peterson. 2004. The influence of top–down, bottom–up and abiotic factors on the moose (Alces alces) population of Isle Royale. Proceedings of the Royal Society of London. Series B: Biological Sciences 271:183-189.

Walter, S. D., and L. M. Irwig. 1988. Estimation of test error rates, disease prevalence and relative risk from misclassified data: a review. Journal of clinical epidemiology 41:923-937.

Williams, B. K., J. D. Nichols, and M. J. Conroy. 2002. Analysis and Management of Animal Populations: Modeling, Estimation, and Decision Making. Academic Press.

Wydeven, A. P., R. N. Schultz, and R. P. Thiel. 1995. Monitoring of a recovering gray wolf population in Wisconsin, 1979-1991. Pages 147-156 in L. N. Carbyn, S. H. Fritts, and D. R. Seip, editors. Ecology and Conservation of Wolves in a Changing World. Canadian Circumpolar Institute, Edmonton, Alberta.

Wydeven, A. P., J. E. Wiedenhoeft, R. N. Schultz, R. P. Thiel, R. L. Jurewicz, B. E. Kohn, and T. R. Van Deelen. 2009. History, population growth, and management of wolves in Wisconsin. Pages 87-105 in A. P. Wydeven, T. R. Van Deelen, and E. J. Heske, editors. Recovery of Gray Wolves in the Great Lakes Region of the United States: An Endangered Species Success Story. Springer, New York, NY, USA.

Table 1. Numbers of endpoints from five causes from adult and non-adult (yearlings and pups) wolves in summer (April – September) and winter (October – March) that were radio-collared and tracked in Wisconsin, USA from 1980 – 2013.

Age	Season	Unknown censoring	Known censoring	Illegal kills	Other human mortality	Other mortality
Adult	Summer	63	20	13	29	28
	Winter	71	44	49	18	52
Non-adult	Summer	8	3	2	1	6
	Winter	52	12	16	4	8
Total		194	79	80	52	94

Table 2. Mean (and 95% credible intervals) of posterior estimates with odds interpretation from a categorical model of the probabilities that an endpoint was from five causes for radio-collared wolves in Wisconsin, USA (1980 – 2013) relative to covariates season, age, and habitat quality. Baseline covariate values were: season = summer, age = adult (≥ 24 months), and habitat = mean habitat quality over all observations.

Logit[1]	Intercept	Non-adults	Winter	Habitat quality
p_K/p_U	0.817 (0.140 - 7.295)	0.535 (0.235 - 1.207)	1.073 (0.569 - 2.143)	1.180 (0.225 - 4.719)
p_I/p_U	**0.094 (0.020 - 0.576)**	0.549 (0.265 - 1.192)	**3.089 (1.493 - 7.042)**	0.469 (0.080 - 1.909)
p_H/p_U	0.385 (0.110 - 1.758)	0.339 (0.101 - 1.055)	**0.454 (0.207 - 0.985)**	**0.173 (0.028 - 0.694)**
p_O/p_U	0.583 (0.123 - 1.979)	**0.320 (0.148 - 0.680)**	1.301 (0.700 - 2.615)	2.018 (0.321 - 9.695)

Bold type indicates that the odds ratio does not overlap 0.
[1] endpoint cause: U = unknown censoring, K = known censoring, I = illegal kill, H = other human mortality, and O = other death.

Table 3. Means, standard deviations (SD), hazard ratios, and 95% credible intervals of hazard ratios from posterior estimates for parameters in a discrete monthly hazard model for the endpoint of wolves in Wisconsin, USA (1980 – 2013).

Parameter	Mean	SD	Hazard ratio	95% CI
Not adult	0.19	0.11	1.21	(0.97 – 1.50)
Winter	0.70	0.10	**2.01**	(1.66 – 2.47)
Habitat	-0.94	0.18	**0.39**	(0.27 – 0.56)

Bold type indicates that the hazard ratio does not overlap 0.

Table 4. Definitions of terms from cause-specific mortality analysis of Wisconsin's wolf population.

Term	Definition
Accurate classification	The true cause of endpoint. For some unknown censoring endpoints, the accurate classification may actually be a mortality endpoint.
Augmented model	The model that includes auxiliary data to inform the misclassification parameters.
Auxiliary data	Population count data that is used to make the misclassification parameters identifiable.
Cause-specific endpoint hazard	The probability of experiencing an endpoint from one of five causes in some month.
Cause-specific mortality hazard	The probability of experiencing a mortality endpoint from one of three mortality causes in some month.
Endpoint	The last location record for a radio-collared wolf.
Error-prone classification	The cause of endpoint that was observed. The error-prone classification pertains to the unknown censoring cause of endpoint.
Hazard	The probability of experiencing an endpoint in some month.
Illegal kill	Cause of endpoint from mortality due to illegal shooting, trapping, or poisoning.
Known censoring	Cause of endpoint from surviving until the end of study or loss-to-follow-up during the study and found dead sometime after its endpoint.
Other death	Cause of endpoint from mortality due to other causes, including disease, intraspecific strife, and unknown causes.
Other human mortality	Cause of endpoint from mortality due to human causes besides illegal killing, including vehicle collision, lethal control action, and harvest.
Overall endpoint hazard	The probability of experiencing an endpoint in some month.
Overall mortality hazard	The probability of experiencing a mortality endpoint in some month.
Unaugmented model	The model that does not include auxiliary data.
Unknown censoring	Cause of endpoint from censoring due to loss-to-follow-up from unknown causes. The cause of endpoint category with possible misclassification.

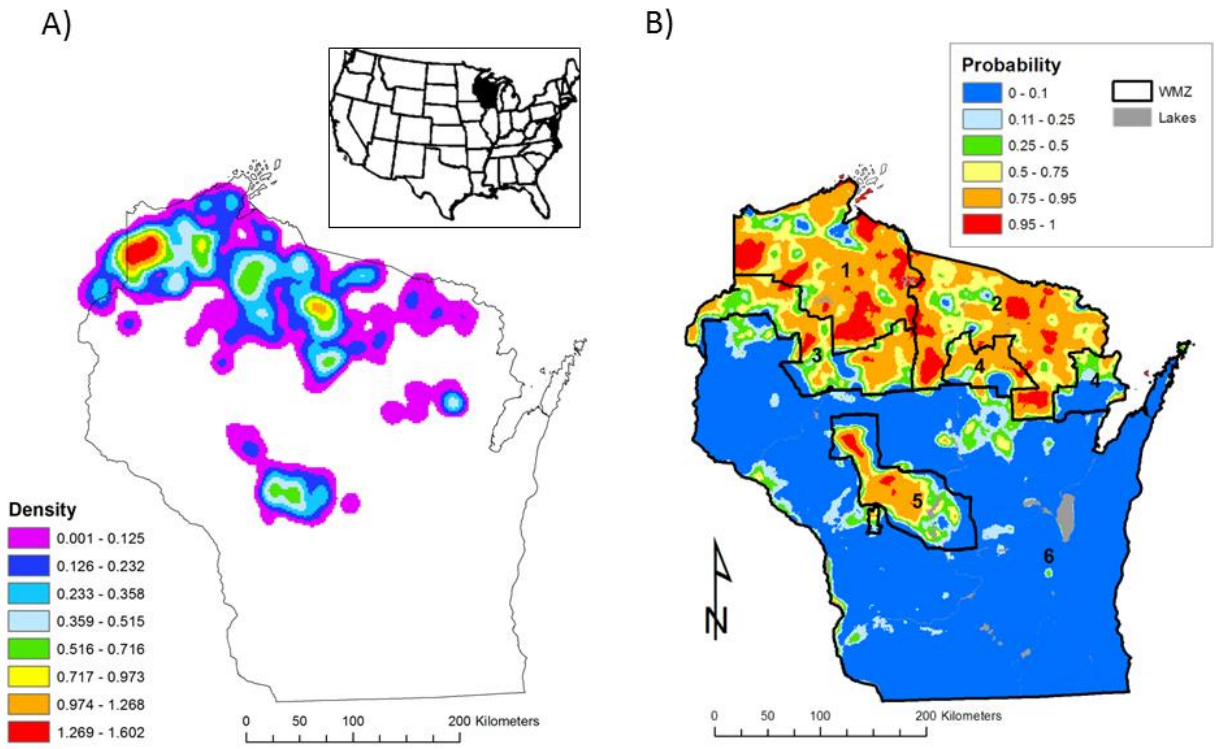

Figure 1. Maps of Wisconsin, USA showing: A) kernel density of radio-collared wolf locations (1980 – 2013), and B) habitat quality class probability from Mladenoff et al. (2009) with six wolf harvest zones (WHZ) labeled as 1 – 6 that was used as the habitat quality covariate in the model.

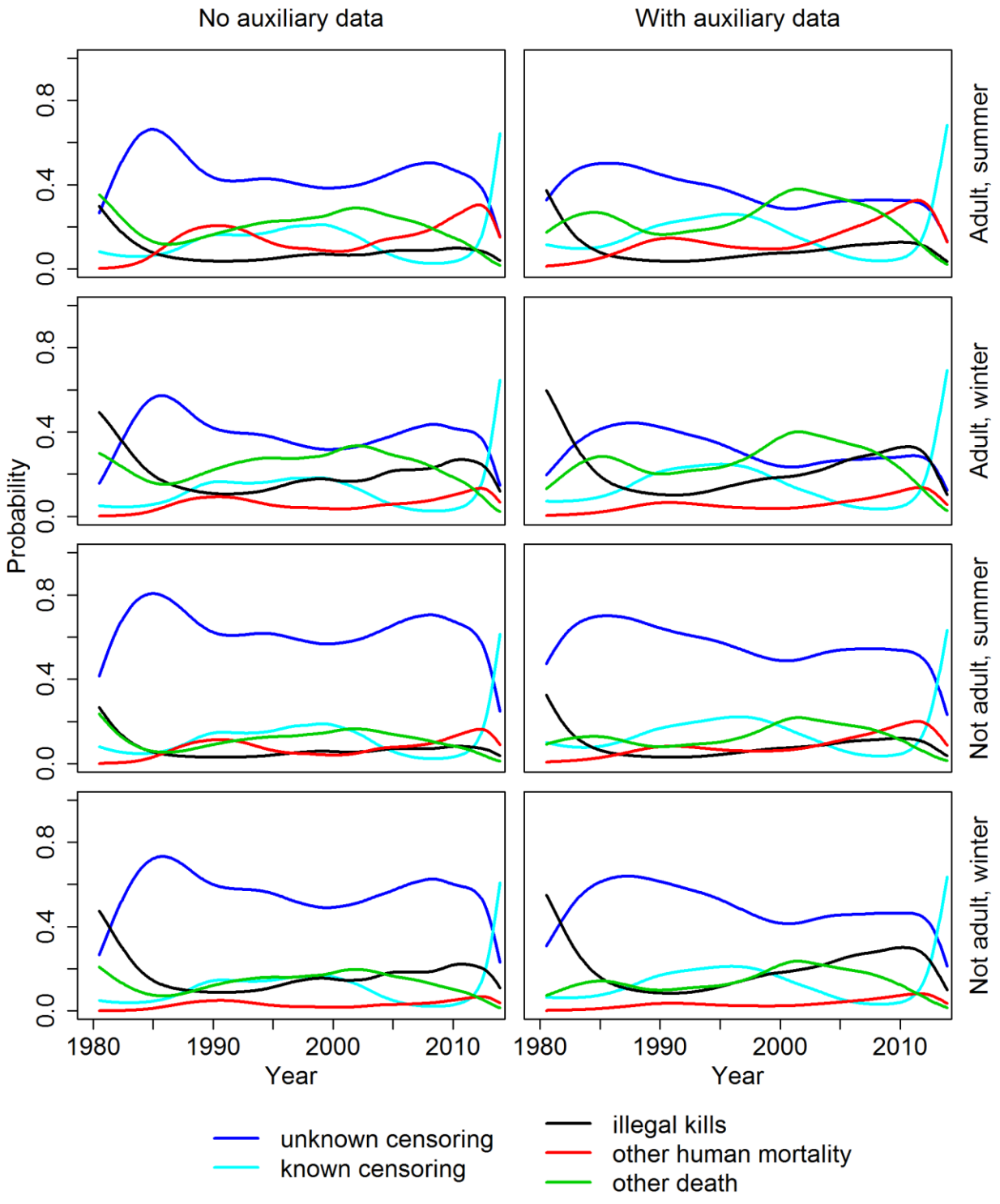

Figure 2. The estimated observed probabilities of endpoints from five different causes for adult and not adult wolves (i.e., yearlings and pups) in summer (April – September) and winter (October – March) from 1980 – 2013 in Wisconsin, USA, modeled from radio-collared data alone and when modeled using auxiliary data from the annual population counts.

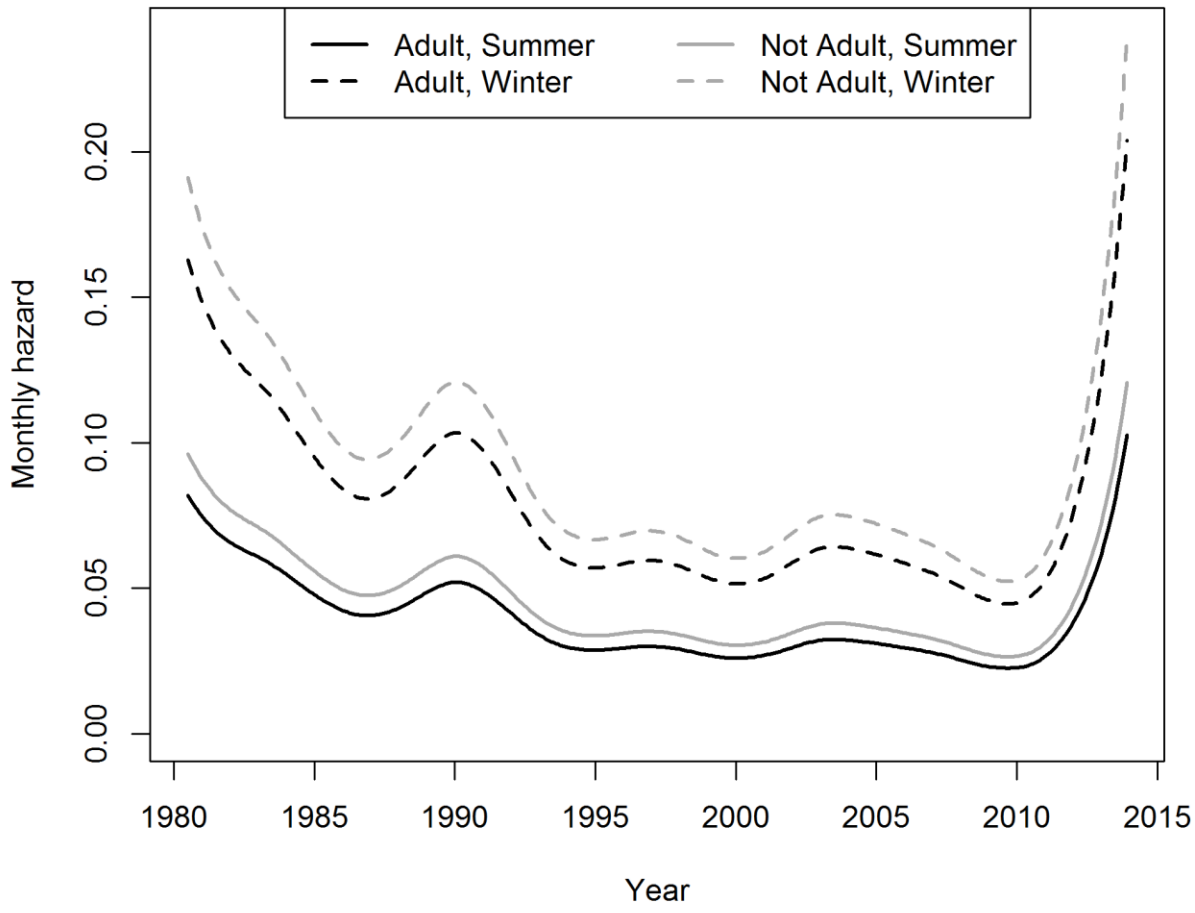

Figure 3. Monthly hazard for endpoints for adult and non-adult (yearlings and pups) radio-collared wolves in summer (April – September) and winter (October – March) in Wisconsin, USA (1980 – 2013).

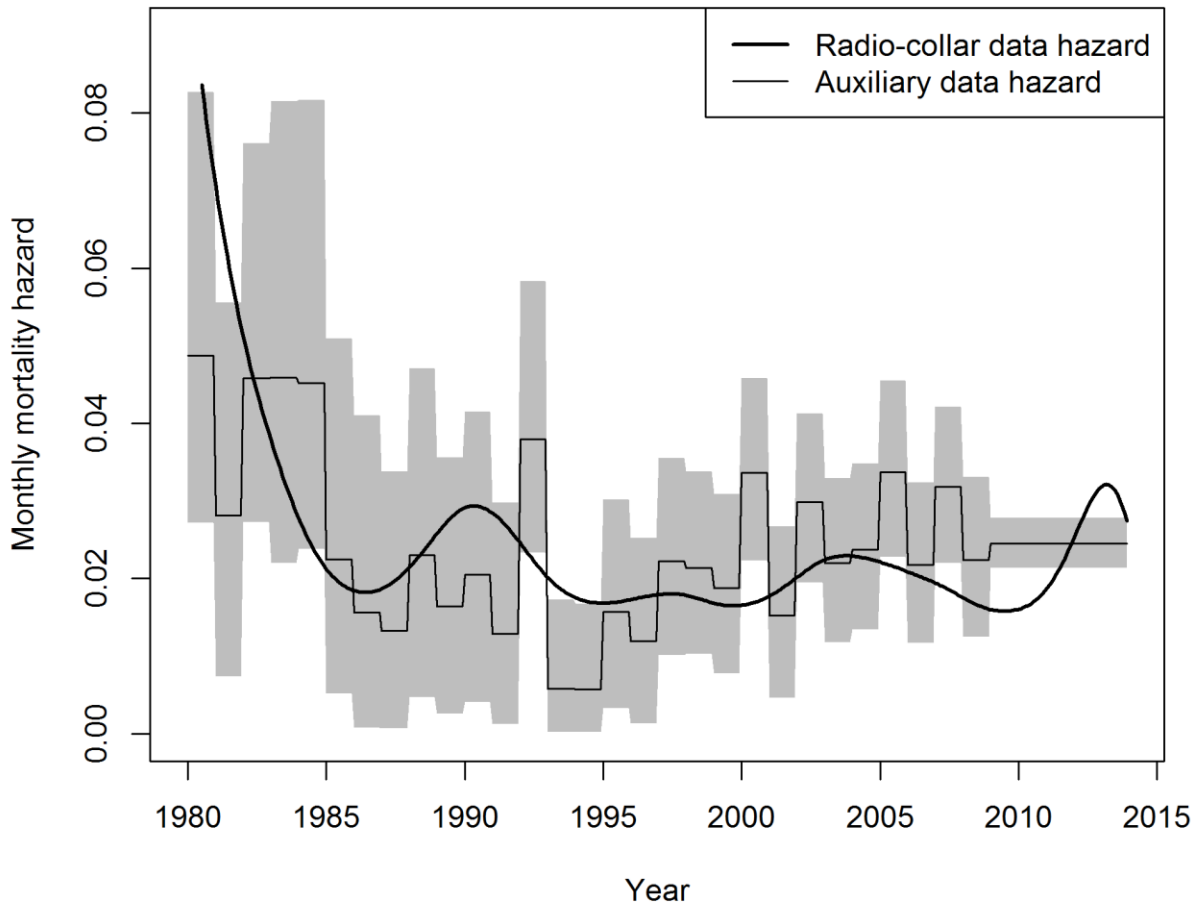

Figure 4. Mean monthly mortality hazards from observed mortality events from radio-telemetry data (thick black line) and from population counts (thin black line) with a 95% credible interval (gray polygon) for the Wisconsin wolf population (1980 – 2013).

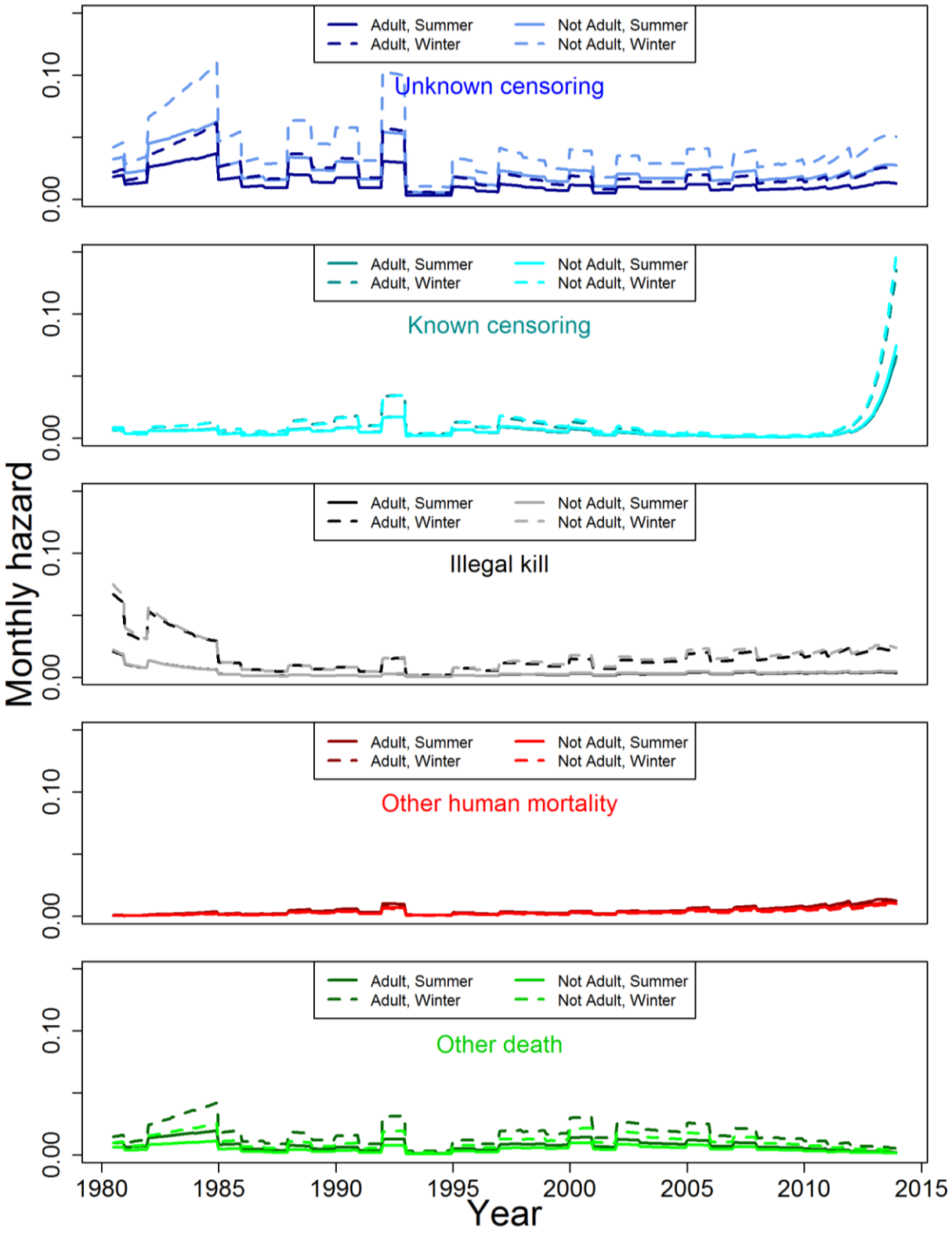

Figure 5. Cause-specific discrete monthly hazards for five enpoint causes for adult and non-adult (yearlings, pups) wolves in summer (April – September) and winter (October – March) in Wisconsin, USA (1980 – 2013).

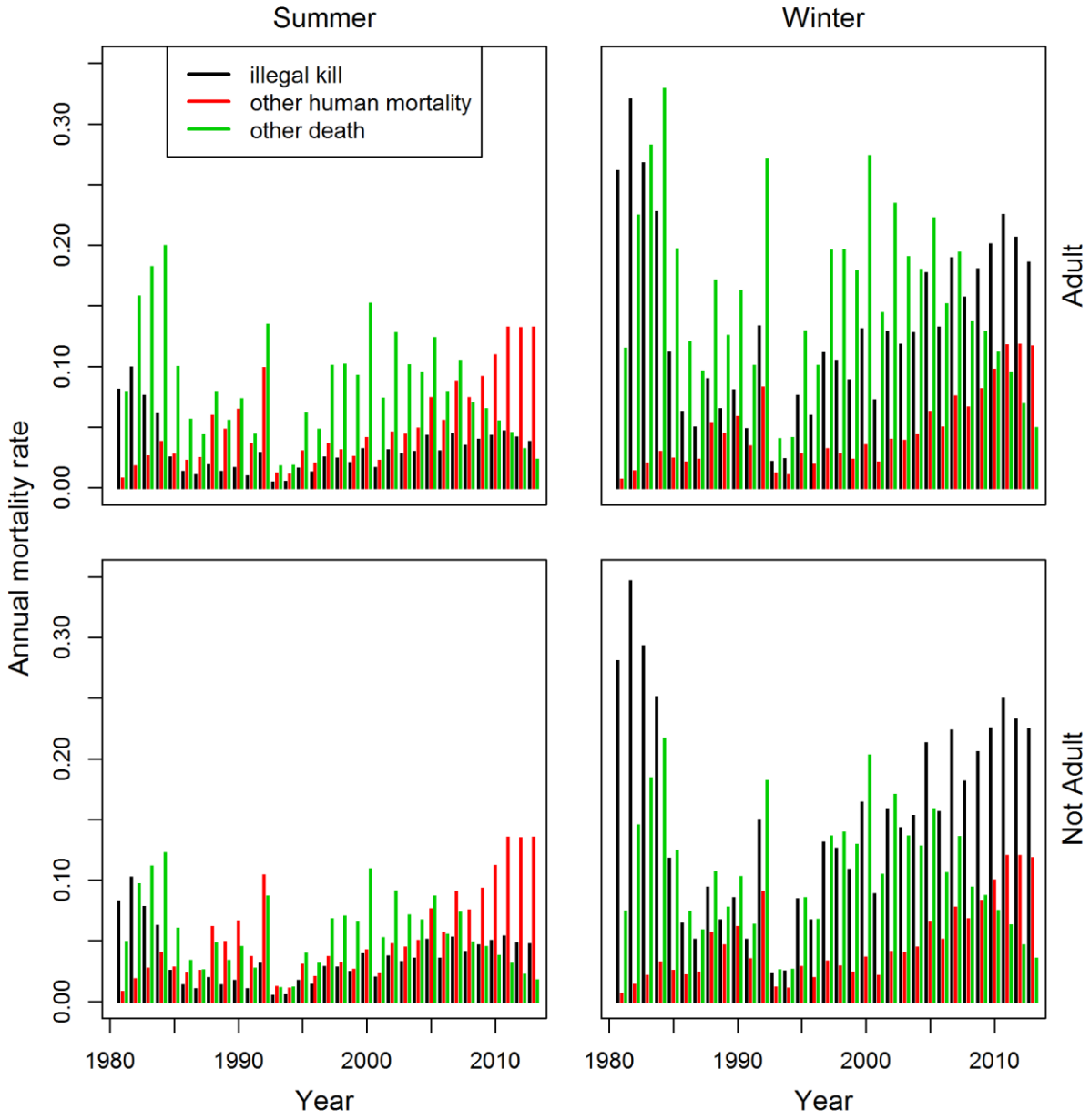

Figure 6. Estimated annual cause-specific mortality rates for adult and non-adult (i.e., yearlings and pups) wolves in summer (April – September) and winter (October – March) in Wisconsin, USA (1980 – 2013).

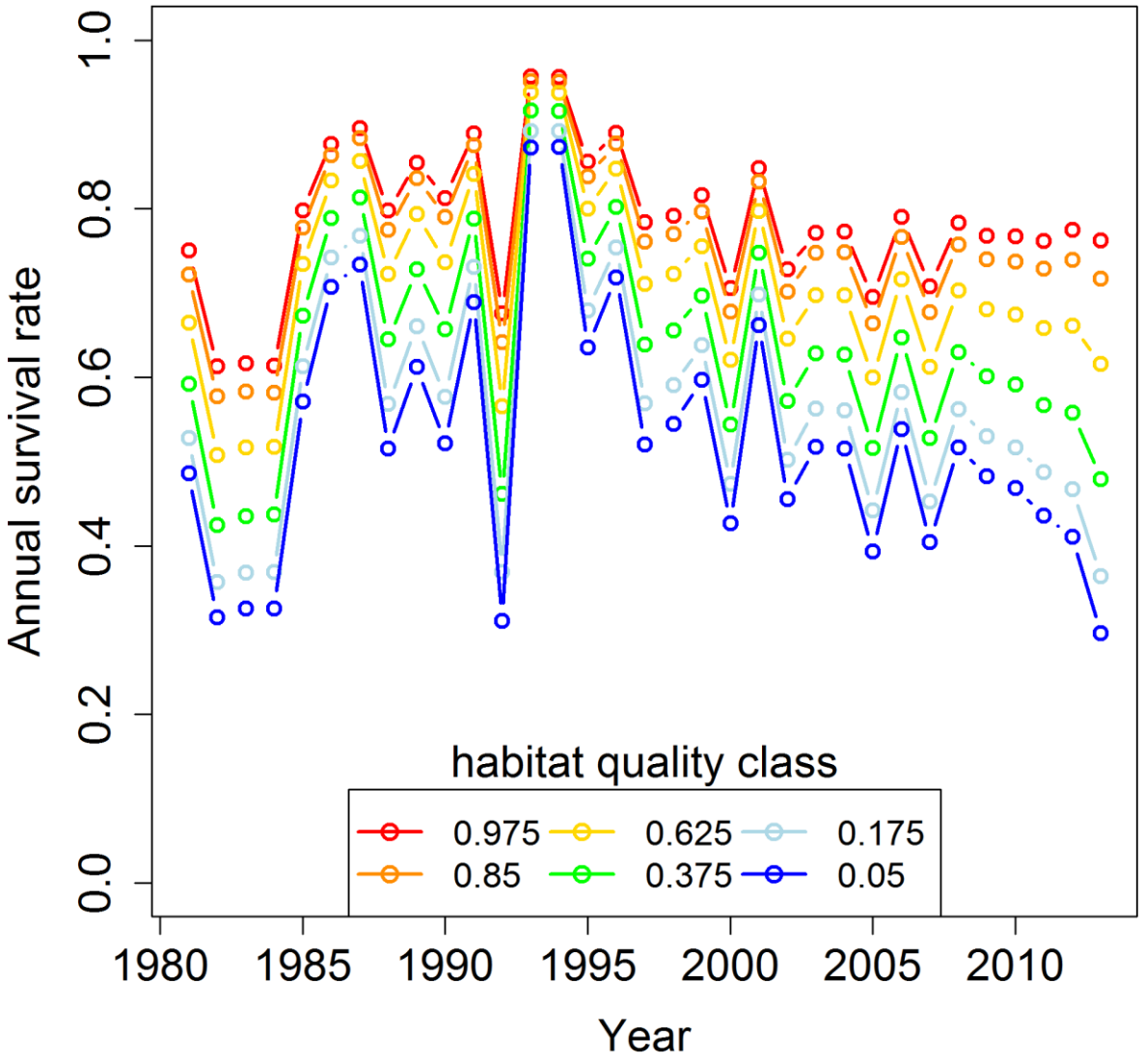

Figure 7. Predicted annual survival rates for adult radio-collared wolves (1981 – 2013) in Wisconsin, USA for each habitat quality class from Mladenoff et al. (2009).

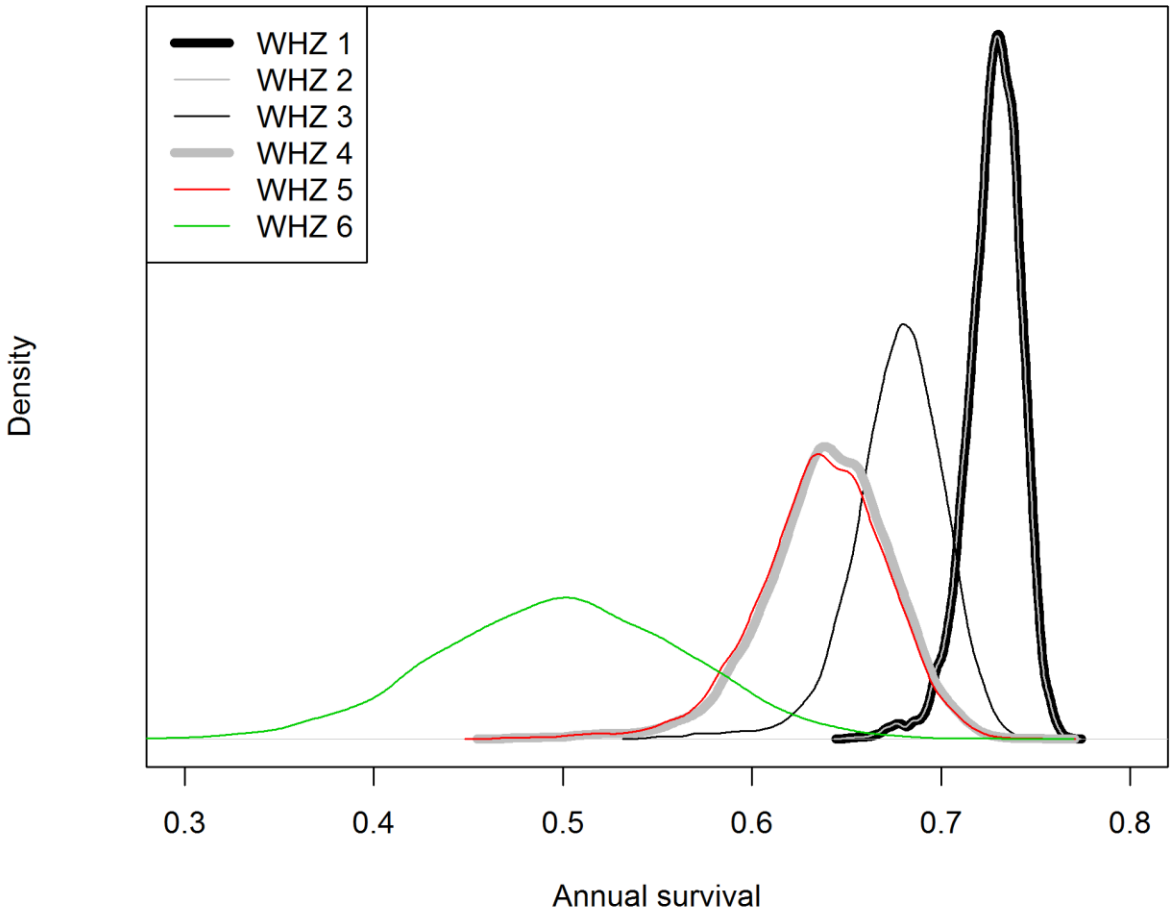

Figure 8. Estimated average annual survival for radio-collared wolves in each wolf harvest zone (WHZ) based on the average habitat quality in each WHZ in Wisconsin, USA.

Appendix A. Population count model for auxiliary monthly hazard data.

We estimated annual survival rate, s_g, from wolf population count data collected by WDNR (1980 – 2009; Wydeven et al. 2009). Our data comprised a time series of annual population counts, $Nobs_g$, and annual estimates of new recruits, $Robs_g$, for year g with $g = 1, 2, \ldots, G$ and G was the total number of years (Fig. A.1, Fig. A.2).

We took the mean of the range in population counts in year g as $Nobs_g$. We assumed that the range in counts each year represented a 95% confidence interval for counts and therefore calculated measurement error as ¼ the difference between the high and low count and took the average among the years as v (i.e., "range rule"; Triola 2010). We modeled the population count, $Nobs_g$, in a given year g using a log-normal distribution. That is, $Nobs_g \sim lognormal(\pi_g, v^2)$, where π_g was the true population size in year g and v was the standard deviation, both on the log scale (Liberg et al. 2012).

We took the mean in the range of the count for the number of new recruits each year as $Robs_g$. We assumed the annual average count of new recruits $Robs_{g+1}$ born into the population and counted on January 1 of year $g + 1$ was represented by a binomial distribution $Robs_{g+1} \sim binomial(Nobs_g, \rho_g)$ with recruitment rate, ρ_g, from the population count in year g, $Nobs_g$, where ρ_g was the true proportion of new recruits that were born into the population and survived until the annual count of $Robs_{g+1}$ for $g = 1,2, \ldots, G-1$ (Fig. A.1). In the normal approximation to the binomial, we modeled $Robs_{g+1} \sim normal(\pi_{R,g+1}, v^2_{R,g+1})$, where $\pi_{R,g+1} = Nobs_g \times \rho_g$ and $v_{R,g+1} = (Nobs_g \times \rho_g \times (1 - \rho_g))^{1/2}$ were the mean and standard deviation of the normal distribution. We let $\rho_g \sim beta(1,1)$ which was equivalent to a $uniform(0,1)$ distribution and both were vague priors on the rate ρ_g.

In the lognormal model for the population counts, we assumed that the mean process, π_{g+1}, was equal to the log of the population count $Nobs_g$ in the previous year g multiplied by the sum of a recruitment rate (ρ_g) and a survival rate (s_g): $\pi_{g+1} = \log(Nobs_g \times (\rho_g + s_g))$ for $g = 1,2, \dots, G-1$. We assumed a closed population where the immigration rate and emigration rate sum to zero and are not included (Gotelli 1995). Annual survival rate s_g was given a vague, uniform prior: $s_g \sim uniform(0,1)$. For years 2010 – 2013 when recruitment data were not collected, we took the average annual survival rate from the previous years: $\bar{s} = \frac{\sum_{g=1}^{G} s_g}{G}$.

We transformed the annual survival rate into a monthly discrete hazard rate, $h_{aux,g}$, where $h_{aux,g} = -\log(s_g)/12$ (Klein and Moeschberger 2003). We replicated each $h_{aux,g}$ twelve times to represent months and created a vector $h(t)_{aux}$ where t indexed month and $t = 1, 2, \dots, T$ and T is the total number of months. The vector $h(t)_{aux}$ was used as auxiliary data in the wolf survival model. We used a Gibbs sampler from program JAGS (Plummer 2003) with the package 'rjags' (Plummer 2011) in program R (R developement Core Team 2013) to sample the posteriors of s_g. We ran multiple chains for 10,000 iterations of burn-in, and an additional 10,000 to sample the posteriors.

From our population count model, annual recruitment rate ranged from 0.218 – 0.600 with an average annual recruitment rate of 0.376 (Fig. A.3). Annual survival rate ranged from 0.565 – 0.935 with an average annual survival rate of 0.756. Both recruitment and survival were more variable and less precise during 1980 – 1992 compared to the years since 1992 (Fig. A.3). Monthly discrete hazard rates ranged from 0.006 – 0.049, and average monthly discrete hazard was 0.025.

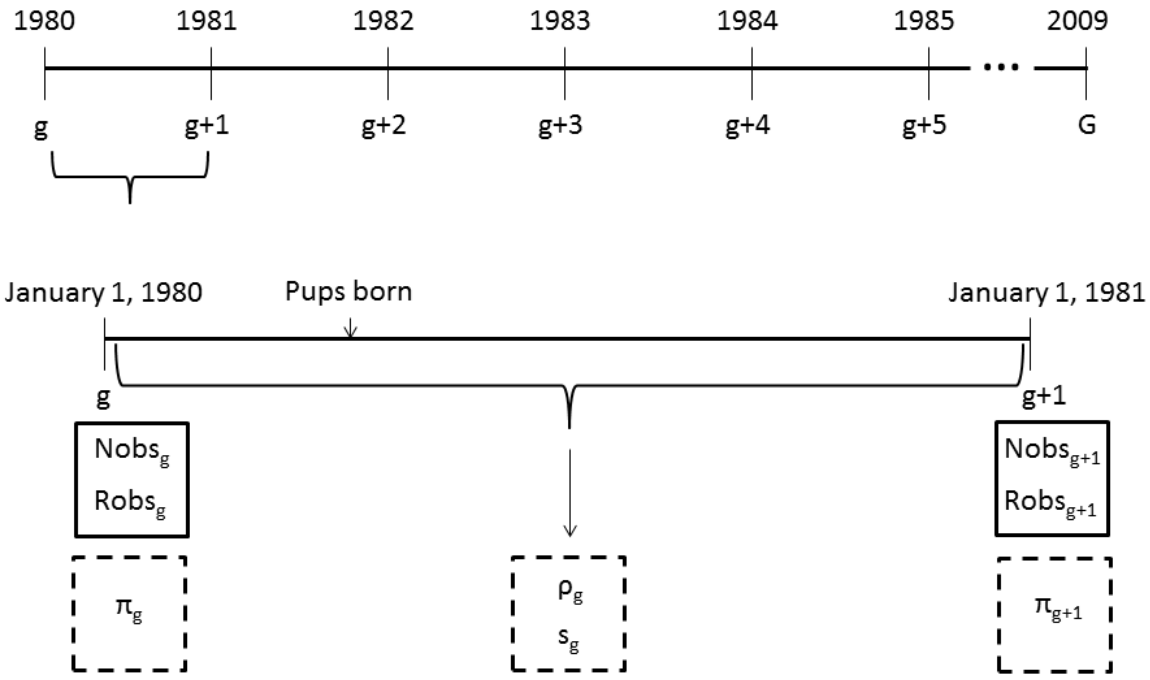

Figure A.1. Timeline of data collection (solid boxes) for wolf population counts ($Nobs$) and wolf pup counts ($Robs$) for year g that were used in a population count model to estimate the true annual population size π, annual recruitment rate ρ, and annual survival rate s for year g.

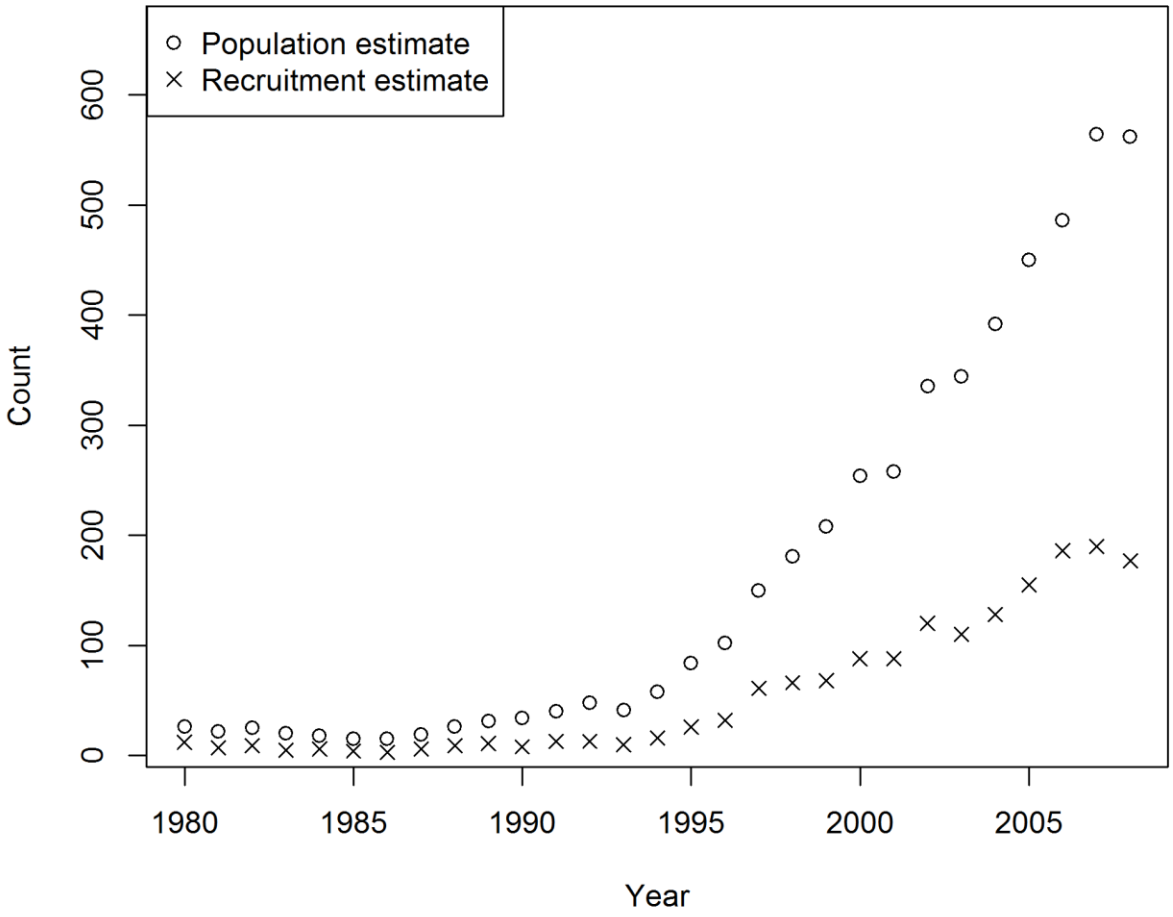

Figure A.2. Annual estimated wolf population size and number of wolf pups (recruitment) in 1980 – 2009 in Wisconsin, USA (Wydeven et al. 2009).

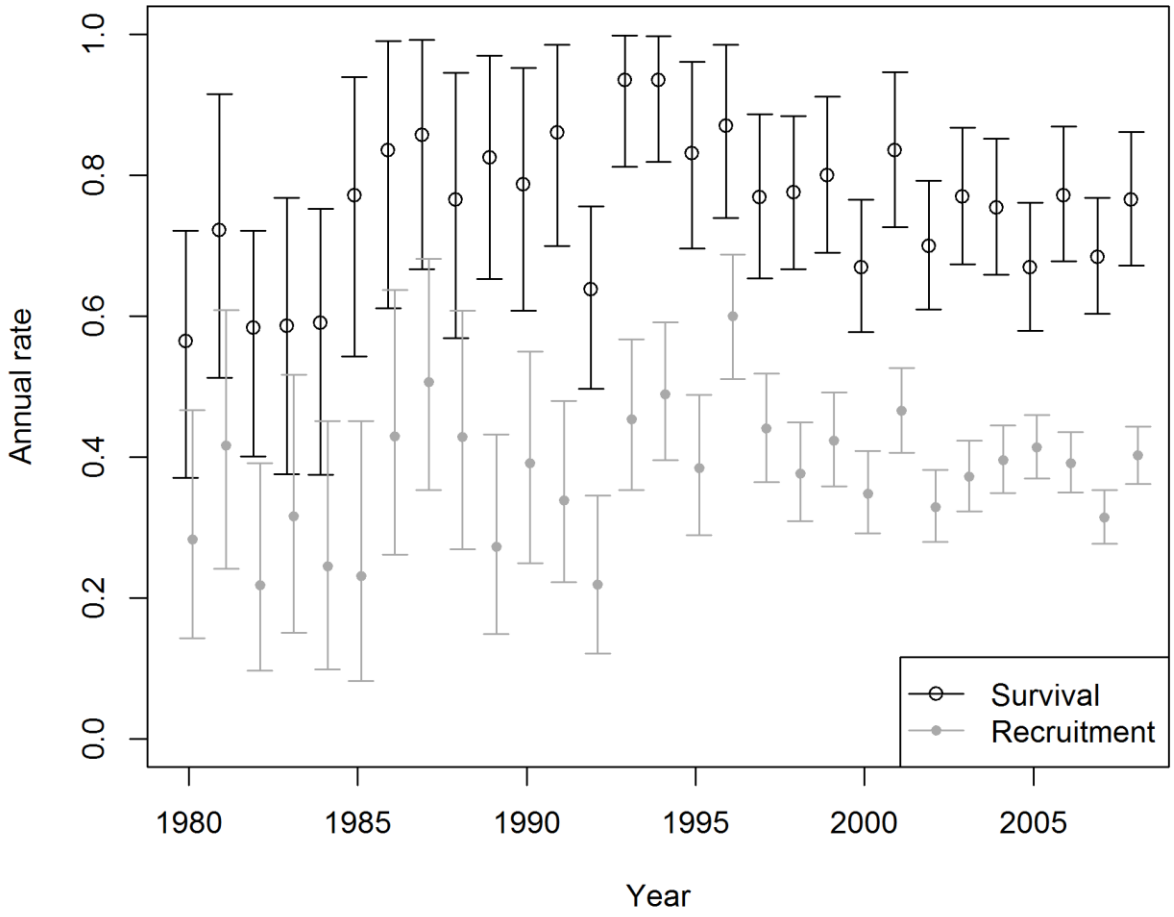

Figure A.3. Posterior means and 95% credible intervals of annual survival and recruitment rates from a population count model of wolves in Wisconsin, USA (1980 – 2009).

Appendix B. Approach to incorporating misclassification in endpoint causes and the relationship to sensitivity and specificity.

We took a generalized sensitivity and specificity approach to estimate misclassification for causes of the endpoints for radio-collared wolves. In this appendix, we give some background on sensitivity and specificity, its application to our study, and work through some examples for interpretation of estimated parameters.

In the medical field, sensitivity and specificity are statistics that can help doctors understand performance of binary diagnostic tests with respect to the true status of infection or disease (Altman and Bland 1994). More generally, sensitivity and specificity are statistical quantities that measure the performance of a classification test. We will first use a disease diagnosis as an example to illustrate notation and structure of a simple classification test. We let D represent the true disease status such that $D = 1$ is disease and $D = 0$ is healthy. We let Y represent the observed and potentially error-prone test for the disease such that $Y = 1$ is a positive test result and $Y = 0$ is a negative test result for the disease. There are four possible outcomes in the classification test (Fig. B.1):

1. True positives$(Y = 1, D = 1)$. True positives occur when there is a positive test for the disease and the disease is actually present. True positives are the numerator in the statistic for test sensitivity.
2. False positives$(Y = 1, D = 0)$. False positives occur when there is a positive test for the disease and the disease is actually absent.
3. False negatives$(Y = 0, D = 1)$. False negatives occur when there is a negative test for the disease and the disease is actually present.

4. True negatives($Y = 0, D = 0$). True negatives occur when there is a negative test for the disease and the disease is actually absent. True negatives are the numerator in the estimate for test specificity.

From these outcomes, we can calculate test sensitivity and specificity. Sensitivity ($P(Y = 1|D = 1)$) is the proportion of diseased individuals that are correctly identified as diseased by the diagnostic test: $sensitivity = \frac{true\ positives}{true\ positives + false\ negatives}$, and specificity ($P(Y = 0|D = 0)$) is the proportion of healthy individuals that are correctly identified as not diseased by the diagnostic test: $specificity = \frac{true\ negatives}{false\ positives + true\ negatives}$ (Altman and Bland 1994, Speybroeck et al. 2013). A perfect test would be completely sensitive and specific ($sensitivity = specificity = 1$).

Now that we set the stage with a disease example, we transition into an example of classification that is relevant in our study of endpoints for wolves. We define the endpoint categories of death and not death (i.e. censored). With the same notation, we define the true endpoint status such that $D = 1$ was a true death and $D = 0$ was definitely not a death. We let Y represent the observed and potentially error-prone categorization of the endpoint such that $Y = 1$ was an endpoint observed as death and $Y = 0$ was an endpoint not observed as death. In this case, we will not have observations in all of the 4 categories (Fig. B.2). We fixed the false positives to 0 because there was no situation where a wolf that was truly censored (and definitely not dead) would actually be categorized as dead. Therefore, all wolves that were actually censored were observed as censored and $specificity = \frac{true\ negatives}{0 + true\ negatives} = 1$. The false negatives were the true dead wolves that were observed as censored, and this category was our primary interest. We defined the parameter φ as the probability that a wolf that was actually

dead was observed as censored ($P(Y = 0|D = 1)$). The more common test sensitivity was then $1 - \varphi$.

In our study, we defined five endpoint categories and therefore extended the binary classification into a 5×5 classification matrix (Fig. B.3). However, we made assumptions about many of the classification categories and kept a single parameter φ. We labeled our causes for the endpoint as 1 = unknown censoring, 2 = known censoring, 3 = illegal kill, 4 = other human mortality, and 5 = other mortality. We present the classification matrix cells as proportions of the total number of true events from each cause, and each row summed to 1. We assumed that all true censoring events (both known and unknown censoring) were observed as censoring events ($P(Y = 1|D = 1) = 1$ and $P(Y = 2|D = 2) = 1$). We treated all of the true known mortality causes($D = 1,2,3$) as a single category because we were not able to differentiate which of the true known mortality causes were misclassified. In other words, we assumed that all true known mortality causes had the same proportion of misclassification. Next, we assumed that misclassification only occurred because true known mortality causes were observed as unknown censoring (i.e., wolves that disappear from follow-up). We let φ be the probability that we observed unknown censoring given that the event was actually a known mortality cause ($P(Y = 1|D = 3) = P(Y = 1|D = 4) = P(Y = 1|D = 5) = \varphi$). Finally, $1 - \varphi$ was the probability of observing a known mortality cause given that the event was actually that known mortality cause ($P(Y = 3|D = 3) = P(Y = 4|D = 4) = P(Y = 5|D = 5) = 1 - \varphi$).

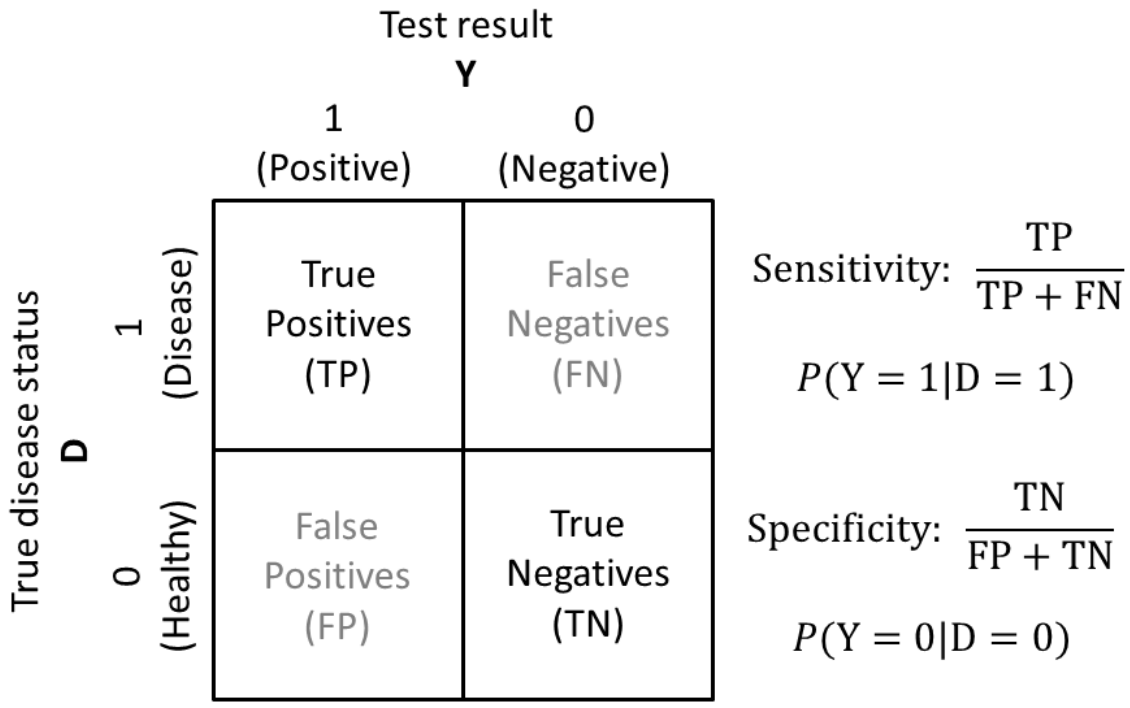

Figure B.1. Diagram of sensitivity and specificity estimates from a binary diagnostic test.

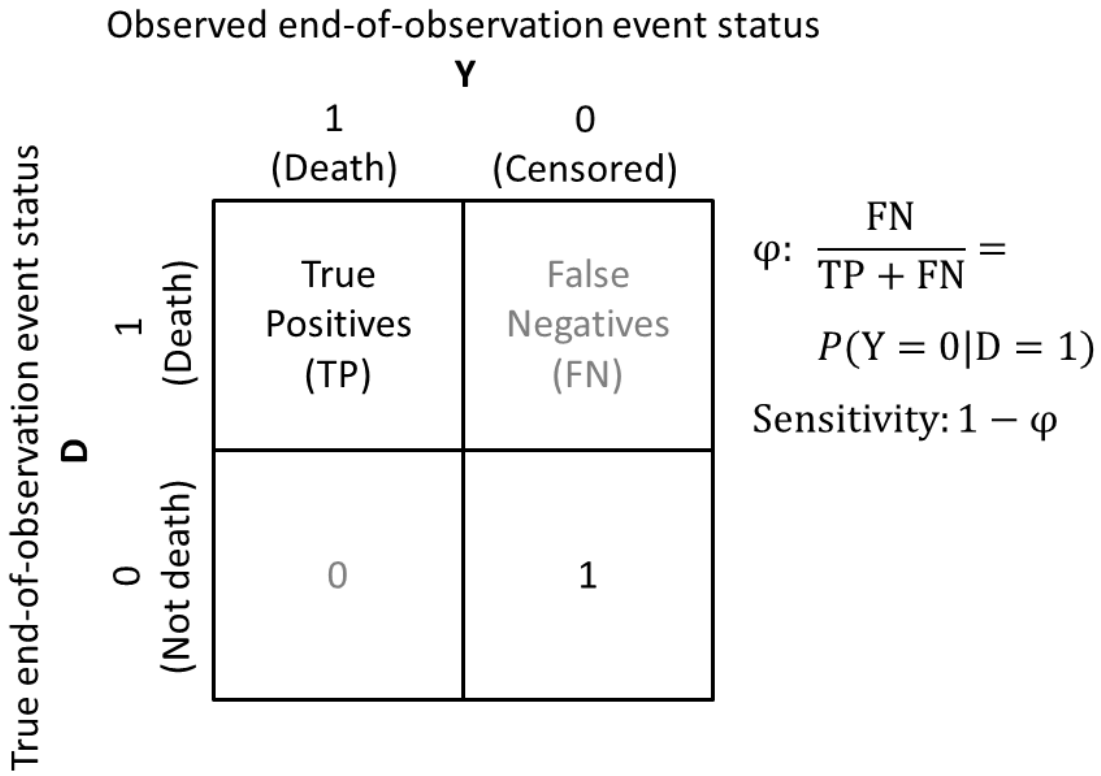

Figure B.2. Diagram of generalized sensitivity and specificity estimates for a misclassification problem of wolf endpoints due death or censoring.

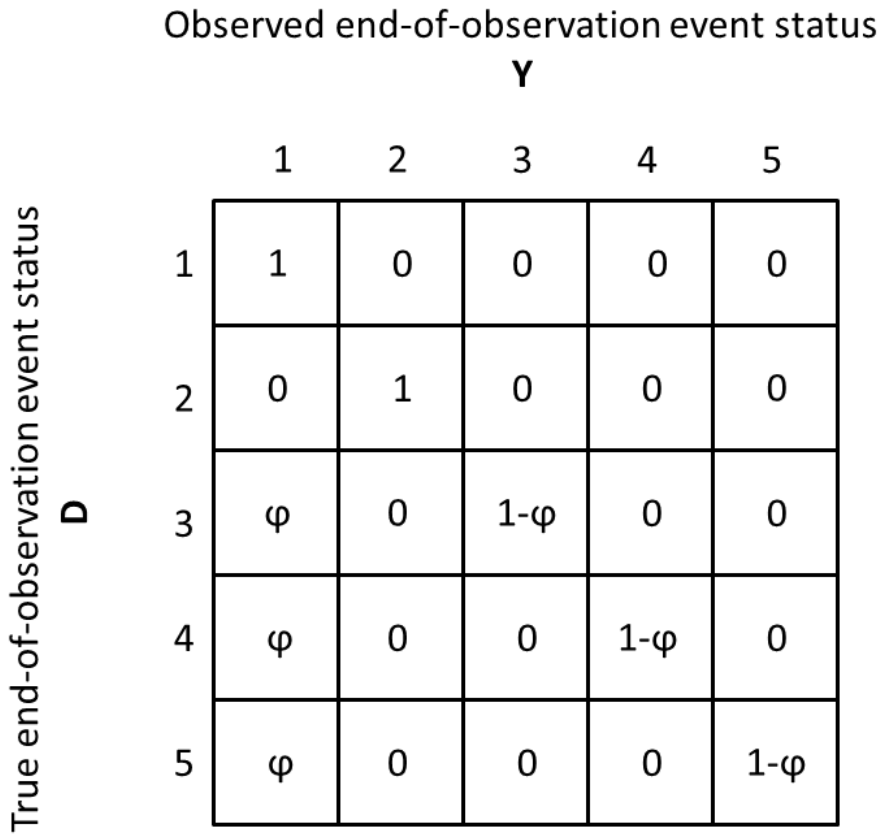

Figure B.3. Generalized sensitivity and specificity matrix relating the classification of observed death status from 5 causes compared to actual death status from 5 causes for wolves in Wisconsin, USA.

Appendix C. Low-rank thin-plate splines to model a smooth function for time.

We used a nonparametric function for time to capture how both cause-specific endpoint probabilities and monthly hazards changed in time. By using a spline for time, we let the data choose the shape of each function with respect to time instead of specifying a functional shape for time through a parametric model. We chose to use penalized splines, specifically low-rank thin-plate splines because of their good mixing properties in the Markov Chain Monte Carlo chains of a Bayesian analysis (Ruppert et al. 2003, Crainiceanu et al. 2007). For the notation and implementation of low-rank thin-plate splines in our analysis, we relied heavily on the methods, notation, and R code from Crainiceanu et al. (2007). Implementation of the spline is very similar in the probability and hazard pieces of our model, but we present them both because they have different dimensions and notation.

Hazard function

The linear predictor for the hazard function was: $\text{cloglog}(\mu_i) = \gamma + \omega_g + X_{i,q}\beta_q + Z_{i,k}b_k$. The $Z_{i,k}b_k$ portion of the linear predictor for observation i is where a smooth function of time was incorporated into the discrete hazard function by way of a low-rank thin-plate spline (Ruppert et al. 2003, Crainiceanu et al. 2007). We chose a number of knots, k with $k = 1, \dots, K$ and K is the total number of knots. We chose to use 20 knots ($K = 20$) to ensure that there was enough flexibility without having too many parameters to estimate in the spline. We let the covariate $X_{i,1}$ represent time for observation i, and we let κ_k represent the sample quantile of $X_{i,1}$ corresponding to the $\frac{k}{1+K}$ probability. Next, we calculated $\boldsymbol{Z}_K$ which was a $N\ x\ K$ matrix with row i equal to the cube of the absolute difference between the time at location i, $X_{i,1}$, and κ_k: $\boldsymbol{Z}_K = \{|X_{i,1} - \kappa_1|^3, |X_{i,1} - \kappa_2|^3, \dots, |X_{i,1} - \kappa_K|^3\}$. We defined a new matrix $\boldsymbol{\Omega}_K$ to have dimensions $Kx\ K$ and let row k be the cube of the absolute difference in time between each

knot, κ_k: $\Omega_{Kk} = \{|\kappa_k - \kappa_1|^3, |\kappa_k - \kappa_2|^3, \ldots, |\kappa_k - \kappa_K|^3\}$. . Next, we let $\boldsymbol{Z} = \boldsymbol{Z}_K\boldsymbol{\Omega}_K^{-1/2}$ so that the matrix Ω_K penalized the coefficients of $\left|X_{i,1} - \kappa_k\right|^3$ in the matrix multiplication and resulted in $N\ x\ K$ matrix $\boldsymbol{Z}$. We defined a new vector $\boldsymbol{b}$ of length K to be vague, random normal variables with mean equal to 0 and standard deviation equal to $\tau^{-1/2}$ and $\tau \sim gamma(0.001, 0.001)$. We let $\boldsymbol{b} = \boldsymbol{\Omega}_K^{1/2}\boldsymbol{u}$ where $\boldsymbol{u}$ is a vector of random parameters of length K, $\boldsymbol{u} = (u_1, u_2, \ldots, u_K)^{\mathrm{T}}$.

Cause-specific endpoint probabilities

In the cause-specific endpoint probability portion of the model, the linear predictor was $\varepsilon_{m,l} = D_{m,r}\alpha_{r,l} + Y_{m,k}a_{k,l}$. The $Y_{m,k}a_{k,l}$ portion of the linear predictor for observation m is where we incorporated a smooth function of time into the cause-specific endpoint probabilities with the spline. We let the covariate $D_{m,2}$ represent time for observation m. We chose a number of knots, k with $k = 1, \ldots, K$ and K is the total number of knots, and we let ς_k represent the sample quantile of $d_{m,2}$ corresponding to the $\frac{k}{1+K}$ probability. Next, we calculated $\boldsymbol{Y}_K$ as an $M\ x\ K$ matrix with row m equal to the cube of the absolute difference between the time at location m, $D_{m,2}$, and ς_k: $\boldsymbol{Y}_{Km} = \{\left|D_{m,2} - \varsigma_1\right|^3, \left|D_{m,2} - \varsigma_2\right|^3, \ldots, \left|D_{m,2} - \varsigma_K\right|^3\}$. We defined a new matrix $\mathbf{O}_K$ to have dimensions $Kx\ K$ and let row k be the cube of the absolute difference in time between each knot, ς_k: $\mathbf{O}_{Kk} = \{|\varsigma_k - \varsigma_1|^3, |\varsigma_k - \varsigma_2|^3, \ldots, |\varsigma_k - \varsigma_K|^3\}$. Next, we let $\boldsymbol{Y} = \boldsymbol{Y}_K\mathbf{O}_K^{-1/2}$ so that the matrix $\mathbf{O}_K$ penalized the coefficients of $\left|D_{m,2} - \varsigma_k\right|^3$ in the matrix multiplication and resulted in $M\ x\ K$ matrix $\boldsymbol{Y}$. We defined a new vector $\boldsymbol{a}$ of length K to be vague, random normal variables with mean equal to 0 and standard deviation equal to $\tau^{-1/2}$ and $\tau \sim gamma(0.001, 0.001)$. We let $\boldsymbol{a} = \mathbf{O}_K^{1/2}\boldsymbol{u}$ where $\boldsymbol{u}$ is a vector of random parameters of length K, $\boldsymbol{u} = (u_1, u_2, \ldots, u_K)^{\mathrm{T}}$.

Appendix D. Mortality rates affecting population growth.

Varying compensation in cause-specific mortality has been documented in wolf populations (Mech 2001). When human-caused mortality was low, as in Minnesota and Denali National Park, Alaska, ~10% of the population was killed because of conflicts with other wolves (Mech 1977, Mech et al. 1998). In contrast, areas in Alaska where wolf hunting is used for management, a negligible proportion of wolves were killed by other wolves, indicating a compensatory mortality mechanism (Ballard et al. 1987). Wolves compensate for hunting pressure by moving on the landscape through dispersal, emigration, and immigration. Recruitment may or may not have a significant role (Adams et al. 2008, Gude et al. 2012).

Recent research into whether human-caused mortality is compensatory or additive with other causes of mortality for a wolf population is controversial, and this has been identified as an important research need in wolf conservation (Vucetich and Peterson 2004). Several analytical approaches have been put forward to try and understand the relationship between mortality sources and population growth. Here, we summarize four different approaches and apply them to wolf data for Wisconsin. For all analyses, we used the midpoint of the population estimates for wolves in Wisconsin from 1980 – 2013 (Wydeven et al. 2009) and the survival and cause-specific mortality rates from Chapter 2.

Approach from Fuller et al. (2003)

Fuller et al. (2003) summarized 19 wolf studies (The Isle Royal study was divided into 2 subsets for a total of 20 data points) and found that, on average, a wolf population would stabilize with an annual mortality rate of 0.34 (SE = 0.06) or a human-caused mortality rate of 0.22 (SE = 0.08). We fit the linear relationship of per capita population growth to annual mortality rate and per capita population growth to human-caused mortality rate (Fig. D.1). We

found that per capita population growth decreased with annual mortality rate ($pgr = 0.455 - 1.261 * mortality$; Adjusted $R^2 = 0.803$) and decreased with human-caused mortality rate ($pgr = 0.334 - 1.514 * mortality$; Adjusted $R^2 = 0.543$). According to this linear relationship, we would estimate that Wisconsin's wolf population would stabilize at 36.1% annual mortality and 22.1% annual human-caused mortality. These are very similar to the total mortality and human-caused mortality rates of 34% and 22% from Fuller et al. (2003) who analyzed data from the 19 North American studies.

Approach from Adams et al. (2008)

Adams et al. (2008) revisited the analyses of Fuller et al. (2003) and separated the population trends from the 19 North American studies into 41 different sub-trends based on notable changes in population trend or management. They left out 3 outliers and fit the relationship between per capita growth rate and annual human-caused mortality. They found that a quadratic was a better fit than a linear function, and reasoned that population trend was not correlated with human-caused mortality rates that were less than 29% annually. Also, populations grew an average of 10% per year when annual human-caused mortality rates were < 29%. Their conclusion was that harvest loss ≤ 29% annually was compensated for by adjustments in dispersal, and at this level there was no relationship between natural mortality and human-caused mortality that would suggest compensation from natural mortality (Adams et al. 2008).

We fit the relationship of per capita population growth and annual human-caused mortality with a quadratic function and compared this model fit compared to the linear model based on Akaike's Information Criterion (AIC). We also fit the relationship of natural mortality to human-caused mortality to consider whether there was evidence of compensation from natural

mortality sources. We found that the quadratic relationship was a better model than the line ($AIC_{quadratic} = -147.1, AIC_{line} = -144.5$; Fig. D.2). The formula for the quadratic function was $pgr = 0.466 - 3.683 * mortality + 6.950 * mortality^2$, and the fit was concave versus the convex relationship found by Adams et al. (2008). The rate of human-caused mortality that would lead to a stable population from the quadratic fit was 0.209. For Wisconsin's wolf population, it appears that there is strong additivity in natural mortality for rates of human-caused mortality < 0.15. After about 15% annual human-caused mortality per year, the relationship is much less clear (Fig. D.2). It is clear, however, that the Wisconsin wolf population had quite a different relationship between per capita growth and human-caused mortality than the findings of Adams et al. (2008).

Approach from Creel and Rotella (2010)

Creel and Rotella (2010) noted that Fuller et al.'s (2003) analysis actually yielded evidence that human harvest was additive to other mortality sources ($\beta/(1-\alpha)$ = 0.91). A linear regression of the total mortality on human-caused mortality rate gives a slope, β, and an intercept, α. The formula $\beta/(1-\alpha)$ yields a value that can be interpreted as evidence for full compensation (0), full additivity (1), partial additivity (between 0 and 1), and super-additivity (> 1; Williams et al. 2002, Lebreton 2005). Using the same 19 studies as Fuller et al. (2003) and an additional 29 population estimates from wolves in the Northern Rocky Mountains, Creel and Rotella (2010) documented super-additive mortality. Also, the model-averaged results from the relationship of population growth rate and human off-take indicated that wolves in the Northern Rocky Mountains had a stable to increasing population growth up to 22.4% annual human-caused mortality and wolves in other areas of North America had stable to increasing population growth up to 24.5% annual human caused mortality (Creel and Rotella 2010).

We fit a line to the total mortality rate versus human-caused mortality rate from our data and calculated $\beta/(1-\alpha)$. We found that the linear relationship was $pgr = 0.088 + 1.256 * mortality$, and that $\beta/(1-\alpha) = 1.38$ (Fig. D.3). The value was very similar to the value of 1.34 that Creel and Rotella (2010) found for wolves in the Northern Rocky Mountain region. These results suggest that human-caused mortality in the Wisconsin wolf population is additive or super-additive.

Approach of Gude et al. (2012)

Gude et al. (2012) noticed that Creel and Rotella (2010) analyzed the Northern Rocky Mountain wolf population dataset without accounting for differences in monitoring and without accounting for recruitment. Therefore, Gude et al. (2012) conducted new analyses of these same data, while attempting to account for some of this extra variation. For a predictor variable of per capita growth rate, the response variables in three competing models were: 1) human-caused mortality rate, 2) recruitment rate, and 3) human-caused mortality rate + recruitment rate. They found that variation in both recruitment and human-caused mortality rate affected the population growth rate.

We fit the same models from Gude et al. (2012) and conducted model selection with AIC. We restricted our analysis to the years 1981 – 2009 because the number of pups each winter was not estimated after 2009. To calculate recruitment rate, we divided the average number of pups in year $t+1$ by the average population size in year t, and took this to be the per capita recruitment rate for year t. We found that per capita growth rate was best explained by the human-caused mortality rate alone ($AIC = -133.3$; Fig. D.4). Recruitment rate had a very weak relationship with per capita growth rate (Adjusted R^2 = -0.031) and AIC was much higher ($AIC = -100.6$; Fig. D.4). The model with both human-caused mortality and recruitment rate

was no better than the model with human-caused mortality rate alone ($AIC = -131.4$). We conclude that the growth rate for wolves in Wisconsin is much more affected by the human-caused mortality rate than by the recruitment rate. This is a different finding than for wolves in the Northern Rocky Mountains where recruitment and human-caused mortality were both contributors to the growth rate (Gude et al. 2012).

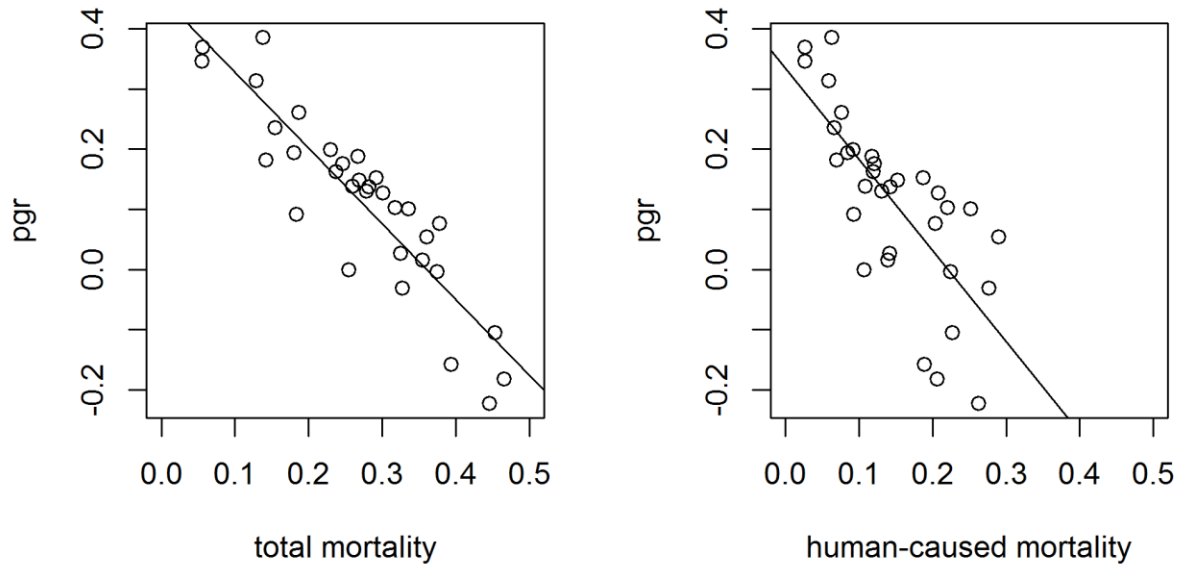

Figure D.1. Plots of per capita growth (pgr) in 1981 – 2013 versus total mortality rate and the human-caused mortality for wolves in Wisconsin, USA. (Approach of Fuller et al. 2003)

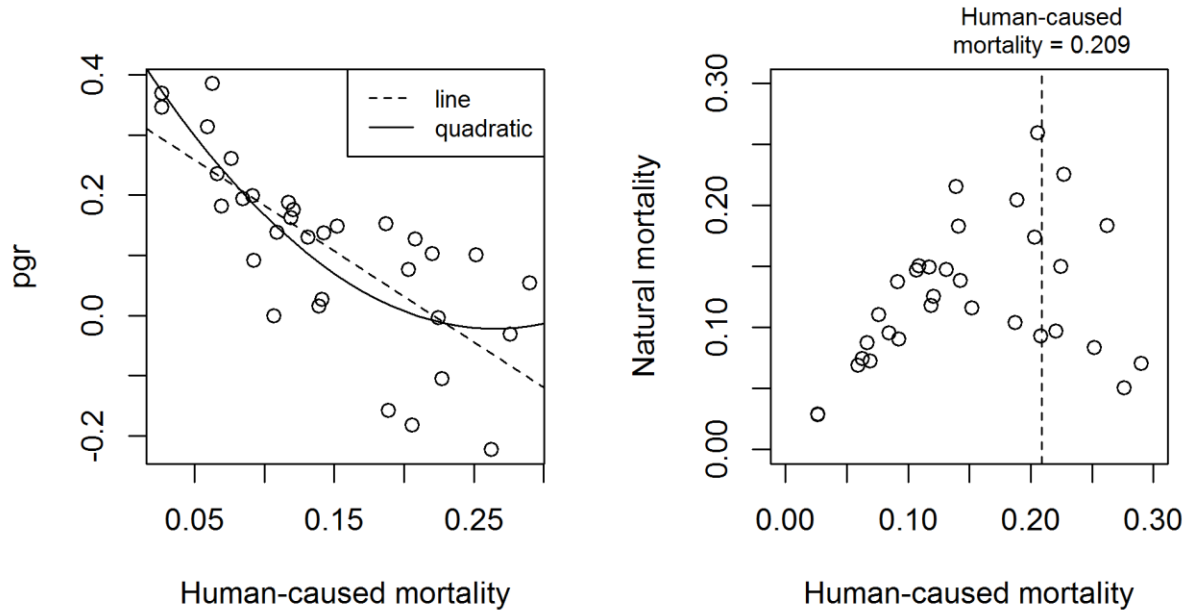

Figure D.2. Plots of per capita growth (pgr) versus human-caused mortality with a linear and a quadratic fit, and of natural mortality versus human-caused mortality with a vertical dashed line for the rate of human-caused mortality that would leads to 0 population growth from the quadratic fit for wolves in Wisconsin, USA from 1981 – 2013. (Approach of Adams et al. 2008)

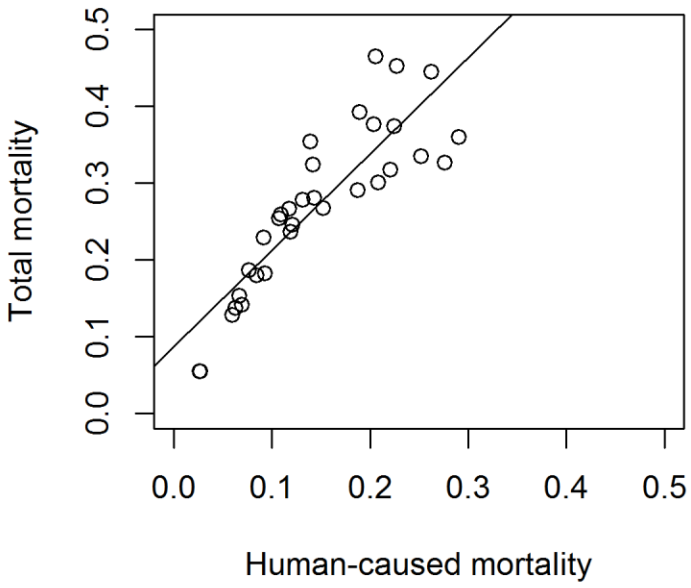

Figure D.3. Relationship of total mortality and human-caused mortality for wolves in Wisconsin, USA (1981 – 2013). (Approach of Creel and Rotella 2010)

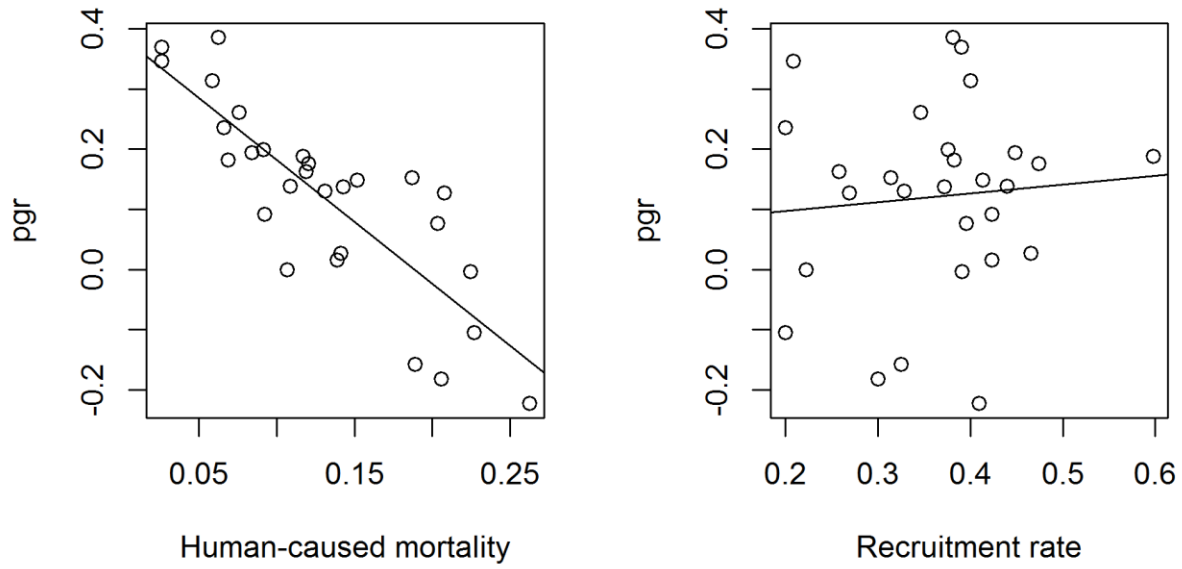

Figure D.4. Plot of per capita growth related to human-caused mortality rate and recruitment rate for wolves in Wisconsin, USA from 1981 – 2009. (Approach of Gude et al. 2012)

Appendix E. Model for use with JAGS.

```
model {

### cause-specific endpoint probability part, pj
for (i in 1:n){
for( k in 1:K ) {
 eta[i,k] <- base1[i,k] + beta1.X1[i,k]
 base1[i,k] <- beta1[1,k] + beta1[2,k]*X1[i,2] + b1.Z1[i,k]
 beta1.X1[i,k] <- beta1[3,k]*X1[i,3] + beta1[4,k]*X1[i,4] + beta1[5,k]*X1[i,5]
 b1.Z1[i,k] <- b1[k,1]*Z1[i,1]+b1[k,2]*Z1[i,2]+b1[k,3]*Z1[i,3]+b1[k,4]*Z1[i,4] +
b1[k,5]*Z1[i,5] + b1[k,6]*Z1[i,6] + b1[k,7]*Z1[i,7] + b1[k,8]*Z1[i,8] +
b1[k,9]*Z1[i,9] + b1[k,10]*Z1[i,10] + b1[k,11]*Z1[i,11] + b1[k,12]*Z1[i,12] +
b1[k,13]*Z1[i,13] + b1[k,14]*Z1[i,14] + b1[k,15]*Z1[i,15] + b1[k,16]*Z1[i,16] +
b1[k,17]*Z1[i,17] + b1[k,18]*Z1[i,18] + b1[k,19]*Z1[i,19] + b1[k,20]*Z1[i,20]
 expeta[i,k] <- exp(eta[i,k])
 # probabilities (link function)
 p[i,k] <- expeta[i,k]/sum(expeta[i,1:K])
}
 # stochastic part
 cause[i] ~ dcat(pstar[i,1:K])
}
 # misclassification
for (i in 1:n) {
for (e in 1:K){
pstar[i,e] <- sum(miss[e,1:K]*p[i,1:K])
}}

for (j in 1:P){
 # coefficients for the baseline category are constrained to zero
 beta1[j,1] <- 0.0
 # independent normal low information priors
 for (k in 2:K){ beta1[j,k] ~ dnorm(0.0, 0.0001) }
}
for (m in 1:20) {b1[1,m] <- 0}
for (k in 2:K) {
for (m in 1:20) {
 b1[k,m] ~ dnorm(0,taub1)
}
}
taub1 ~ dgamma(0.001,0.001)
sigmab1 <- 1/sqrt(taub1)

### the hazard part, h
# i for records, and N for number of records
for (i in 1:N) {
 outcome[i] ~ dbern(mu[i])
 cloglog(mu[i]) <- beta.X[i] + base.beta.X[i]
 base.beta.X[i] <- gm + beta0[year[i]] + beta[2]*X[i,2] + b.Z[i]
 beta.X[i] <- beta[3]*X[i,3] + beta[4]*X[i,4] + beta[5]*X[i,5]
 b.Z[i] <- b[1]*Z[i,1]+b[2]*Z[i,2]+b[3]*Z[i,3]+b[4]*Z[i,4] + b[5]*Z[i,5] + b[6]*Z[i,6]
+ b[7]*Z[i,7] + b[8]*Z[i,8] + b[9]*Z[i,9] + b[10]*Z[i,10] + b[11]*Z[i,11] +
b[12]*Z[i,12] + b[13]*Z[i,13] + b[14]*Z[i,14] + b[15]*Z[i,15] + b[16]*Z[i,16] +
b[17]*Z[i,17] + b[18]*Z[i,18] + b[19]*Z[i,19] + b[20]*Z[i,20]
 hazard[i] <- -log(1-mu[i])
}
for (k in 1:20) {b[k] ~ dnorm(0,taub)}
taub ~ dgamma(0.001,0.001)
sigmab <- 1/sqrt(taub)
for (i in 2:P) {
 beta[i] ~ dnorm(0,0.0001)
 haz.ratio[i] <- exp(beta[i])}
```

```
for (i in 2:34) {
 beta0[i] ~ dnorm(0,0.0001)
}
gm ~ dnorm(0,0.0001)
beta0[1] <- 0

### for prediction of pj(t) and h(t)
for (i in 1:T) {
# for pj(t)
for (k in 1:K){
eta2[i,k] <- beta1.X2[i,k] + base2[i,k]
base2[i,k] <- beta1[1,k] + beta1[2,k]*X2[i,2] + b1.Z2[i,k]
base.seasonave[i,k] <- beta1[1,k] + beta1[2,k]*X2[i,2] + b1.Z2[i,k] + (beta1[4,k]/2)
beta1.X2[i,k] <- beta1[3,k]*X2[i,3] + beta1[4,k]*X2[i,4] + beta1[5,k]*mean.value
b1.Z2[i,k] <- b1[k,1]*Z2[i,1]+b1[k,2]*Z2[i,2]+b1[k,3]*Z2[i,3]+b1[k,4]*Z2[i,4] +
b1[k,5]*Z2[i,5] + b1[k,6]*Z2[i,6] + b1[k,7]*Z2[i,7] + b1[k,8]*Z2[i,8] +
b1[k,9]*Z2[i,9] + b1[k,10]*Z2[i,10] + b1[k,11]*Z2[i,11] + b1[k,12]*Z2[i,12] +
b1[k,13]*Z2[i,13] + b1[k,14]*Z2[i,14] + b1[k,15]*Z2[i,15] + b1[k,16]*Z2[i,16] +
b1[k,17]*Z2[i,17] + b1[k,18]*Z2[i,18] + b1[k,19]*Z2[i,19] + b1[k,20]*Z2[i,20]
expeta2.base.seasonave[i,k]<-exp(base.seasonave[i,k])
expeta2[i,k]<-exp(eta2[i,k])
# probabilities (link function)
p.pred[i,k] <- expeta2[i,k]/sum(expeta2[i,1:K])
p.base.seasonave[i,k] <-
expeta2.base.seasonave[i,k]/sum(expeta2.base.seasonave[i,1:K])
}

# for h(t)
cloglog(mu2[i]) <- base.beta.X3[i] + beta.X3[i]
base.beta.X3[i] <- gm + beta0[year2[i]] + beta[2]*X3[i,2] + b.Z3[i]
beta.X3[i] <- beta[3]*X3[i,3] + beta[4]*X3[i,4] + beta[5]*mean.value
cloglog(h.base.seasonave[i]) <- gm + beta0[year2[i]] + beta[2]*X3[i,2] + b.Z3[i] +
(beta[4]/2)
b.Z3[i] <- b[1]*Z3[i,1]+b[2]*Z3[i,2]+b[3]*Z3[i,3]+b[4]*Z3[i,4] + b[5]*Z3[i,5] +
b[6]*Z3[i,6] + b[7]*Z3[i,7] + b[8]*Z3[i,8] + b[9]*Z3[i,9] + b[10]*Z3[i,10] +
b[11]*Z3[i,11] + b[12]*Z3[i,12] + b[13]*Z3[i,13] + b[14]*Z3[i,14] + b[15]*Z3[i,15] +
b[16]*Z3[i,16] + b[17]*Z3[i,17] + b[18]*Z3[i,18] + b[19]*Z3[i,19] + b[20]*Z3[i,20]
 hazard.pred[i] <- -log(1-mu2[i])
 hazard.base.seasonave[i] <- -log(1-h.base.seasonave[i])
}

### hj(t) part. Cause-specific hazard
for (i in 1:T) {
 p.interesting[i] <- sum(p.base.seasonave[i,3:5])
 haz.interesting[i] <- p.interesting[i]*hazard.base.seasonave[i]
 log.haz.auxiliary[i] ~ dnorm(log(haz.interesting[i]),tau.auxiliary)
}

### predict survival
for (i in 1:T) {
 p.mort[i] <- sum(p.pred[i,3:5])
 cause.haz[i] <- p.mort[i]*hazard.pred[i]
}

for (j in 1:4) {
for (i in 1:33) {
 annual.surv[i,j] <- exp(-sum(cause.haz[((i-1)*12+7+(j-1)*402):((i-1)*12+18+(j-
1)*402)]))
}
 mean.surv[j] <- mean(annual.surv[1:33,j])
}
tot.surv <- (mean.surv[1]*153 + mean.surv[2]*234 + mean.surv[3]*20 +
mean.surv[4]*92)/499
```

```
### misclassification matrix
miss[1,1] <- 1
miss[2,1] <- 0
miss[3,1] <- 0
miss[4,1] <- 0
miss[5,1] <- 0

miss[1,2] <- 0
miss[2,2] <- 1
miss[3,2] <- 0
miss[4,2] <- 0
miss[5,2] <- 0

miss[1,3] <- phi
miss[2,3] <- 0
miss[3,3] <- 1 - phi
miss[4,3] <- 0
miss[5,3] <- 0

miss[1,4] <- phi
miss[2,4] <- 0
miss[3,4] <- 0
miss[4,4] <- 1 - phi
miss[5,4] <- 0

miss[1,5] <- phi
miss[2,5] <- 0
miss[3,5] <- 0
miss[4,5] <- 0
miss[5,5] <- 1 - phi

phi ~ dunif(0,1)

}
```

Chapter 3: An individual-based model for southern Lake Superior wolves: A tool to explore the effect of human-caused mortality on a landscape of risk

Abstract

Gray wolves (*Canis lupus*) have complex life-histories due, in part, to mating systems that depend on dominance hierarchies and a social structure linked to philopatric social groups known as packs. In addition, mortality risk associated with interactions with humans vary spatially. We developed an individual-based spatially-explicit (IBSE) model for the southern Lake Superior wolf population to better capture the life-history of wolves in a harvest model. Simulated wolves underwent an annual cycle of stage-dependent mate-finding, dispersal, reproduction, and aging on a simulated landscape reflecting spatially-explicit state and water boundaries, Ojibwe Indian reservation boundaries, wolf harvest zones, livestock depredation areas, and a spatial mortality risk map that scaled an individual's probability of mortality to the influence of road density and percent of agriculture. Additional mortality sources included recreational harvest and lethal control focused on areas of chronic livestock depredations. We built, documented, and calibrated the IBSE model to the observed growth of the combined Wisconsin and Michigan wolf population. We found that without harvest, the Wisconsin wolf population attained an average carrying capacity of 1242 wolves after 50 years and breeding pairs persisted for a mean 1.8 years. We simulated six management scenarios with varying rates and timings of harvest and assessed effects on wolf populations in terms of numbers, pack sizes, age ratios, dispersal and immigration rates, and breeding pair tenures. The simulated harvest with rates corresponding to the 2012 harvest in Wisconsin reduced the population 4% in the first year of harvest and stabilized the wolf population at about 600 wolves after 20 years of harvest. A 30% harvest rate across the simulation reduced the population by 65% after 20 years with

some simulated populations going extinct before 100 years. In general, harvest increased the proportion of pups in the population and decreased breeding pair tenure. Targeted lethal control was more effective than harvest for reducing the number of wolves near known livestock depredation sites. This model facilitates prediction of important population patterns that is simultaneously dependent on complexities associated with life history and spatially structured mortality.

Introduction

During the last three decades, gray wolves recolonized the upper southern Lake Superior (SLS) region, USA from a source population in Minnesota. Gray wolves reintroduced into central Idaho and Yellowstone National Park (Wyoming, USA) have expanded their range across the Rocky Mountain region into portions of Washington and Oregon (United States Fish and Wildlife Service et al. 2013). Recovery has been so successful that both the Great Lakes and Rocky Mountain populations are now harvested. Other pockets of habitat are now home to less established wolf populations. Reintroduced Mexican wolves (*Canis lupus baileyi*) in the southwestern USA and red wolves (*Canis rufus*) in the southeastern USA each have populations around 100 individuals (United States Fish and Wildlife Service 2012, 2013). The success of wolves in these different habitats demonstrates wolves' ability to exist in human-dominated landscapes, especially when wolves are protected from heavy harvests associated with early eradication campaigns and poaching (Merrill 2000, Thiel et al. 2009). Nevertheless, having humans and wolves sharing modern landscapes requires a thorough understanding of how active management, including harvest, affects population dynamics.

Individual-based modeling is increasing in ecology to answer pragmatic questions and to explore ecological theories (Grimm and Railsback 2005). Interest in individual-based models is

not usually in the individuals per se, but rather in the population properties that emerge because of the decisions and behaviors of individuals (Grimm and Railsback 2005, Macal and North 2010). In populations with complex social structures, population prediction can be especially difficult because individuals contribute differently to the population depending on their social role. Wolves have a social structure where breeding pairs and their offspring make up packs (Mech and Boitani 2003). Because not all wolves are breeders, the population effect from the death of a wolf depends on that wolf's social status, the time of year, and the size of the population. The death of a pregnant female wolf would reduce population recruitment while the death of non-reproductive yearling would have no effect on population recruitment in the next year beyond its own contribution to overall mortality. Concerning the time of the year when a wolf death occurs, the death of a potential breeder before breeding season may or may not have a population effect depending on whether there is time for replacement of that breeder (Brainerd et al. 2008). All of these population effects are more pronounced at small population sizes because of demographic stochasticity and possible Allee effects (Berec et al. 2001, Stenglein et al. *unpublished*). With individual-based models, individual differences can be modeled explicitly leading to a more realistic population model.

Individual-based models are sometimes used to understand the effect of various management actions (Grimm et al. 2005). Anticipating the need for removal strategies of problem wolves from the growing SLS wolf population, Haight et al. (2002) developed an individual-based model to test the effect of three wolf removal strategies and the combinations of multiple strategies. This individual-based model provided guidance to managers on wolf removal strategies by showing that proactive removal of wolves in areas near farms reduced depredations, removed fewer wolves than the reactive strategy, and was the least costly strategy

(Haight et al. 2002). In another example, an individual-based spatially-explicit (IBSE) model to understand the effect of social structure on canid populations was used to evaluate coyote management strategies (Pitt et al. 2003, Conner et al. 2008). This IBSE model showed that spatially intensive removal of coyotes was longer-lasting and more effective than random removal of coyotes (Conner et al. 2008). These examples demonstrate the utility inherent in individual-based models and their use as realistic management tools.

An IBSE model, though complex, makes explicit assumptions that enhance model transparency (Grimm 1999). IBSE models are often more realistic than population-based models and this makes them easier to conceptualize by different groups of people. Stakeholders interested in an issue can include science in their discussions through IBSE models that simulate different management scenarios (Bousquet and Le Page 2004). However, it is important that IBSE models used to make management decisions are well-documented. This documentation should include model assumptions, parameter values, and model predictions over a range of scenarios (Bart 1995).

We developed an IBSE model to explore the effects of human-caused mortality sources on wolves in the SLS region. The purpose of our model was to understand how wolf colonization and distribution in the SLS region was affected by roads, agriculture, and different mortality sources linked to the landscape, political boundaries, and management. Our model provided a visual and quantitative tool to understand and predict wolf population growth in Wisconsin. The model also enabled evaluation of spatially-structured harvest scenarios on the Wisconsin wolf population. In particular, our objectives were to: 1) build and document a plausible IBSE model of the colonization of the Wisconsin and Michigan wolf population from resident Minnesota wolves, 2) calibrate the model using observed population growth of

Wisconsin and Michigan populations, 3) use the model to explore the effects of different types and timing of human mortality sources that occurred on different parts on the simulated landscape, and 4) demonstrate the use of the IBSE model as a platform for evaluating management proposals.

Methods

Spatial mortality risk map

The IBSE model derived population parameters based on the collective behaviors and fates of individual wolves interacting with mortality risk that varied spatially. To create a spatial mortality risk component, we took a heuristic approach to scaling a simulated wolf's annual probability of mortality on the basis of road density and amount of agriculture in the SLS region (Wydeven et al. 2009b). The response variable was the dead (N = 195) or alive (N = 15,134) status of radio-telemetry locations for each of 195 wolves in Wisconsin's radio-telemetry database that were monitored consistently and found dead sometime during 1979 – 2012 (see Wydeven et al. 2009b for wolf capture, handling, radio-collaring, and tracking methods). We used logistic regression conditioned on a wolf's identity to remove unobserved individual heterogeneity (Gail et al. 1981).

We used roads and agriculture as predictors because these variables were selected from a suite of 16 variables (some highly correlated) in a pack-level analysis of wolf habitat quality in Wisconsin by Mladenoff et al. (2009). We quantified road density (km/km^2) and percentage of agriculture in 1 km buffers around each radio-telemetry location (see Appendix A for details on road and agriculture parameter derivation). We performed the conditional logistic regression in Program R (Version 3.0.1, R Development Core Team 2013) using function 'clogit' in the 'survival' package (Therneau 2013).

We gridded a 630 km x 554 km landscape of the SLS region centered on Wisconsin into 1 km^2 pixels, and obtained road density and percent agriculture covariates for each land pixel. Next, we obtained a value from the fitted model for each land pixel using Raster Calculator in ArcMap (Version 9.2, Environmental Systems Research Institute 2009). These fitted values were the probabilities that an average wolf's radio-telemetry location would be a death location, and the predicted values did not directly translate to annual mortality rates. Therefore, we scaled these fitted values to reflect the annual mortality rate for wolves in Wisconsin (Wydeven et al. 2009b). The scaling reflected the estimated annual mortality rate for wolves in primary wolf range in Wisconsin from our survival analysis in Chapter 2 (Appendix A). Therefore, the spatial mortality risk map reflected the majority of the annual probability of mortality for the simulated wolves.

The IBSE model

We built an IBSE model of the SLS wolf population in NetLogo v. 5.0.1 (Wilensky 1999) and describe it following the Overview, Design concepts, and Details protocol (Grimm et al. 2006, Grimm et al. 2010). We assumed that observed population dynamics were primarily driven by the model rules that affected the behaviors and decisions of individual virtual wolves (hereafter, wolves). Wolves faced decisions on life stage events reflecting wolf phenology in the SLS wolf population (Wydeven et al. 2009a). In addition to the phenomological realism, our model used the best-available data from the SLS wolf population to parameterize life stage events, including dispersal (Treves et al. 2009), litter size (Fuller et al. 2003), territory size, and pack size (Wydeven et al. 2009b).

Because of our interest in inferences about the SLS wolf population, and in particular the Wisconsin wolf population, we constructed a SLS landscape for simulated wolves. This

particular SLS landscape focused our model inference on the specifics of colonization and the interaction of different mortality factors for wolves in the SLS region. Despite criticism for the complexity of IBSE models (Grimm 1999), the level of complexity we included in this IBSE model was necessary to address our questions about the SLS wolf population.

State variables and scales

The IBSE model included four hierarchical levels of organization: individual wolves, territories, the wolf population, and the landscape (Table 1). The model incremented population dynamics in 1 year time steps designed to match wolf life history events during an annual cycle (Fig. 1). The simulation ran for 100 years or until all wolves were extinct.

We defined territories as 15 x 15 km square patches of habitat where the center of the territory was in breeding range (Table 1, Fig. 2E). We used the average territory size of wolf packs with ≥ 20 radio-telemetry locations in Wisconsin from 2001 – 2006 (mean = 136 km^2, SD = 67) to inform mean territory sizes in the model (Wydeven et al. 2009b). However, calculation of mean territory size from minimum convex polygons is a minimum estimate and did not include the interstitial area between packs, which increase average pack size by 37% (Fuller et al. 1992). Therefore, we gridded the landscape into potential territories of 225 km^2, and territories were considered occupied if there were ≥ 2 wolves within the territory boundary.

Virtual packs of wolves (hereafter, packs) were identified as aggregates of 2 – 12 wolves located in discrete territories. Packs consisted of a breeding pair, their offspring of multiple generations, and any unrelated wolves that dispersed into the pack. Packs could also have a single breeder or no breeders if one or both breeders died. Wolves were identified as either a member of a certain pack or as lone wolves. Lone wolves were wolves that were outside pack

territories or wolves that did not have any full siblings within an 8 km radius of their location (the size of 1 territory). When within territories, lone wolves were considered part of the pack.

State variables for individual wolves were identification number, sex, age, breeder status, disperser status, immigrant status, pack status, mother's identification number, and father's identification number (Table 1). Breeder status, pack status, and genetic heritage (i.e., mother's identification number, father's identification number) were the primary determinants of wolf movement and behavior on the landscape.

Process overview and scheduling

In each year of simulation, wolves searched for mates, dispersed and searched for mates again, reproduced, experienced a targeted lethal control event (once the Wisconsin population >349 wolves), dispersed (if pack sizes were larger than 12 wolves), were hunted (once the Wisconsin population >843 wolves), faced spatial mortality risk, and aged (Fig. 1). Aside from aging and the spatial mortality risk event, not all wolves participated in or were affected by each event. Within each event, individuals were processed randomly and transitions associated with all state changes apart from aging occurred according to probability distributions (Table 2).

Initialization and input data

Simulations began with 20 male wolves and 20 female wolves that formed breeding pairs in 20 randomly chosen pack territories in northeastern Minnesota. The initial individuals were given a random age (1 – 12) and pack membership as breeders.

The landscape was read into the model by its x and y coordinates (spaced 1 km apart) and all associated landscape variables. We constructed this file in ArcMAP beginning with a point layer with a grid of points spaced 1 km apart over the entire landscape. We included the following layers: state boundaries (Minnesota, Wisconsin, Michigan, Iowa) or water (Fig. 2A),

Ojibwe ceded territories of Wisconsin (a region where bands of the Ojibwe Tribe may exercise treaty rights to hunt and gather resources, Fig. 2B), Ojibwe Indian reservations of Wisconsin (Fig. 2B), Wisconsin wolf harvest zones (WHZs, Fig. 2C), Wisconsin chronic depredation farms, livestock depredation sites, and a 5 km buffer around depredation areas (depredation buffer, hereafter, Fig. 2D), pack territories (Fig. 2E), and the spatial mortality risk map (Fig. 2F). The value of each layer at each set of coordinates became the value for the 1×1 km pixel. The percent harvest per WHZ in Wisconsin and the percent harvest across Minnesota and Michigan were inputs to the model and used to construct the harvest scenarios. Also, the timing of harvest was input into the model.

Submodels

Mate-finding

Mate finding was an action taken by lone wolves and single breeders, and occurred ≤ 2 times per year (Fig. 1). Lone wolves would search for mates, have an opportunity to disperse if a mate was not found (see dispersal for mate-finding section, below), and then search for mates a second time. We defined single breeders as territorial breeding wolves whose mates died. We allowed single breeders to pair up by first allowing any subordinate, unrelated adult wolves of the opposite sex in their own pack to fill the vacant breeding position and by allowing any unrelated lone wolves of the opposite sex from up to 2 territories away to usurp the empty breeding position if breeders were unavailable within the pack.

Any remaining lone wolves would then search out each other. A male lone wolf would search for an unrelated female lone wolf within 2 territories of his location; if found, the male and female would move to the closest territory. They would form a breeding pair if the territory was unoccupied by another breeding pair. We chose a distance of 2 territories away because a

sensitivity analysis demonstrated that this distance resulted in simulated population growth that matched the observed population growth more closely than using other distances (Stenglein, *unpublished data*).

Dispersal for mate-finding (winter dispersal)

Wolves dispersed after a first round of mate-finding if they were not part of a breeding pair, were not single breeders, and were not part of a pack. Dispersing wolves chose a random direction and dispersed a distance drawn from a lognormal probability distribution with mean = 3.918 and SD = 1.005 on the log scale (Treves et al. 2009). According to this distribution, wolves dispersed an average of 50 km.

The wolves that dispersed outside of the land area (i.e., into the water pixels) were considered emigrants. An equal number of immigrants were then generated and entered the simulation in randomly chosen locations in breeding range. Wolves that entered the simulation as immigrants were given a random age (1 – 12) and random sex assignment, pack membership if they arrived in an occupied territory, status as an immigrant, and no mother and father identification numbers. The immigrants represented wolves that entered the SLS region from Canada, and did not represent wolves that moved from one area of the SLS region into another area of the SLS region (e.g., wolves from Minnesota that moved into Wisconsin were not considered immigrants).

Reproduce

Females in breeding pairs would reproduce each year producing a single litter. Litter sizes were drawn from a normal distribution with mean = 5.406 and SD = 0.790 reflecting the mean and standard deviation of litter sizes from North American studies (Fuller et al. 2003). We rounded the value drawn from the distribution to the next whole number to represent litter size as

a whole number of pups. Wolves born into the simulation were given age 0, a random sex assignment, a membership into their current pack, and their mother's and father's identification numbers.

Targeted lethal control

The Wisconsin portion of the simulated wolf population was exposed to targeted lethal control during summer when the Wisconsin winter population count was > 350 wolves, and every year thereafter. We chose to initiate the targeted lethal control event when the simulated Wisconsin population reached 350 wolves because a minimum count of 353 wolves was recorded in Wisconsin in 2003 when the targeted lethal control program actually began (Ruid et al. 2009, Wydeven et al. 2009b).

Targeted lethal control events removed 10% of the wolves (calculated from the Wisconsin winter population count) primarily from the depredation buffer (Fig. 2D). We chose 10% of the winter count because in the years since 2003 when lethal control was allowed at least half of the year, 5.1 – 9.3% of the winter population was killed from lethal control action (Olson 2013). In 2012 and 2013, once wolves were delisted, lethal control action removed 9.3% and 8.2% of the winter population, respectively. For the IBSE model, we chose the slightly higher value of 10% lethal control of the winter population to represent the proportion of lethal control that we expected in a delisted population. Also, 10% lethal control of the winter population translates to < 10% mortality due to lethal control in the population once it implemented because there are many more wolves in the summer (season of lethal control) after the birth of pups. In the IBSE model, we removed 90% of the targeted lethal control quota from the depredation buffer and restricted to areas outside of Ojibwe Indian reservations. If there were not enough wolves within the depredation buffer, then wolves were removed from an additional 5 km buffer

around the depredation buffer to fill the quota (Fig. 2D). The remaining 10% of the quota (1% of the Wisconsin winter population count) were removed from random locations in Wisconsin outside of Ojibwe Indian reservations. We chose for most (90% of the lethal control quota) of lethal control events to focus in the depredation buffers because most depredations are related to livestock loss and they occur in very specific locations, like the chronic depredation farms and known depredation sites that we used in our model (Ruid et al. 2009, Olson 2013).

Dispersal due to resource limitation (Fall dispersal)

We used a threshold pack size of 12 wolves as a trigger for a second type of dispersal to model resource limitation in the pack (Fig. 1). This number was based on the observations that maximum pack sizes in Wisconsin were 12 wolves from 1980 – 2007 (Wydeven et al. 2009b). In the model, packs with > 10 non-breeding pack members would assign a number of members in excess of this non-breeder pack maximum to disperse out of the pack. The individuals were chosen randomly from among the non-breeding pack members. For example, if there were 12 non-breeding pack members, the model would randomly select 2 of them to disperse out of the pack. These dispersers were assigned a random direction and dispersed a distance of kilometers drawn from a lognormal distribution (3.918, 1.005). Dispersers died unless they arrived in an occupied territory with < 12 wolves, a vacant pack territory, or other land area.

Harvest

We initiated harvest when the winter population count was > 843 wolves in Wisconsin since this was the population size observed during winter of 2011-2012 before the first actual harvest. Harvest quotas were calculated as user-determined percentages of the population harvested per WHZ times the winter population count in each WHZ. We chose a constant harvest level for Minnesota and Michigan and harvest quotas in these states were calculated as

the percent harvest multiplied by the previous winter's population count. In most cases, harvest occurred as a fall harvest after dispersal and before the spatial mortality risk event. However, in some cases, a percentage of the harvest was allocated as a winter harvest which occurred early in the calendar year, after mate-finding and before reproduction. Wolves were chosen randomly for harvest. We did not expect that harvest rates would be different for different age and sex classes because mortality rates overall do not vary by age and sex class (Wydeven et al. 2009b).

Spatial mortality risk

The spatial mortality risk event scaled an individual wolf's probability of mortality to the spatial mortality risk map (Appendix A). Each wolf was assigned a number from Uniform distribution (0, 1) and if this number was less than the spatial mortality risk value at their location (1 km^2 pixel), they would die. We chose for spatial mortality risk to occur just one time per year in the winter because this is when actual wolves in Wisconsin experience their highest mortality rates (see Chapters 1 and 2).

Age

At the very end of the calendar year, all wolves aged 1 year. Wolves died if they were > 12 years old. Wild wolves as old as 15 years old (Theberge and Theberge 1998) and breeding wolves as old as 11 years have been documented (Mech 1988). However, these old-aged wild wolves are very rare (Mech 1988, 2006).

Model calibration

We calibrated the model by comparing how simulated population growth matched observed population growth in Wisconsin and the wider SLS region. In particular, using the first 35 years of the simulation without any harvest, we documented: 1) the yearly mean Wisconsin winter population count, 2) the yearly mean winter population count in the SLS region, and 3)

the yearly mean number of pups in Wisconsin in the winter. For each of the quantities counted in the simulation, we compared them to data collected on the wolf population in Wisconsin and Michigan from 1979 – 2012 (Beyer et al. 2009, Wydeven et al. 2009b). We assessed correspondence by running 100 simulations and quantifying how often the 95% confidence intervals from the IBSE model simulations contained the observed population trend.

Simulations

Simulations in the IBSE model served two purposes: 1) to show the effects of different sources, rates, and timings of mortality on population counts, structure, and distribution, and 2) demonstrate the use of the IBSE model as a platform for evaluating management proposals. We ran six different simulations where we varied the intensity, location, and timing of harvest: 1) no harvest, 2) the 2012 Wisconsin harvest rates, 3) the 2012 Wisconsin harvest rates with 75% fall harvest and 25% winter harvest, 4) the 2013 Wisconsin harvest rates, 5) 30% harvest across the entire simulation, and 6) a rate of Wisconsin harvest that would enable a stable to increasing wolf population in the ceded territories of Wisconsin (Table 3).

Each simulation consisted of 100 iterations. In each simulation, we tracked number and age structure of wolves, number of packs, number of wolves in the depredation buffer, number and age structure of harvested wolves, number of pups born, the proportion of disrupted packs because of harvest (the number of packs that lost at least 1 breeder because of harvest divided by the number of packs that bred prior to harvest), and dispersal and immigration rates. We recorded these quantities at the end of each simulated year.

Results

Spatial mortality risk map

According to the model, an increase in road density and an increase in percent agriculture increased the probability that a location was a death location (Appendix A). The scaled spatial mortality risk probabilities ranged from 0.229 to 0.452, and the average spatial mortality risk for simulated wolves was 26 – 27%, which was the same as the average annual mortality of 26% that we estimated for wolves in Wisconsin (Chapter 2). There were no substantial differences in survival by age and sex class for wolves, so we assumed the same spatial mortality risk map for all wolves (see Chapters 1 and 2; Wydeven et al. 2009b). The risk map showed generally a lower probability of mortality in the northern and central forest regions of Wisconsin, the upper peninsula of Michigan, and the northeastern portion of Minnesota (Fig. 2F).

The IBSE model

All simulated wolf populations persisted for 100 years. Simulated populations that were not harvested stabilized at 1242 wolves (SD = 34) in Wisconsin after 50 years and at 2453 wolves (SD = 56) in the SLS region after 60 years (Fig. 3A). The average annual per capita growth rate was 7.2% (SD = 13.7) in Wisconsin (Fig. 3B). Average winter pup:yearling:adult ratio after 50 years of simulation was 37:23:40, and mean breeder:nonbreeder ratio was 13:87. On average after 50 years of the simulation, 45.9% (SD = 4.3) of the packs that produced pups retained both breeders through the next winter count and the breeding pair tenure averaged 1.8 (SD = 0.1) years.

Mean pack size in Wisconsin after 50 years was 8.1 wolves (SD = 0.2) and an average of 52% of the pups born survived to the winter count. Mean dispersal rate during mating was 6.7% (SD = 0.01), and 2.1% (SD = 0.003) of the Wisconsin population emigrated from the study area (and an equal proportion immigrated into the study area). After 50 years, the summer-targeted lethal control events killed 5.9% (SD = 0.001) of the summer population (10% of the winter

population, but there are more wolves in summer with the birth of pups), and disproportionately targeted pups in relation to their availability. Wolves were removed at random from within the depredation buffer areas, so a higher proportion of pups removed meant that depredation buffer areas had proportionally more pups compared to the rest of Wisconsin. On average, 18.1% (SD = 0.01) of the fall population dispersed during fall dispersal because of resource limitation at the pack level, and 27.9% (SD = 0.01) of the Wisconsin population died because of spatial mortality risk with pups, yearlings, and adults dying in proportion to their availability.

After 50 years of simulation, most wolves in the depredation buffer occurred in summer after birth of pups and before the targeted lethal control event (mean = 43, SD = 14). Targeted lethal control removed typically all wolves in the depredation buffer. Spatial mortality risk reduced the mean number of wolves in the depredation buffer from 25 (SD = 5) to 17 (SD = 4) after 50 years. The birth of pups led to a spike in the number of wolves in the depredation buffer (19 wolves pre-pup birth to 43 wolves post pup birth, on average, in the depredation buffer), followed by the fall dispersal (0 wolves pre-fall dispersal to 25 wolves post fall dispersal in the depredation buffer).

Model calibration

Simulated winter population counts were within 1 SD of the estimated Wisconsin and SLS population counts in all except the first 5 years of the simulation (Fig. 4A). Similarly, the winter pup counts in Wisconsin were within 1 SD of the estimated Wisconsin pup counts in all except the first 5 years of the simulation and in 1993 when the simulated wolf pup count was larger than the estimated wolf pup count (Fig. 4B).

Simulations

Mean winter population count in Wisconsin after 100 years of simulation ranged from 19 (SD = 25) to 1257 (SD = 38) wolves depending on harvest scenarios. There was 30% more variation among simulations in the 2012 long-harvest scenario after 100 years compared to the other scenarios. In the 30% harvest scenario, 14% of simulations went extinct before 100 years, while all simulations from all other scenarios persisted for 100 years. Harvest generally began in year 33 of the simulation (range: 26 – 43) when there was a mean of 878 (SD = 24) wolves in Wisconsin outside of Ojibwe Indian reservations. Harvest reduced the Wisconsin population size by an average of 1.2% (SD = 3.1) to 17.3% (SD = 2.9) in the first year, and -9.2% (SD = 6.3) to 94.7% (SD = 3.9) in the 50th year (Fig. 5). The only harvest simulation that resulted in population growth after 50 years was the stable population harvest scenario that had a goal of a stable to increasing population in the ceded territories (Fig. 5). Composition of harvests was generally 62 – 65% pups and yearlings and this was the approximate proportion of pups and yearlings in the population.

The 2012 harvest scenario achieved a mean 4.1% (SD = 2.9) population reduction in the first year, similar to the estimated actual reduction of Wisconsin's wolf population of 3.1% after the 2012 hunt (based on midpoints of 847.5 wolves in 2011/2012 and 821.5 wolves in 2012/2013 during winter population counts). After the first year decrease in the simulated populations, populations under the 2012 harvest scenario equilibrated at pre-harvest levels by year 20 of harvest (Fig. 5). Compared to the 2012 harvest scenario, the 2012 long-harvest scenario had less population reduction in the first year of harvest (mean = -1.7%, SD = 3.1), but more population reduction every year thereafter (Fig. 5). The 2012 long-harvest scenario had a 7.3% population reduction (SD = 6.4) by the 50th year of harvest, and variation in population reduction was always higher in the 2012 long harvest scenario compared to the 2012 harvest scenario (Fig. 5).

We suspect that the possibility of harvesting mated females in the long-harvest scenario led to more variation in next year's population size because the harvest of each mated female resulted in reproductive loss for an entire pack.

The 2013 harvest scenario reduced the Wisconsin wolf population by 24.9% (SD = 4.0) on average after 5 years of harvest and 36.0% (SD = 4.9) after 50 years of harvest to stabilize at a mean of 597 (SD = 39) wolves after 100 years (Fig. 5). At a 30% constant harvest rate (i.e., 30% harvest scenario), the simulated wolf populations had a similar reduction of 24.9% (SD = 4.0) in the population after 5 years of harvest, but then continued to decline and sometimes went extinct. There was a reduction of 94.7% (SD = 3.9) in the population on average after 50 years of harvest (Fig. 5).

After 5 years of harvest, there were 1 – 3% more pups in the winter population for all scenarios that had harvest (Table 4). This result was probably because harvest reduced the number of adults. Overall, the winter breeder:nonbreeder ratio stayed very consistent across scenarios and years since harvest. Average pack size increased with time in the no harvest scenario, and decreased with harvest by 0.6 – 1.7 wolves per pack after 5 years of harvest (Table 4). Average dispersal and immigration rates increased with time in the no harvest scenario but decreased proportionally with harvest in harvest scenarios (Table 4). Mortality from the spatial mortality risk remained at 26 – 27% regardless of the time or harvest scenario (Table 4). On average, 42% of breeding pairs bred for ≥ 1 year in the no harvest simulations and the rate did not vary as growth decelerated in later years. However, percentage of breeding pairs that bred for ≥ 1 year decreased 3 – 12% after the first year of harvest compared to the no harvest scenarios (Table 4). Average tenure of breeding pairs was 1.8 years in the no harvest scenario, and decreased to 1.5 in the 30% harvest scenario after 5 years of harvest (Table 4).

The sequence of the life history events during simulation affected the number of wolves located in the depredation buffer areas (Fig. 1, Fig. 6). In all harvest simulations after the first and twentieth years of harvest, targeted lethal control was the most important event in reducing wolves in the depredation buffer reactively and corresponded to the time of year when most depredations occurred (Olson 2013; Fig. 6). This result was not surprising because the rules for targeted lethal control directly removed wolves in the buffer zones from the simulation (see Targeted lethal control, above). The second most important source of mortality for wolves in the depredation buffer was spatial mortality risk. In the simulation, fall harvest had a proactive impact on the number of wolves in the depredation buffer, but the effect was smaller because harvest was not directed into depredation buffer areas (Fig. 6). The largest increase in wolves in the depredation buffer during the simulated year occurred because of reproduction and then fall dispersal (Fig. 6).

Discussion

We built, documented and calibrated an IBSE model of the colonization and population dynamics of SLS wolves. Our approach enabled modelling dynamics associated with the complex life history of wolves relating to pack structure, breeding status, age, sex, kin relationships, and location with respect to other wolves and features on a particular landscape. Our IBSE model currently is used by managers at Wisconsin Department of Natural Resources to explore how different harvest scenarios may impact Wisconsin's wolf population (Wolf harvest rule to Natural Resources Board, July 2012 board meeting), and the model-estimated population reduction we predicted matched observed reduction following the 2012 and 2013 wolf harvests in Wisconsin. The Great Lakes Indian Fish and Wildlife Commission used our IBSE model to explore the effect of harvest on the wolf population defined by the ceded

territories of Wisconsin. They developed a harvest scenario with the goal of a stable to increasing wolf population in the ceded territories of Wisconsin because of the spiritual and cultural importance of wolves to the Ojibwe people (David 2009, Stenglein and Gilbert 2012). Harvest rates of 5 – 20% in WHZs 1 – 5 and 75% in WHZ 6 led to a stable population size of 1000 wolves after 20 years of harvest and an average harvest of > 90 wolves per year. These uses demonstrate the utility of an IBSE model that multiple agencies and members of the public can use and understand.

Calibration of our IBSE model to observed growth in Wisconsin's wolf population was vital. Our model closely aligned with actual wolf population and pup counts documented in Wisconsin and the SLS region from 1985 – 2012. Our calibration required that the IBSE model begin with wolf packs in Minnesota that recolonized Wisconsin and Michigan for each simulation, because the SLS landscape has a corridor of patchy habitat between Lake Superior to the north and agricultural areas to the south (Mladenoff et al. 1995, Mladenoff et al. 1999). The landscape configuration required simulated wolves in Minnesota to disperse east to find breeding range and increase their population size. This simulated recolonization allowed for the development of simulated pack structure and a realistic distribution of wolves across the simulated SLS landscape.

The IBSE model generated at least three emergent components of wolf biology for wolves in the SLS region. First, the simulated unharvested wolf population reached a carrying capacity that we can compare to other estimates of carrying capacity from the literature. Van Deelen (2009) fit growth curves to the SLS wolf data from 1985 – 2007 and estimated a carrying capacity of 1,321 (95% CI: 1,215 – 1,427) wolves with ~650 wolves as the carrying capacity for Wisconsin alone. The equilibrium population size from our IBSE model suggests that an

unharvested wolf population would stabilize at nearly double the level previously estimated by Van Deelen (2009). Second, simulated wolves had a limited perception neighborhood for mate searching. We calibrated the IBSE model using a mate search distance of two territories away because our previous work with this model demonstrated that a mate search distance of < 2 territories and > 2 territories resulted in a population that grew too slowly (and sometimes went extinct) and a population that grew too quickly compared to actual growth. Therefore, we suggest two territories (30 km) as a realistic biological perception neighborhood for mate searching in the SLS region, which is similar to the perception neighborhood of ~20 – 40 km used for wolves in the Greater Yellowstone Ecosystem, USA (Hurford et al. 2006). This perception neighborhood may change due to landscape configuration, environmental factors, and proximity to other conspecifics (Berec et al. 2001, Hurford et al. 2006).

Third, we documented social effect of harvest in a simulated wolf population. Our IBSE model is the first model that can infer effects of human-caused mortality on social structure of packs. Wolves exist in packs consisting of a breeding pair and multiple generations of offspring, and exploitation may disrupt pack structure and lead to a higher proportion of pups (Fuller et al. 2003, Rutledge et al. 2010). We documented these effects of harvest in our IBSE simulation because harvest increased the proportion of pups in the population and caused more disruption in packs by killing breeders and decreasing the average tenure of breeding pairs. The mechanism in the model to produce this result was harvest mortality that was homogeneous by WHZ. A change in the composition of packs or the loss of a breeder could have additional cascading effects that were not well captured in our model (Brainerd et al. 2008). Our IBSE model did not include explicitly a lag effect of breeding pairs reestablishing once one or both breeders were

lost, which is a phenomenon documented in wolves (Brainerd et al. 2008). Therefore, our IBSE model may underestimate the social effect of harvest on the wolf population.

Our IBSE model demonstrated that the timing and location of mortality events affected the wolf population in different ways depending on wolf phenology. For example, extending harvest into the mating season resulted in more pack disturbance, higher population reduction, and more variability compared to the same amount of harvest restricted to the fall months. We suspect that this result is because some of the simulated female breeders were killed in the late harvest and this precluded pack reproduction for the year. The higher spatial mortality risk of mortality in agricultural areas and areas with high road density in Wisconsin prevented wolves from establishing packs outside of their primary range. The annual targeted lethal control removed the wolves in the depredation buffer areas and was the single-most important mortality event for maintaining low wolf populations in known depredation areas. Moreover, targeted removal events coincided with the time of year of when wolf depredations were occurring (Olson 2013). After targeted lethal control, the general spatial mortality risk was more effective at reducing the number of wolves in the depredation buffer compared to harvest. Harvest could have been a more important factor in reducing the number of wolves in the depredation buffer areas if WHZs were configured around these areas of known high livestock depredation and harvest rates were high in these areas (Haight et al. 2002).

We highlight differences between political and biological boundaries for the SLS wolf population. The timing, level, and distribution of harvest affected the distribution, composition, and size of the wolf population. However, the most striking harvest effects occurred when Michigan and Minnesota wolves were harvested as intensively as Wisconsin's proposed 2013 harvest. Instead of Wisconsin's population stabilizing at some 600 wolves with the proposed

2013 harvest rates and Michigan and Minnesota harvesting at much lower rates, the wolves in the entire simulation plummeted. This is evidence of source-sink dynamics in our Great Lakes simulated landscape, and these dynamics become more apparent with increasing harvest (Pulliam and Danielson 1991). When Wisconsin harvests at high levels compared to the Upper Peninsula of Michigan and Minnesota, Wisconsin likely becomes a population sink, with a source of wolves (mainly from the Upper Peninsula of Michigan) that supplement the diminishing Wisconsin wolf population. Wisconsin, Michigan, and Minnesota have a single wolf population, and the management decisions in one state affect the dynamics across this region.

An IBSE model is only as good as the parameter estimates that drive it. We were fortunate to have access to a long history of wolf research in the SLS region, and could derive the parameter estimates for our model from many sources (Mech 1970, Thiel 1993, Wydeven et al. 1995, Thiel 2001, Mech and Boitani 2003, Wydeven et al. 2009a). We fit distributions to empirical data and our simulations drew from these distributions. However, some processes are not easy to parameterize in an IBSE model because of lack of information or complexity. Decisions for parameterization of each life history event were needed despite relatively poor understanding of these events. For example, general dispersal rates across age and sex classes for different times of the year are not well documented. In our simulation, we decided to not treat dispersal decision as a random draw from a distribution. Rather, we decided that dispersers were all wolves that fit certain criteria and these criteria changed depending on the time of the year. Also, we used a very simplistic understanding of pack structure based around an unrelated mated pair and their offspring of multiple generations, even though we know that inbreeding does occur occasionally in the wild (Mech and Boitani 2003, Vonholdt et al. 2008, Rutledge et al. 2010, Stenglein et al. 2011).

Nonetheless, complex life histories largely preclude the use of simple phenomenological models especially for questions that are driven by controversial management actions such as the aggressive harvests being proposed for newly recovered wolf populations (Levins 1966). Our IBSE model is a simplification of how we understand wolves to be interacting on the landscape, and simplification is inherent in modelling (Levins 1966). It is not necessary for our model to be a perfect depiction of wolf life history, because our interest is in population-level questions and our model reflects wolf population growth and effects of harvest thus far. We advocate modelling, not as an endpoint, but as a step in an iterative process of integrating current knowledge, identifying critical information needs, and conducting research to advance our understanding and ability to predict population dynamics. For wolves, we see a main research need of understanding how harvest affects the social structure of wolf populations and the behavior of individual wolves.

Management Implications

It is appropriate to view the Great Lakes wolf population as a single population that is managed jointly by Minnesota, Wisconsin, Michigan, and Ontario, Canada. It is clear from our model that the management decisions in one place affect the entire population. We highlight the annual Midwest Wolf Steward meeting that brings together managers, researchers, non-profit organizations, and other stakeholders to have important conversations about wolves in this region. We estimate that harvest rates well below 30% of the winter population across the Great Lakes Region will be necessary to ensure long-term population viability.

Pertaining to wolf management in Wisconsin, we highlight that a reconfiguration of the location and number of WHZ for harvest could be an effective way of reducing wolf numbers in depredation areas. Some zones could be smaller areas where there is a high incidence of livestock depredations, and harvest rates could be much higher in these zones. Livestock

depredation sites have been predicted from environmental variables, and this information could be used to delineated different WHZ (Treves et al. 2004, Olson 2013).

We demonstrate the use of IBSE models in an adaptive management framework to assess the effects of harvest and exploitation of other wolf populations and populations of other large carnivores with the goal of better decision-making for management of populations. Adaptive management is an iterative decision-making process that is essentially an optimization problem to maximize an objective in the face of uncertainty (Walters and Hilborn 1978). We demonstrated how our model could be optimized to meet an objective, by simulating a wolf harvest with a goal of a stable to increasing population. The process of developing an IBSE model is useful in itself to identify research questions, management needs, stakeholders, available data, and gaps in available data. Our model has already been used effectively in the beginning stage of an adaptive management approach to wolf harvest in Wisconsin, and may continue to be used to inform harvest decisions and improve future management of wolves.

Literature Cited

Bart, J. 1995. Acceptance criteria for using individual-based models to make management decisions. Ecological Applications 5:411-420.

Berec, L., D. Boukal, and M. Berec. 2001. Linking the allee effect, sexual reproduction, and temperature-dependent sex determination via spatial dynamics. American Naturalist 157:217-230.

Beyer, D. E., Jr., R. O. Peterson, J. A. Vucetich, and J. H. Hammill. 2009. Wolf population changes in Michigan. Pages 65-85 in A. P. Wydeven, T. R. Van Deelen, and E. J. Heske, editors. Recovery of Gray Wolves in the Great Lakes Region of the United States: An Endangered Species Success Story. Springer.

Beyer, H. L. 2004. Hawth's analysis tools for ArcGIS.

Bousquet, F., and C. Le Page. 2004. Multi-agent simulations and ecosystem management: a review. Ecological Modelling 176:313-332.

Brainerd, S., H. Andren, E. Bangs, E. Bradley, J. Fontaine, W. Hall, Y. Iliopoulos, M. Jimenez, E. Jozwiak, O. Liberg, C. Mack, T. Meier, C. Niemeyer, H. Pedersen, H. Sand, R.

Schultz, D. Smith, P. Wabakken, and A. Wydeven. 2008. The effects of breeder loss on wolves. Journal of Wildlife Management 72:89-98.

Breslow, N. E., and N. E. Day. 1980. Statistical methods in cancer research. International Agency for Research on Cancer Lyon.

Center for Shared Solutions and Technology Partnerships. 2013. Michigan Geographic Framework: State of Michigan.in Center for Shared Solutions and Technology Partnerships, editor.

Conner, M., M. Ebinger, and F. Knowlton. 2008. Evaluating coyote management strategies using a spatially explicit, individual-based, socially structured population model. Ecological Modelling 219:234-247.

Cox, D. R. 1972. Regression models and life tables. JR stat soc B 34:187-220.

David, P. 2009. Ma'iingan and the Ojibwe. Pages 267-277 in A. P. Wydeven, T. R. Van Deelen, and E. J. Heske, editors. Recovery of Gray Wolves in the Great Lakes Region of the United States: An Endangered Species Success Story. Springer.

Environmental Systems Research Institute. 2009. ArcGIS Desktop. Environmental Systems Research Institute, Redlands, CA.

Fry, J., Xian, G., Jin, S., Dewitz, J., Homer, C., Yang, L., Barnes, C., Herold, N., and Wickham, J. 2011. Completion of the 2006 National Land Cover Database for the conterminous United States. Photogrammetric Engineering and Remote Sensing 77:858–864.

Fuller, T., W. Berg, G. Radde, M. Lenarz, and G. Joselyn. 1992. A history and current estimate of wolf distribution and numbers in Minnesota. Wildlife Society Bulletin 20:42-55.

Fuller, T. K., L. D. Mech, and J. F. Cochrane. 2003. Wolf Population Dynamics. Pages 161 - 191 in L. D. Mech and L. Boitani, editors. Wolves: Behavior, Ecology, and Conservation. The University of Chicago Press, Chicago, Illinois.

Gail, M., J. Lubin, and L. Rubinstein. 1981. Likelihood calculation for matched case-control studies and survival studies with tied death times. Biometrika 68:703-707.

Grimm, V. 1999. Ten years of individual-based modelling in ecology: what have we learned and what could we learn in the future? Ecological Modelling 115:129-148.

Grimm, V., U. Berger, F. Bastiansen, S. Eliassen, V. Ginot, J. Giske, J. Goss-Custard, T. Grand, S. Heinz, G. Huse, A. Huth, J. Jepsen, C. Jorgensen, W. Mooij, B. Muller, G. Pe'er, C. Piou, S. Railsback, A. Robbins, M. Robbins, E. Rossmanith, N. Ruger, E. Strand, S. Souissi, R. Stillman, R. Vabo, U. Visser, and D. DeAngelis. 2006. A standard protocol for describing individual-based and agent-based models. Ecological Modelling 198:115-126.

Grimm, V., U. Berger, D. DeAngelis, J. Polhill, J. Giske, and S. Railsback. 2010. The ODD protocol A review and first update. Ecological Modelling 221:2760-2768.

Grimm, V., and S. F. Railsback. 2005. Individual-based modeling and ecology. Princeton university press.

Grimm, V., E. Revilla, U. Berger, F. Jeltsch, W. Mooij, S. Railsback, H. Thulke, J. Weiner, T. Wiegand, and D. DeAngelis. 2005. Pattern-oriented modeling of agent-based complex systems: Lessons from ecology. Science 310:987-991.

Haight, R., L. Travis, K. Nimerfo, and L. Mech. 2002. Computer simulation of wolf-removal strategies for animal damage control. Wildlife Society Bulletin 30:844-852.

Hurford, A., M. Hebblewhite, and M. Lewis. 2006. A spatially explicit model for an Allee effect: Why wolves recolonize so slowly in Greater Yellowstone. Theoretical Population Biology 70:244-254.

Klein, J. P., and M. L. Moeschberger. 2003. Survival analysis: statistical methods for censored and truncated data. Springer-Verlag, New York, NY.

Levins, R. 1966. The strategy of model building in population biology. American scientist 54:421-431.

Macal, C., and M. North. 2010. Tutorial on agent-based modelling and simulation. Journal of Simulation 4:151-162.

McCullagh, P. 1984. Generalized linear models. European Journal of Operational Research 16:285-292.

Mech, L. 1988. Longevity in wild wolves. Journal of Mammalogy 69:197-198.

Mech, L. 2006. Estimated age structure of wolves in northeastern Minnesota. Journal of Wildlife Management 70:1481-1483.

Mech, L. D. 1970. The Wolf. The Natural History Press, Garden City, N.Y.

Mech, L. D., and L. Boitani. 2003. Wolf Social Ecology. Pages 1 - 34 in L. D. Mech and L. Boitani, editors. Wolves: Behavior, Ecology, and Conservation. The University of Chicago Press, Chicago, Illinois.

Merrill, S. 2000. Road densities and Gray Wolf, Canis lupus, habitat suitability: an exception. Canadian Field-Naturalist 114:312-313.

Mladenoff, D., T. Sickley, R. Haight, and A. Wydeven. 1995. A regional landscape analysis and prediction of favorable gray wolf habitat in the norther Great Lakes region. Conservation Biology 9:279-294.

Mladenoff, D., T. Sickley, and A. Wydeven. 1999. Predicting gray wolf landscape recolonization: Logistic regression models vs. new field data. Ecological Applications 9:37-44.

Mladenoff, D. J., M. K. Clayton, S. D. Pratt, T. A. Sickley, and A. P. Wydeven. 2009. Change in occupied wolf habitat in the northern Great Lakes region. Pages 119-138 in A. P. Wydeven, T. R. Van Deelen, and E. J. Heske, editors. Recovery of Gray Wolves in the Great Lakes Region of the United States: An Endangered Species Success Story. Springer.

Olson, E. R. 2013. As a wolf: A Wisconsin case-study of wolf-human conflict and predator-prey ecology. University of Wisconsin - Madison, Madison, WI.

Pitt, W., P. Box, and F. Knowlton. 2003. An individual-based model of canid populations: modelling territoriality and social structure. Ecological Modelling 166:109-121.

Pulliam, H. R., and B. J. Danielson. 1991. Sources, sinks, and habitat selection: a landscape perspective on population dynamics. American Naturalist:S50-S66.

R Development Core Team. 2013. R: A language and environment for statistical computing. R Foundation for Statistical Computing, Vienna, Austria.

Ruid, D. B., W. J. Paul, B. J. Roell, A. P. Wydeven, R. C. Willging, R. L. Jurewicz, and D. H. Lonsway. 2009. Wolf–human conflicts and management in Minnesota, Wisconsin, and Michigan. Pages 279-295 in A. P. Wydeven, T. R. Van Deelen, and E. J. Heske, editors. Recovery of Gray Wolves in the Great Lakes Region of the United States: An Endangered Species Success Story. Springer, New York, NY, USA.

Rutledge, L., B. Patterson, K. Mills, K. Loveless, D. Murray, and B. White. 2010. Protection from harvesting restores the natural social structure of eastern wolf packs. Biological Conservation 143:332-339.

Stenglein, J., L. Waits, D. Ausband, P. Zager, and C. Mack. 2011. Estimating gray wolf pack size and family relationships using noninvasive genetic sampling at rendezvous sites. Journal of Mammalogy 92:784-795.

Stenglein, J. L., and J. Gilbert. 2012. Population effects of proposed Wisconsin wolf harvest with varying responses by Ojibwe Tribes. Odanah, WI.

Theberge, J., and M. Theberge. 1998. Wolf country: eleven years tracking the Algonquin wolves. Random House LLC.

Therneau, T. 2013. A Package for Survival Analysis in S.

Thiel, R. P. 1993. The Timber Wolf in Wisconsin: The Death and Life of a Majestic Predator. University of Wisconsin Press.

Thiel, R. P. 2001. Keepers of the wolves: the early years of wolf recovery in Wisconsin. Univ of Wisconsin Press.

Thiel, R. P., W. Hall Jr, E. Heillhecker, and A. P. Wydeven. 2009. A disjunct gray wolf population in Central Wisconsin. AP Wydeven, TR Van Deelen, and EJ Heske. Recovery of Gray Wolves in the Great Lakes Region of the United States: An Endangered Species Success Story. Springer, New York, NY, USA:107-117.

Treves, A., K. A. Martin, J. E. Wiedenhoeft, and A. P. Wydeven. 2009. Dispersal of gray wolves in the Great Lakes region. Pages 191-204 in A. P. Wydeven, T. R. Van Deelen, and E. J. Heske, editors. Recovery of Gray Wolves in the Great Lakes Region of the United States: An Endangered Species Success Story. Springer.

Treves, A., L. Naughton-Treves, E. K. Harper, D. J. Mladenoff, R. A. Rose, T. A. Sickley, and A. P. Wydeven. 2004. Predicting Human- Carnivore Conflict: a Spatial Model Derived from 25 Years of Data on Wolf Predation on Livestock. Conservation Biology 18:114-125.

United States Department of Commerce. 2010. TIGER/Line Files.in U. S. C. B. G. Division, editor., Washington, D.C.

United States Fish and Wildlife Service. 2012. Mexican wolf recovery program: Progress report #15, reporting period: January 1 – December 31, 2012.

United States Fish and Wildlife Service. 2013. Red wolf recovery program: 3rd quarterly report, April – June 2013.

United States Fish and Wildlife Service, Idaho Department of Fish and Game, W. P. Montana Fish, Nez Perce Tribe, National Park Service, Blackfeet Nation, Confederated Salish and Kootenai Tribes, Wind River Tribes, Confederated Colville Tribes, Washington Department of Fish and Wildlife, Oregon Department of Fish and Wildlife, Utah Department of Natural Resources, and U. W. Services. 2013. Northern Rocky Mountain Wolf Recovery Program 2012 Interagency Annual Report. Helena, Montana.

Van Deelen, T. R. 2009. Growth characteristics of a recovering wolf population in the Great Lakes region Pages 139-153 in A. P. Wydeven, T. R. Van Deelen, and E. J. Heske, editors. Recovery of Gray Wolves in the Great Lakes Region of the United States: An Endangered Species Success Story. Springer, New York, NY, USA.

Vonholdt, B., D. Stahler, D. Smith, D. Earl, J. Pollinger, and R. Wayne. 2008. The genealogy and genetic viability of reintroduced Yellowstone grey wolves. Molecular Ecology 17:252-274.

Walters, C. J., and R. Hilborn. 1978. Ecological optimization and adaptive management. Annual review of Ecology and Systematics 9:157-188.

Wilensky, U. 1999. NetLogo. Center for Connected Learning and Computer-Based Modeling, Evanston, IL.

Wydeven, A. P., R. N. Schultz, and R. P. Thiel. 1995. Monitoring of a recovering gray wolf population in Wisconsin, 1979-1991. Pages 147-156 in L. N. Carbyn, S. H. Fritts, and D. R. Seip, editors. Ecology and conservation of wolves in a changing world. Canadian Circumpolar Institute, Edmonton, Alberta.

Wydeven, A. P., T. R. Van Deelen, and E. J. Heske. 2009a. Recovery of Gray Wolves in the Great Lakes Region of the United States: An Endangered Species Success Story. Springer.

Wydeven, A. P., J. E. Wiedenhoeft, R. N. Schultz, R. P. Thiel, R. L. Jurewicz, B. E. Kohn, and T. R. Van Deelen. 2009b. History, population growth, and management of wolves in Wisconsin. Pages 87-105 in A. P. Wydeven, T. R. Van Deelen, and E. J. Heske, editors. Recovery of Gray Wolves in the Great Lakes Region of the United States: An Endangered Species Success Story. Springer, New York, NY, USA.

Table 1. Landscape, wolf population, territories, and individual wolf state variables with definitions and descriptions used in an individual-based spatially-explicit model of wolves in the southern Lake Superior region, USA.

Entity	Variable	Description
Landscape	Spatial mortality risk	Land pixels with a probability of mortality for wolves derived from agriculture and road density.
	Breeding range	Areas of Minnesota, Wisconsin Wolf Management Units 1 – 5, and the Upper Peninsula of Michigan where the spatial mortality risk is < 0.75.
	Ceded territories	Wisconsin land pixels that make up the territories ceded from the United States in various treaties.
	Chronic depredation farms	Farms in Wisconsin with at least 2 verified livestock depredations in a 5 year period.
	Depredation sites	Farms in Wisconsin with a verified depredation in 2010 or 2011.
	Depredation buffer	Areas within 5 km of chronic depredation farms or depredation sites.
	Ojibwe Indian reservation	Wisconsin land pixels categorized as belonging to an Ojibwe Indian Tribe, including Red Cliff, Bad River, Lac Courte Oreilles, Lac du Flambeau, and Menominee/Stockbridge-Munsee.
	State	Land pixels categorized as Wisconsin, Upper Peninsula of Michigan, lower peninsula Michigan, Minnesota, and Iowa.
	Territory	15 km x 15 km blocks of land pixels in Minnesota, Wisconsin, and the Upper Peninsula of Michigan with a center in breeding range.
	Wolf harvest zones (WHZ)	Wisconsin land pixels categorized by WHZ 1, 2, 3, 4, 5, or 6.
Wolf population	Number harvested	The number of wolves harvested and sometimes divided into a fall harvest and winter harvest.
	Number killed from spatial mortality risk	The number of wolves killed because of an annual mortality event in late fall correlated with road density and percent agriculture.
	Number killed from depredation	The number of wolves killed because of livestock depredation activity mainly in a targeted fashion around depredation buffer areas.
	Number of breeders	A winter count for the number of wolves that were breeders in the past Spring and were still alive for the winter count.
	Number of nonbreeders	A winter count for the number of wolves that were not breeders the previous Spring.
	Number of pups	A count of the new Spring recruits still alive in the winter count.
	Population size	The number of wolves at various times in the simulation and for various spatial delineations of wolves (e.g., Wisconsin population size).
Territories	Identification number	Each territory has a unique identification number that remained throughout the simulation.
	Pack size	The number of wolves in the territory.
	Pack members	The set of wolves in the territory.
	Number of breeders	The number of breeding wolves in the territory.
	Litter size	A count of the number of pups that are produced each summer by a breeding pair.
Individual wolves	Identification number	Each wolf's unique identification that it is given when it enters the simulation.
	Sex	Male or female and determined randomly at birth and for immigrants entering the simulation.
	Age	A whole number 0, 1, 2, …, 12 and defined randomly for immigrants. Pups were born with age = 0 and all wolves die at age of 12.
	Pack status	A categorization given to wolves in a pack territory.
	Immigrant status	Wolves that enter the simulation as immigrants.
	Breeder status	Wolves that have a breeding position in the pack and given to at most 1 male and 1 female in a pack. A breeder maintains breeder status in a pack as long as he/she is alive.

(Table 1 continued on next page)

Table 1 (continued). Landscape, wolf population, territories, and individual wolf state variables with definitions and descriptions used in an individual-based spatially-explicit model of wolves in the southern Lake Superior region, USA.

Entity	Variable	Description
Individual wolves	Disperser status	Wolves that disperse at any one or more of the dispersal opportunities in the year.
	Dispersal direction	Wolves that disperse chose a random direction each time they disperse.
	Dispersal distance	Wolves that disperse chose a dispersal distance from a distribution each time they disperse.
	Loner status	Wolf that is not a breeder and does not have any siblings or a parent in its pack or is outside of breeding range.
	Mother identification number	Every wolf born in the simulation took its mother's identification number. Immigrants and wolves that begin the simulation took their own number.
	Father identification number	Every wolf born in the simulation took its father's identification number. Immigrants and wolves that begin the simulation took their own number.
Definitions	Breeding pair	Two unrelated wolves of the opposite sex that resided on a pack territory and bred.
	Breeding pair tenure	The number of years that the same breeding pair produced pups.
	Disrupted pack	Reproductive pack that lost at least 1 breeder to some mortality event.
	Lone wolf	Wolf outside of breeding range or within breeding range but without parents or siblings within an 8 km radius.
	Pack	2 – 12 wolves that resided on a pack territory.
	Pack size maximum	The maximum number of wolves in pack above which there were not enough resources.
	Single breeder	Wolf that was part of a breeding pair and remained on the breeding pack territory after death of its mate.
	Targeted lethal control	Mortality event in Wisconsin that focused on killing wolves in depredation buffer areas.
	Unrelated wolves	Wolves that were not parent-offspring, full siblings, or half-siblings.
	Winter population count	Count of wolves in January of each year, after aging and before mate-finding.
	Wisconsin winter population count	Count of the wolves in Wisconsin, but outside of the reservation, in January of each year.

Table 2. Overview of processes, parameters, and default values parameters in an individual-based spatially explicit model for wolves in the southern Lake Superior region, USA.

Parameter	Value or distribution
Number of initial breeding pairs	20
Number of 1 km x 1 km pixels	349,020
Number of km in east – west direction	630
Number of km in north – south direction	554
Number of potential territories	363
Number of potential territories in Wisconsin	151
Mate-finding	
Search distance (number of territories away)	2
Dispersal for mate-finding	
Probability of dispersing in degree direction 1, 2, …, 360	1/360
Distribution for distance	lognormal
Mean distance (km)	50
Standard deviation of distance (km)	3
Probability immigrant sex is male	0.5
Probability immigrant age is 1, 2, …, 12	1/12
Reproduction	
Distribution for litter size	normal
Mean litter size (number of pups)	5.4
Standard deviation of litter size	0.8
Probability that pup sex is male	0.5
Targeted lethal control	
Proportion of Wisconsin's winter population that is killed	0.1
Number of chronic depredation farms	111
Number of livestock depredation sites	236
Depredation buffer distance from sites (km)	5
Dispersal due to resource limitation	
Probability of dispersing in degree direction 1, 2, …, 360	1/360
Mean distance (km)	50
Standard deviation of distance (km)	3
Pack size maximum	12
Spatial mortality risk mortality	
Average probability of death from spatial mortality risk	0.35
Average probability of death in WI from spatial mortality risk	0.37
Average prob. of death in WHZ 1 from spatial mortality risk	0.29
Average prob. of death in WHZ 2 from spatial mortality risk	0.29
Average prob. of death in WHZ 3 from spatial mortality risk	0.32
Average prob. of death in WHZ 4 from spatial mortality risk	0.33
Average prob. of death in WHZ 5 from spatial mortality risk	0.33
Average prob. of death in WHZ 6 from spatial mortality risk	0.40
Age	
Maximum age of wolves	12

Table 3. Wolf harvest rates in wolf harvest zones (WHZ) of Wisconsin, Michigan (MI), and Minnesota (MN), USA with percent of harvest occurring in the fall before mating season for 6 wolf harvest scenarios.

Brief description	Motivation	WHZ 1	WHZ 2	WHZ 3	WHZ 4	WHZ 5	WHZ 6	MI	MN	Fall percent
No harvest	Baseline understanding of simulated wolf population without harvest	0	0	0	0	0	0	0	0	NA
2012 harvest	Harvest Wisconsin wolves by WHZ as was observed during 2012 harvest	9.0	9.4	19.4	18.5	14.7	47.5	7.0	14.0	100
2012 long harvest	Harvest Wisconsin wolves by WHZ as was observed during 2012 harvest, except extend 25% of the harvest into the winter after mating season	9.0	9.4	19.4	18.5	14.7	47.5	7.0	14.0	75
2013 harvest	Harvest Wisconsin wolves by WHZ as was proposed for 2013 harvest	21.4	16.6	66.4	48.0	23.6	90.9	7.0	14.0	100
30% harvest	Harvest all wolves with a 30% harvest rate which is the overall rate of wolf harvest proposed for the 2013 Wisconsin wolf harvest	30.0	30.0	30.0	30.0	30.0	30.0	30.0	30.0	100
Stable population harvest	Harvest Wisconsin wolves by WHZ at a low enough rate to maintain a stable to increasing wolf population in the ceded territories of Wisconsin	5.0	5.0	10.0	10.0	20.0	75.0	7.0	14.0	100

Table 4. Averages (and standard deviations) for percent of pups in winter, number of breeders and non-breeders in winter, breeding pair tenure, percent of breeding pairs that breed for at least 1 year, pack size, and dispersal and immigration rates for 100 simulated Wisconsin wolf populations harvested for 1, 5 and 20 years (Yr) under 6 different scenarios.

		Harvest scenario					
Measure	Yr	No harvest	2012 harvest	2012 long harvest	2013 harvest	30% harvest	Stable pop harvest
Percent pups in winter	1	38.7 (2.2)	38.6 (2.5)	38.7 (2.3)	38.6 (3.0)	38.8 (2.8)	38.7 (2.3)
	5	38.0 (2.4)	39.5 (2.7)	39.7 (2.7)	40.8 (3.9)	41.2 (3.5)	38.8 (2.5)
	20	36.9 (1.8)	39.3 (2.6)	39.2 (3.2)	40.7 (4.0)	38.5 (8.4)	38.7 (2.4)
Breeders in winter	1	139 (9)	127 (9)	130 (9)	109 (9)	111 (9)	131 (9)
	5	155 (10)	130 (12)	127 (10)	100 (11)	100 (10)	134 (9)
	20	168 (10)	134 (11)	124 (11)	88 (10)	44 (10)	144 (10)
Non-breeders in winter	1	845 (30)	770 (27)	787 (30)	662 (29)	682 (28)	787 (31)
	5	961 (38)	781 (35)	769 (38)	602 (41)	597 (33)	816 (35)
	20	1077 (30)	806 (36)	753 (46)	526 (42)	279 (50)	864 (42)
Breeding pair tenure ≥1 yr (%)	1	42.4 (4.8)	36.4 (5.3)	39.0 (4.7)	30.9 (4.6)	30.3 (4.6)	39.6 (4.5)
	5	42.4 (4.8)	38.0 (4.9)	38.0 (4.7)	33.6 (4.9)	33.3 (5.3)	39.4 (4.8)
	20	42.2 (4.5)	38.2 (5.2)	37.3 (5.2)	34.5 (5.3)	36.5 (7.8)	39.7 (4.1)
Breeding pair tenure (years)	1	1.77 (0.11)	1.67 (0.12)	1.71 (0.12)	1.57 (0.11)	1.55 (0.11)	1.73 (0.11)
	5	1.79 (0.12)	1.66 (0.11)	1.64 (0.10)	1.56 (0.10)	1.53 (0.10)	1.71 (0.11)
	20	1.76 (0.10)	1.65 (0.11)	1.63 (0.12)	1.56 (0.11)	1.60 (0.16)	1.70 (0.10)
Average pack size	1	7.82 (0.20)	7.21 (0.20)	7.39 (0.23)	6.40 (0.18)	6.42 (0.20)	7.44 (0.19)
	5	7.94 (0.23)	7.14 (0.23)	7.17 (0.24)	6.38 (0.24)	6.23 (0.20)	7.39 (0.22)
	20	8.05 (0.19)	7.20 (0.23)	7.15 (0.22)	6.58 (0.28)	5.87 (0.39)	7.42 (0.21)
Winter dispersal rate	1	0.059 (0.007)	0.057 (0.007)	0.058 (0.007)	0.054 (0.006)	0.058 (0.008)	0.055 (0.007)
	5	0.064 (0.007)	0.050 (0.007)	0.048 (0.006)	0.044 (0.006)	0.037 (0.006)	0.051 (0.006)
	20	0.067 (0.007)	0.051 (0.005)	0.048 (0.005)	0.043 (0.006)	0.034 (0.008)	0.051 (0.005)
Fall dispersal rate	1	0.161 (0.007)	0.145 (0.008)	0.142 (0.009)	0.132 (0.009)	0.135 (0.010)	0.147 (0.009)
	5	0.170 (0.007)	0.139 (0.007)	0.133 (0.008)	0.127 (0.009)	0.096 (0.006)	0.143 (0.007)
	20	0.181 (0.006)	0.146 (0.006)	0.140 (0.006)	0.134 (0.007)	0.081 (0.009)	0.150 (0.006)
Immigration rate	1	0.018 (0.004)	0.018 (0.003)	0.018 (0.003)	0.018 (0.004)	0.017 (0.004)	0.018 (0.003)
	5	0.019 (0.003)	0.016 (0.003)	0.015 (0.003)	0.014 (0.003)	0.011 (0.003)	0.016 (0.003)
	20	0.021 (0.003)	0.016 (0.003)	0.016 (0.003)	0.015 (0.003)	0.010 (0.004)	0.016 (0.002)
Spatial mortality risk rate	1	0.273 (0.012)	0.270 (0.014)	0.270 (0.012)	0.264 (0.015)	0.269 (0.014)	0.266 (0.012)
	5	0.276 (0.011)	0.267 (0.012)	0.268 (0.014)	0.266 (0.013)	0.267 (0.017)	0.267 (0.012)
	20	0.279 (0.011)	0.270 (0.012)	0.267 (0.012)	0.263 (0.015)	0.260 (0.020)	0.268 (0.012)
Fall harvest rate	1	0 (0)	0.087 (0.003)	0.067 (0.003)	0.174 (0.007)	0.174 (0.005)	0.063 (0.005)
	5	0 (0)	0.084 (0.003)	0.064 (0.003)	0.161 (0.008)	0.176 (0.006)	0.062 (0.004)
	20	0 (0)	0.084 (0.003)	0.062 (0.003)	0.146 (0.008)	0.165 (0.010)	0.062 (0.004)
Winter harvest rate	1	0 (0)	0 (0)	0.035 (0.002)	0 (0)	0 (0)	0 (0)
	5	0 (0)	0 (0)	0.032 (0.002)	0 (0)	0 (0)	0 (0)
	20	0 (0)	0 (0)	0.031 (0.002)	0 (0)	0 (0)	0 (0)

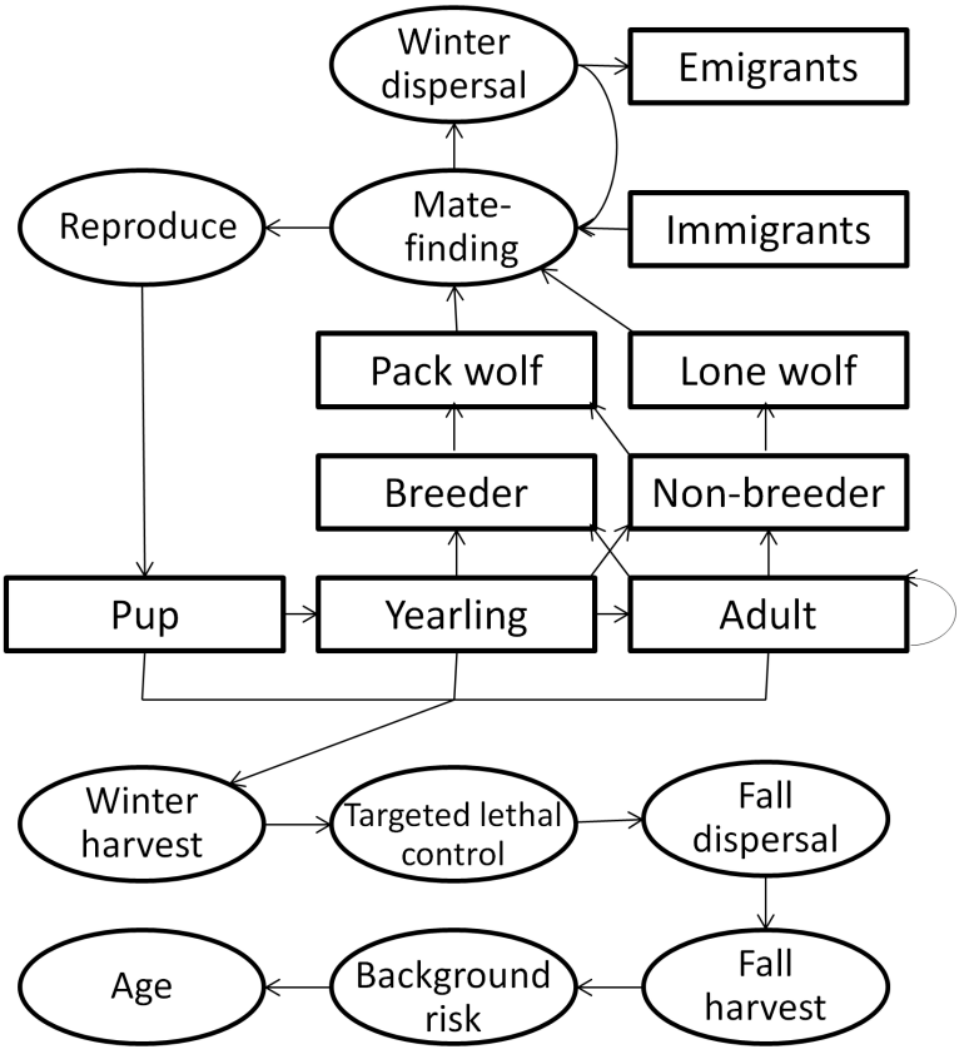

Figure 1. Annual events of simulated wolves in an individual-based spatially-explicit model for wolves in the southern Lake Superior region, USA.

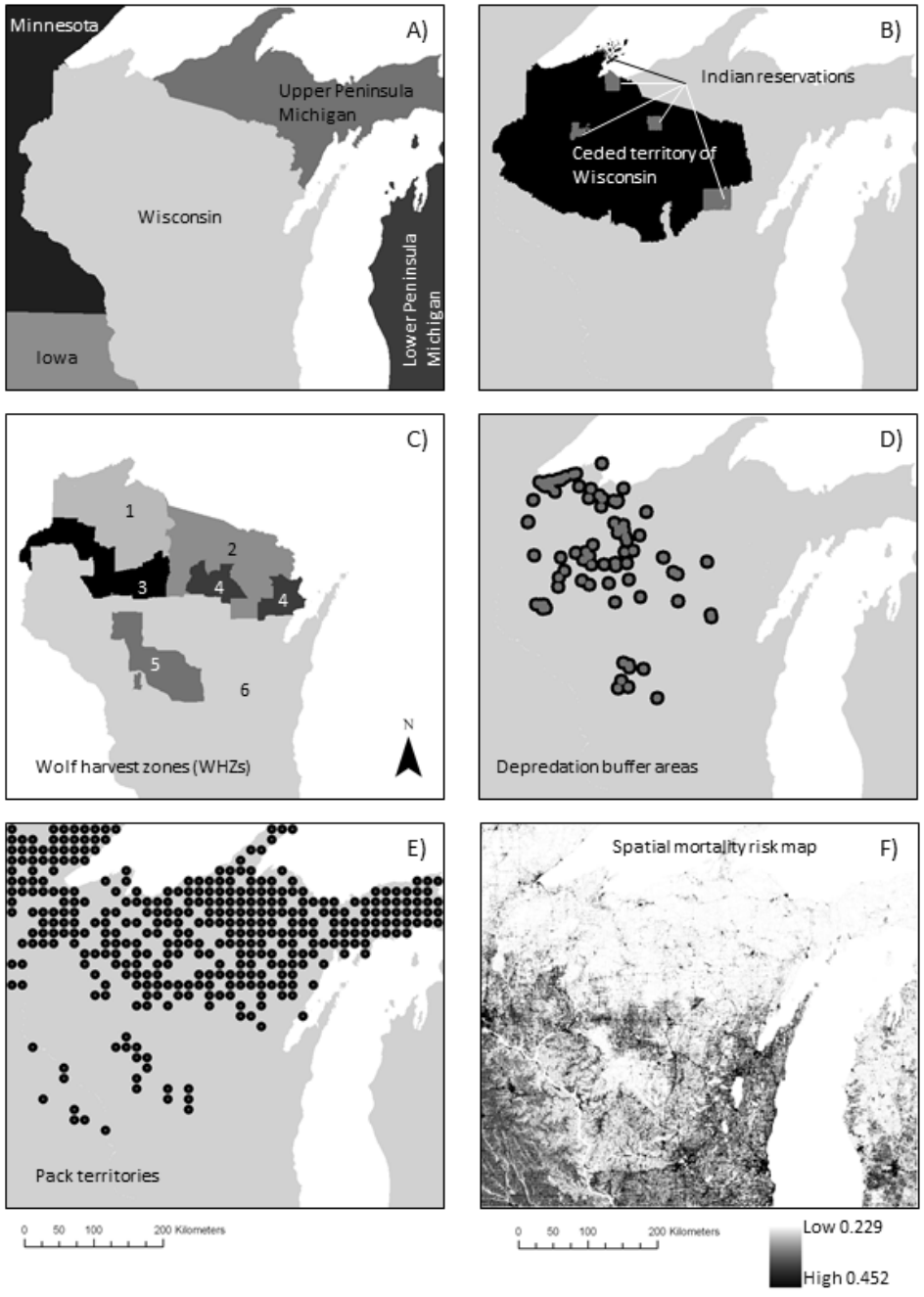

Figure 2. Landscape variables in an individual-based spatially-explicit simulation for wolves in the southern Lake Superior region, USA, including: A) state and water boundaries, B) Ojibwe Indian reservation boundaries and the ceded territories in Wisconsin, C) wolf harvest zones in Wisconsin, D) locations of farms with chronic depredation problems and farms with a depredation in 2010 or 2011 surrounded by a 5 km buffer (light gray; depredation buffer) and a 10 km buffer (black), E) centers of pack territories that denote 15 km x 15 km square sections of habitat, and F) a spatial mortality risk map.

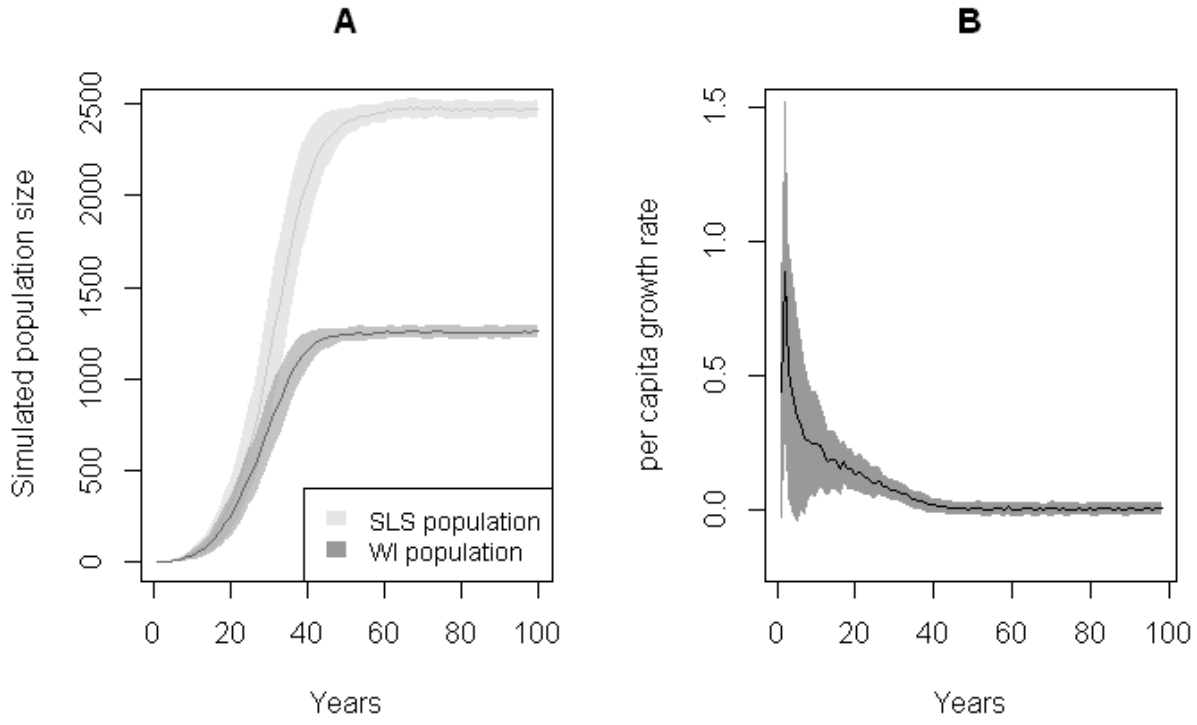

Figure 3. A) The mean and standard deviation from 100 simulations of the Wisconsin (WI) and southern Lake Superior (SLS) wolf population sizes for 100 years of an individual-based spatially-explicit simulation, and B) the mean and standard deviation of the per capita growth rate for the simulated Wisconsin wolf population.

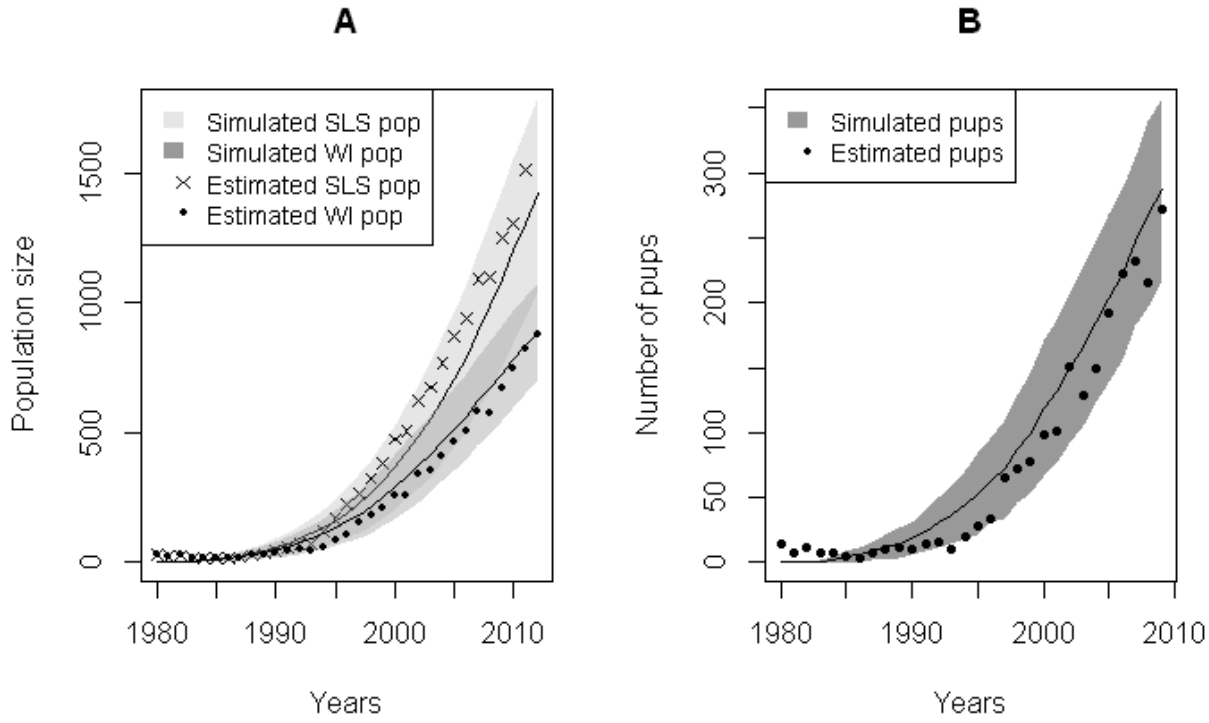

Figure 4. Model calibration showing the mean and 1 standard deviation from 100 simulations of an individual-based spatially-explicit model of A) wolf population growth in Wisconsin (WI) and the southern Lake Superior region (SLS) plotted with the estimated population sizes from 1980 – 2012, and B) number of pups in Wisconsin plotted with estimated number of pups in Wisconsin from 1980 – 2010.

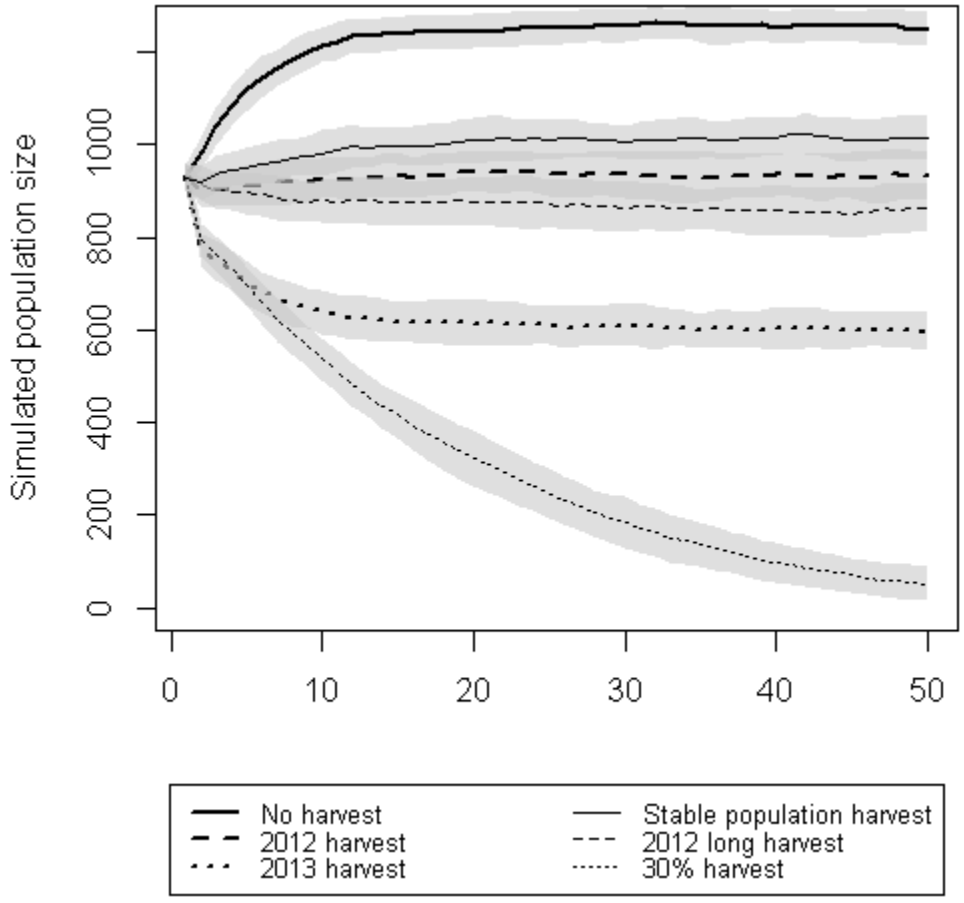

Figure 5. The average and 1 standard deviation of estimated wolf population sizes in Wisconsin, USA, under 6 harvest scenarios for 50 years of harvest using an individual-based spatially-explicit model of wolves in the southern Lake Superior region, USA.

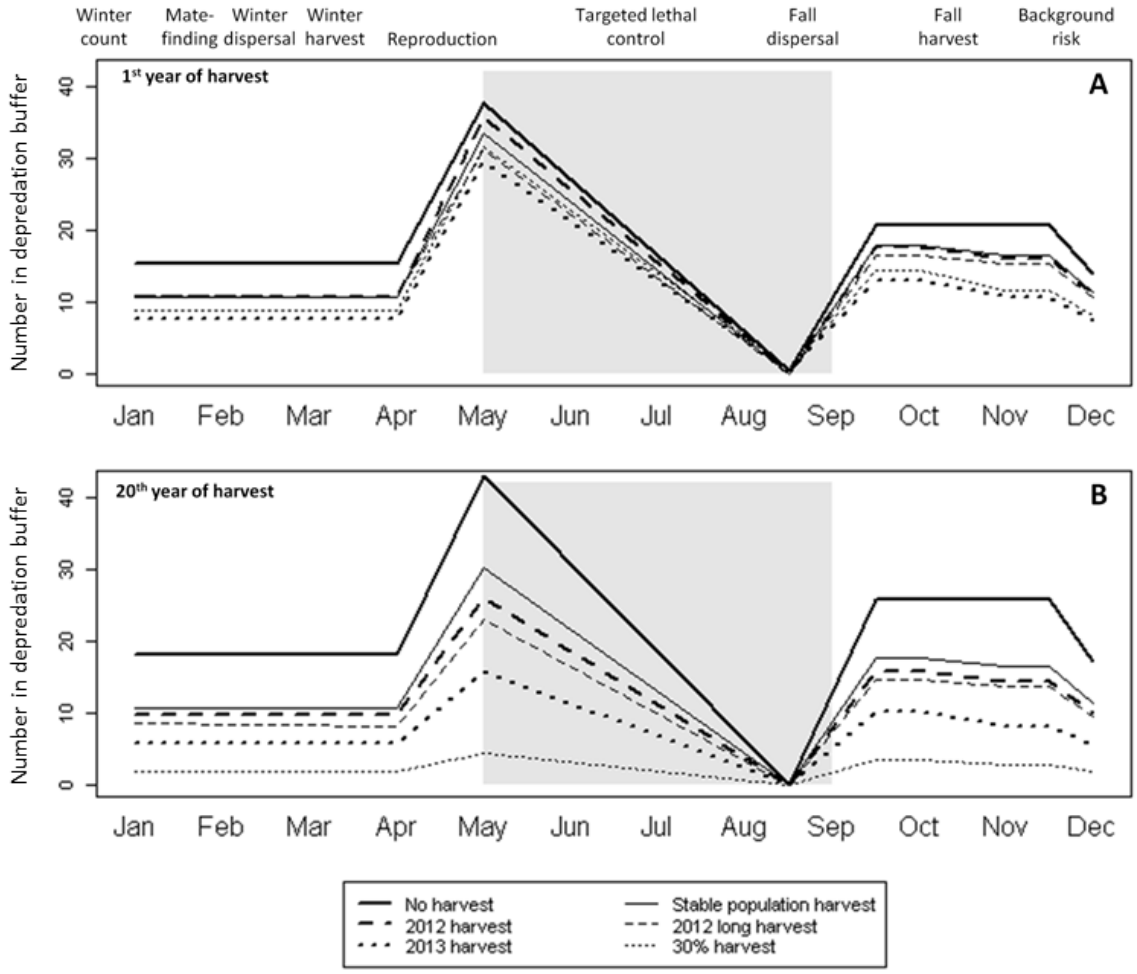

Figure 6. The number of simulated wolves in the depredation buffer in Wisconsin from an individual-based spatially-explicit model for southern Lake Superior wolves, USA, from 6 harvest scenarios throughout the simulated year after A) 1 year and B) 20 years of harvest. The gray shaded area shows when the majority of the depredation events occur in Wisconsin (Olson 2013).

Appendix A. Details on spatial mortality risk surface model and use.

The following details the construction and interpretation of the spatial mortality risk surface used in the individual-based spatially-explicit wolf harvest model. In this model, we used the alive (0) or dead (1) status of 195 radio-collared wolves from 15,329 radio-telemetry relocations in Wisconsin, USA from 1979 – 2012 as the response variable in a logistic regression. Radio-collared wolves had a mean of 78 locations (N = 195, range 2 – 422). We performed a logistic regression with a conditional likelihood by stratifying on individual wolf. Individuals were treated as nuisance parameters in the model. By using a conditional logistic regression, we took into account that the radio-telemetry locations for an individual wolf are inherently similar, and wolves contributed to the likelihood only if they had some change in the covariates between their alive locations and death location (Breslow and Day 1980). Therefore, the stratification by individual wolf led to some loss of information, but the gain was a robust model with unbiased estimates for the parameters of interest (Gail et al. 1981, McCullagh 1984).

The likelihood from the conditional logistic regression model was equivalent to the partial likelihood from the Cox model when each wolf was assigned to its own stratum and time was constant (Cox 1972, Gail et al. 1981). We had 195 strata from 195 individual wolves that we indexed by k and $k = 1, 2, \ldots, K$ and K was the number of strata. We took time to be constant which meant that time did not enter into the model and we assumed that all locations for a wolf occurred simultaneously. Each stratum k was its own risk set composed of n alive locations and 1 death location. For each stratum, we estimated a partial likelihood $L_k(\boldsymbol{\beta})$ where $\boldsymbol{\beta}$ were the parameters of interest and $\boldsymbol{Z}$ were the coefficients, with row $\boldsymbol{Z}_{n+1}$ of coefficients for the death location: $L_k(\boldsymbol{\beta}) = \exp(\boldsymbol{\beta Z}_{n+1}) / \sum_{i=1}^{n+1} \exp(\boldsymbol{\beta Z}_i)$. The numerator of the partial

likelihood used only the information from the single death location and the denominator of the likelihood used information about all locations for the wolf in stratum k (Klein and Moeschberger 2003). After computing $L_k(\boldsymbol{\beta})$ separately for each stratum k, the log partial likelihood $LL(\boldsymbol{\beta})$ was the sum of the log partial likelihoods by stratum: $LL(\boldsymbol{\beta}) = \sum_{k=1}^{K} LL_k(\boldsymbol{\beta})$, where $LL_k(\boldsymbol{\beta}) = \log(L_k(\boldsymbol{\beta}))$. By stratifying, we assumed that the covariates $\boldsymbol{\beta}$ did not change for individual wolves (Klein and Moeschberger 2003). Instead, the differences among wolves were absorbed in the baseline hazards which canceled out of the partial likelihoods. The log partial likelihood $LL(\boldsymbol{\beta})$ was then maximized with respect to $\boldsymbol{\beta}$ which can be done numerically by taking partial derivatives of $LL(\boldsymbol{\beta})$ and solving a set of nonlinear equations using a Newton-Raphson procedure (Gail et al. 1981, Klein and Moeschberger 2003).

The covariates of interest $\boldsymbol{Z}$ were road density and percent of agriculture. Using ArcMap, we aggregated statewide road layers from Wisconsin (United States Department of Commerce 2010), Minnesota (United States Department of Commerce 2010) and Michigan (Center for Shared Solutions and Technology Partnerships 2013) and used road designations that corresponded to primary roads, secondary roads, city streets, local roads, rural roads, ramps, and service drives (TIGER/Line 2010 Classes of S1100, S1200, S1400, S1630, and S1640). Second, we used the National Land Cover Database 2006 (Fry 2011) and aggregated the categories of pasture and crops to represent agriculture. In each buffered location, we measured road density and percentage of agriculture using Hawth's Tools (Beyer 2004) in ArcMap. We standardized both covariates to have mean 0 and standard deviation (SD) 1 so that they were on the same scale for interpretation.

We used the function 'clogit' in the survival library of program R to fit the model. The results were the same when we used the function 'coxph' in the survival library, thereby confirming the equivalence of the conditional logistic regression and Cox proportional hazards likelihoods under certain conditions (Gail et al. 1981). We used the Wald chi-squared test to test the null hypothesis of the estimated parameters different than 0: $H_{0,road}: \beta_{road} = 0$ and $H_{0,ag}: \beta_{ag} = 0$ (Table A.1). Both tests were highly significant, leading to rejection of both null hypotheses and we concluded that both parameter estimates were different than 0. Next, we converted the estimated parameters into relative risks, RR, for easier interpretation: $RR_{road} = e^{\beta_{road}}$ and $RR_{ag} = e^{\beta_{ag}}$ (Table A.1).

The road and agriculture effects were similar to each other and both positive. A wolf in a location with road density 1 SD higher than average road density had a probability of a death location 1.432 times greater than a wolf in a location with average road density, assuming average percent agriculture. Similarly, a wolf in a location with percent agriculture 1 SD greater than a wolf in a location with average percent agriculture had a probability of a death location 1.362 times greater than a wolf in a location with average percent agriculture, assuming average road density (Table A.1). To interpret another way, for every 0.5 km roads / km^2 (1 SD) increase in road density, a wolf was 1.432 times more likely to have its location be a death location. For every 10% increase in percent agriculture (1 SD), a wolf was 1.362 times more likely for that location to be a death location.

Next, we extrapolated this fitted model to every 1 km^2 pixel of a 630 km x 554 km landscape centered on Wisconsin. We made a landscape layer of road density and percent agriculture and standardized them based on the original model. Road density in km road / km^2 in

each 1 km^2 pixel was subtracted from the mean (0.552 km / km^2) and divided by the SD (0.603 km / km^2) road density calculated from the radio-telemetry locations (Fig. A.1). Percent agriculture in each 1 km^2 pixel was subtracted from the mean (3.620%) and divided by the SD (9.931%) percent agriculture calculated from the radio-telemetry locations (Fig. A.2). We used the standardized road density and standardized percent agriculture values at each 1 km^2 pixel as predictors, and calculated the linear predictor for each pixel, $\beta_{road} * Z_{road} + \beta_{ag} * Z_{ag}$ (Fig. A.3).

The linear predictor was the log hazard. We scaled the log hazard to represent a spatial mortality risk surface to range from 0.229 to 0.452 (Fig. A.4). The low and high spatial mortality risks of 0.229 and 0.452 represented the average annual mortality for the simulated wolves that live in the best wolf range and poorer quality wolf range as defined from the highest wolf pack habitat suitability class in Mladenoff et al. (2009) . We took the best wolf range to represent the highest probability class of 0.96 – 1, and we estimated wolf survival in this habitat as 0.771 (SD = 0.015, see Chapter 2). We took poorer quality wolf range to represent the much lower probability class of 0.11 – 0.25, and we estimated wolf survival as 0.548 (SD = 0.055, see Chapter 2). We did not scale our spatial mortality risk surface to the very lowest probability class of Mladenoff et al. (2009) because very little of this lowest class was in wolf range (WHZs 1 – 5) and the radio-collared wolves from this analysis were primarily in wolf range. The high spatial mortality risk of 0.452 was double the low spatial mortality risk and was an estimate of the annual mortality rate for wolves in Wisconsin that are mostly outside of wolf range. Most the radio-collared wolves in Wisconsin have been radio-collared and tracked in primary wolf range, so we do not have a very good idea of survival rates outside of wolf range. We assumed

that the riskiest parts of the landscape in areas with high road density and high percent agriculture had double the spatial mortality risk compared to primary wolf range (Fig. A.4).

Table A.1. Parameter values and relative risk (with 95% confidence interval) for a conditional logistic regression model describing the conditional probability that a location was a death location for wolves in Wisconsin, USA (1979 – 2012). The Wald chi-square test and p-value test the null hypothesis that the parameter value equals 0.

Parameter	Mean estimate	Wald chi-square test	p-value	Mean relative risk	95% CI
Roads[1]	0.359	5.49	< 0.0001	1.432	1.260 – 1.628
Agriculture[1]	0.309	4.91	< 0.0001	1.362	1.204 – 1.541

[1] Roads stands for road density in km^2/km and agriculture stands for percent agriculture.

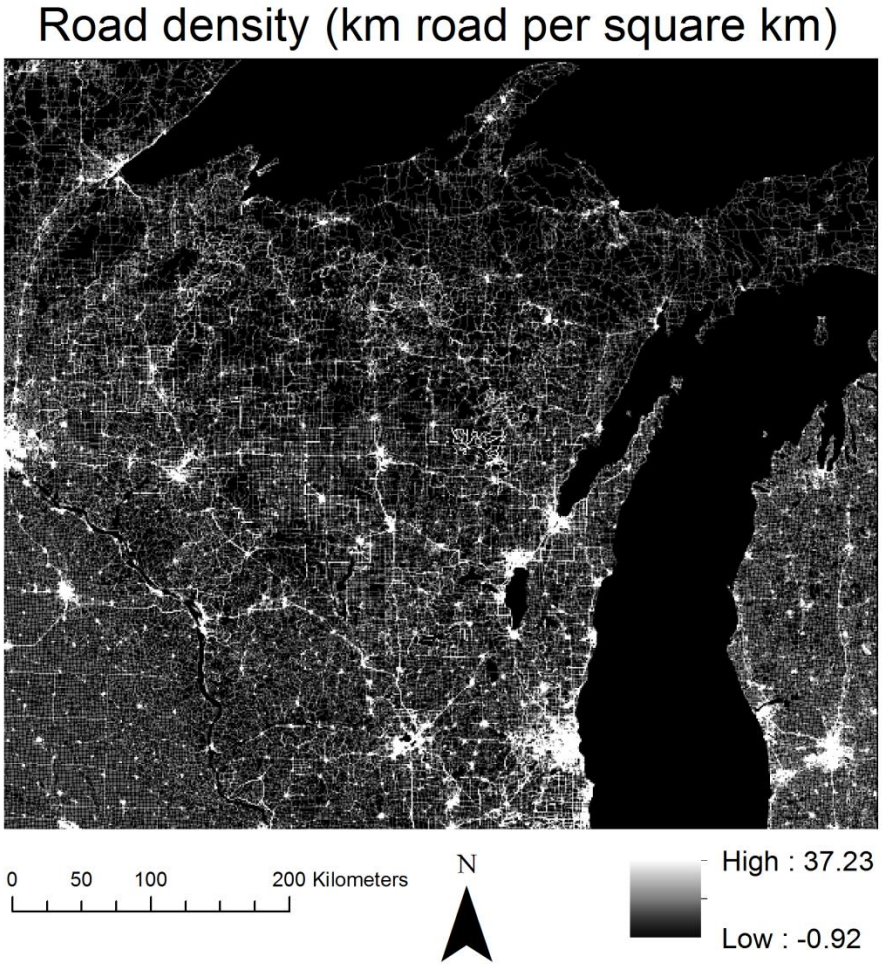

Figure A.1. Paved road density in km road / km^2 mapped in 1 km^2 pixels for Wisconsin, the upper peninsula of Michigan, and a portion of Minnesota, USA (2010).

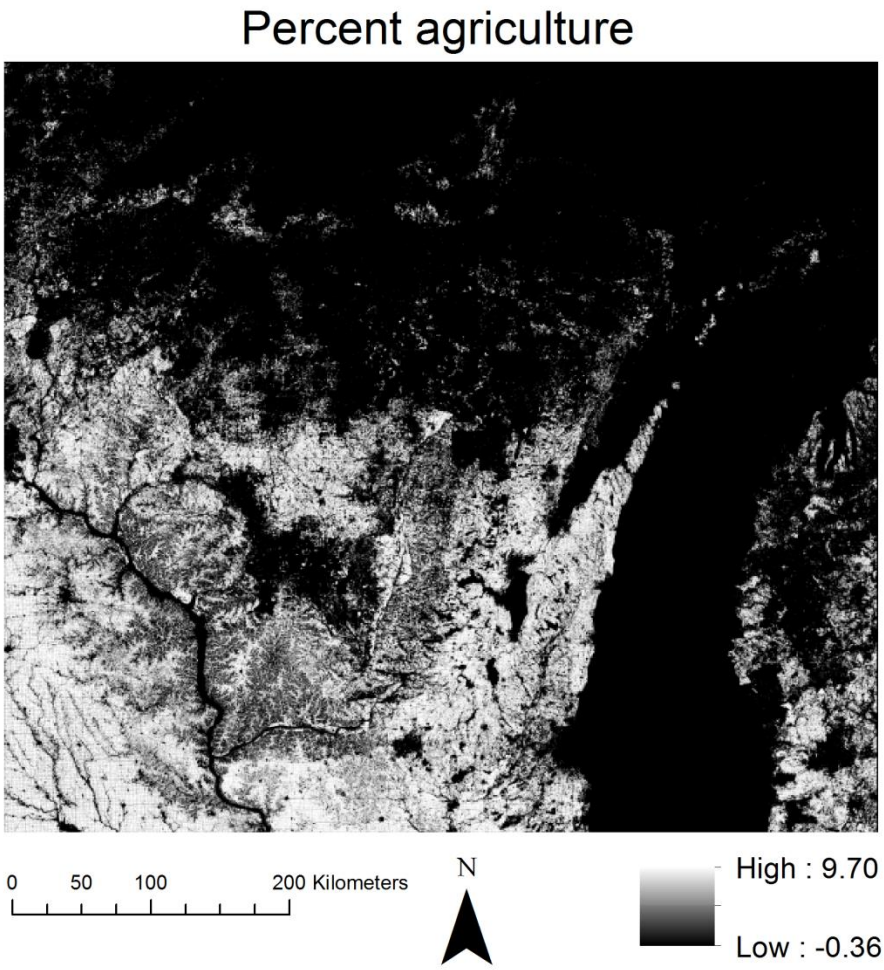

Figure A.2. The percent of agriculture mapped in 1 km^2 pixels across Wisconsin, the upper peninsula of Michigan, and Minnesota, USA (2006).

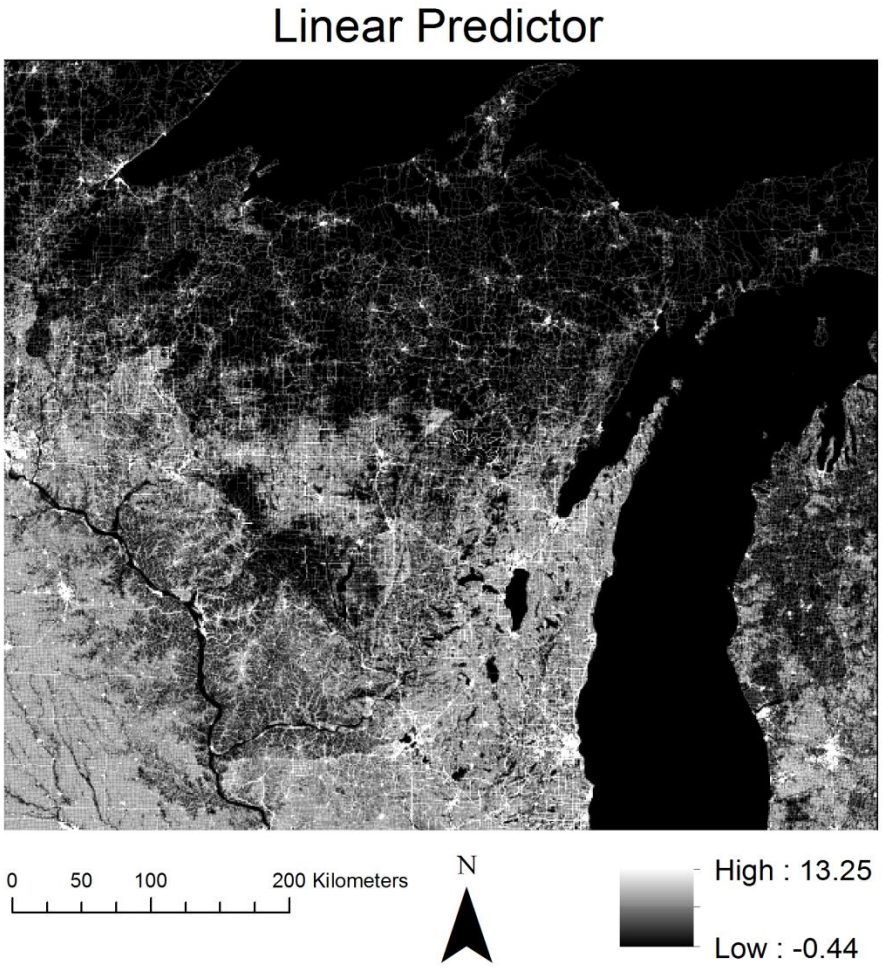

Figure A.3. A map of the linear predictor (log hazard) from a fitted conditional logistic regression model of the alive or dead status of wolf radio-telemetry locations based on the variables of road density and percent of agriculture in 1 km^2 pixels mapped across Wisconsin, the upper peninsula of Michigan, and Minnesota, USA.

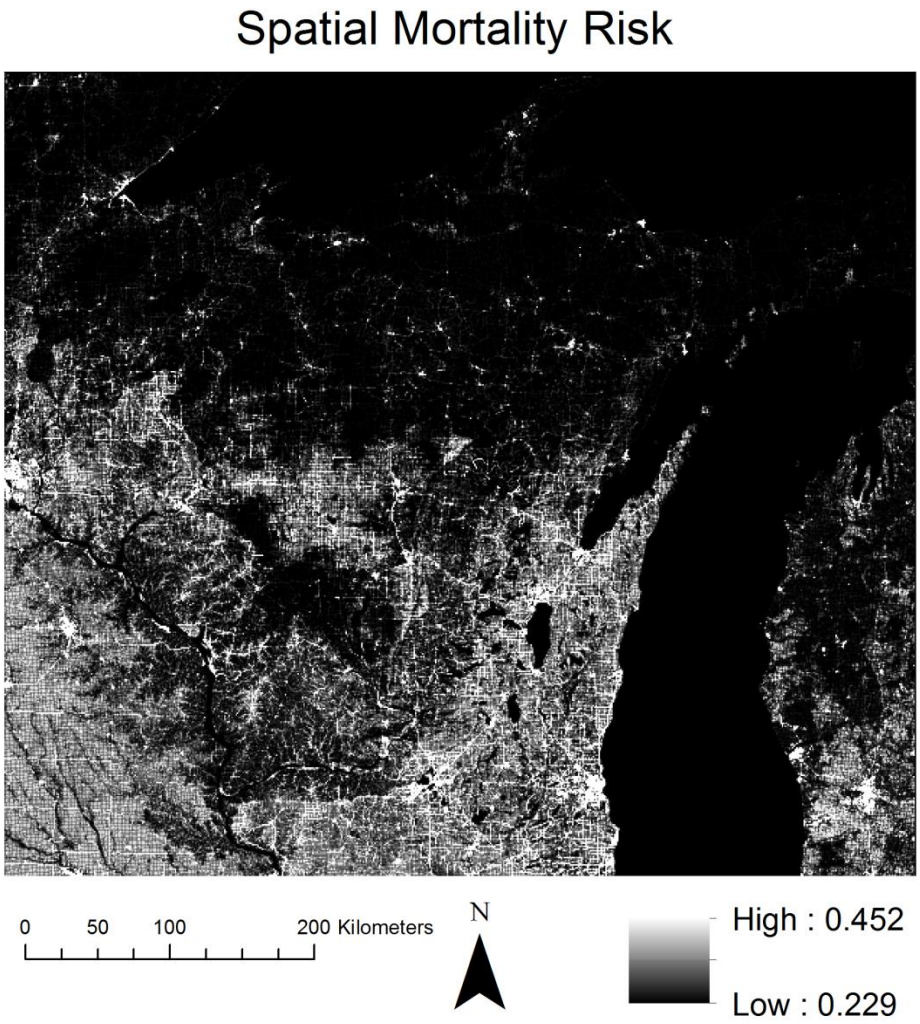

Figure A.4. A map of spatial mortality risk that has been scaled to estimated mortality rates for wolves living in the best quality and poorer quality habitat (defined in Mladenoff et al. 2009) and mapped in 1 km^2 pixels across Wisconsin, the upper peninsula of Michigan, and Minnesota, USA.

Appendix B: Design concepts from individual-based spatially-explicit model for wolves in the southern Lake Superior region, USA.

Design concepts

Sensing

The probability of breeding between any discrete pair of wolves was dependent on life history stage and relationships, including: age, sex, pack status, pack size, breeding status, immigrant status, disperser status, parents, and sibling relationships. After a breeder died, wolves that were within two territories could sense a single breeder occupying a pack territory and could occupy the open breeding position. Wolves evaluated status as siblings and offspring/parents and avoided inbreeding when choosing a mate.

Emergence

We observed the emergent properties primarily through simulated population dynamics, because the individuals' responsiveness to social position and spatial context imposed limitations. Colonization and subsequent distribution patterns of simulated wolves emerged from the process of wolves searching for mates and joining/forming packs within a defined search distance of two territories away. Consequently, sparse distribution of wolves during the first years of a simulation resulted in reduced population growth consistent with a suspected Allee effect (Stenglein et al., *unpublished*). The pattern of reduced population growth at high density after many years was also an emergent property because of a fixed number of territories and pack size limits. As territories become saturated density-driven leveling off of the population growth rate occurred. The number of territories and a pack size maximum within territories defined the resource limitation in our simulation. Otherwise, we did not explicitly

model the distribution of food resources because we did not believe SLS wolves to be food limited (Van Deelen 2009). Wolves' primary food source in the SLS region is deer and deer densities were roughly 5 to 13 deer/km^2 across the SLS region– a level roughly 3 times higher than the level at which wolf populations become food-limited (Fuller et al. 2003, Van Deelen 2009).

Reduced or improved fitness resulting from pack status was an emergent property of the model as well. Nonbreeding individuals that were not members of packs or were members of large packs (> 12 wolves) dispersed ≤ 2 times a year and this increased their exposure to riskier parts of the landscape. Individuals dispersed in random directions and for distances drawn from an empirically derived distribution (Treves et al. 2009), so they tended to move through or arrive in areas where spatial mortality risk was up to 2 times higher than in core habitat areas (Appendix A). However, dispersing individuals potentially increased their reproductive potential by leaving their natal packs and moving to nearby vacant territories. Wolves increased their fitness when they found a mate and a pack territory to establish a new pack because breeding range was defined as areas with the lowest spatial mortality risk. Also, breeders had increased survival because they did not disperse from the pack.

Pack structure and age structure were also emergent properties of the simulation. Packs emerged as an unrelated adult male and adult female paired and occupied territories. Each year the pack bred and the offspring mainly stayed in the pack as long as pack sizes remained < 12 wolves. Occasionally, a non-breeding member would enter the pack through dispersal. Therefore, a typical pack structure of an unrelated breeding pair with multiple generations of offspring and an occasional unrelated wolf in a defined territory emerged from the simulation

(Mech and Boitani 2003). Age structure emerged and stabilized as the simulated population increased their distribution across the landscape. Age structure was a result of the annual aging event interacting with variable survival as well as the birth pulse of pups each simulated year.

Interaction

We modeled interactions between wolves and the landscape and between individual wolves explicitly. First, wolves experienced variable mortality risks from four sources of mortality as they moved around the landscape: 1) Wolves' spatial mortality risk changed as a result of different road density and agricultural density (Appendix A), 2) Wolves' probability of being killed through targeted lethal control was linked to depredation buffer areas, 3) Wolves' probability of being harvested was determined by the harvest quota and wolf density in whichever wolf harvest zone they were in, and 4) Wolves' probability of dying because of resource limitation (too many wolves in a pack) was linked to the number of wolves in their current pack and the density of wolves in pack-areas serving as potential dispersal sinks. Second, wolves interacted with other wolves by searching for receptive, unrelated mates and for vacant pack territories. New breeding packs were only formed if there was a potential breeding pair and a vacant pack territory, thereby interacting with each other and the landscape during mate-finding. Third, wolves in packs interacted with each other. For example, presence of breeding wolves suppressed breeding by other pack members – making them subordinates. Related wolves stayed with their parents and litter mates in their natal pack, but avoided inbreeding when searching for a mate. Resource limitation occurred as a threshold pack size that triggered increased dispersal.

Stochasticity

Stochasticity was implemented at the level of probability distributions for outcomes associated with individual life-history events; hence in the early years where there were fewer individuals, stochasticity had a larger impact on population trend. Initialization of each simulation began with 20 breeding pairs located in Minnesota's pack areas. Their offspring began the colonization of the SLS region. If these packs were initiated in areas with higher relative mortality risk, they might have died out before producing many pups to colonize the SLS region. Also, dispersers from the original wolf packs chose a random direction and drew a distance from a probability distribution. Because mate-finding distance was restricted, there was a chance that lone wolves would not find mates in the sparsely populated parts of SLS region before they died.

Other elements of stochasticity were variable litter sizes and numbers of immigrants. The number of wolves in a litter was drawn from a probability distribution and sex was randomly assigned. With few packs, an unequal sex ratio of small litter sizes could have prevented the population from increasing. Another stochastic process was the number and location of the arrival of immigrants. The number of immigrants was determined by the number of dispersers that emigrated from the study area. New immigrants increased potential breeding opportunities, especially in a small inter-related population.

Collectives

Individual wolves grouped into packs based on presence inside a territory and presence within a territory of ≥ 1 breeder. Packs either had a breeding pair (most often) or a single breeder that lost its mate and was waiting for a wolf to fill that breeding position. All other wolves in the pack were subordinate, and most were related to each other and the breeders. A

second collective designation was based on landscape and administrative boundaries (e.g., state boundaries, WHZ boundaries, ceded territory boundaries). These boundaries were simply used to subset the population during annual counts.

Observation

Counts of wolves by area occurred during different times in the simulated calendar year and totals were reported at the end of the year. Generally, counts occurred before and after each dispersal or mortality event, and were enumerated for the SLS region, each of the states, the ceded territory, the Ojibwe Indian reservations, and each WHZ. The winter population count was made at the end of the calendar year after all wolves aged 1 year and before mate-finding. Timing of the winter population count in the simulation mirrored the timing of winter population counts of wolves made by Wisconsin and Michigan each year (Beyer et al. 2009, Wydeven et al. 2009b).

We also quantified numbers of individuals and rates for immigration, dispersal, and pup production events. We counted the number of wolves (by age class) that died as a result of each mortality event, the number of packs disrupted as a result of harvest (loss of at least one breeding wolf), and the number of wolves that were in the depredation buffer after dispersal and mortality events, and the average number of wolves in Wisconsin packs. Most of these counts were made at the end of the calendar year. We quantified breeding pair tenure of Wisconsin packs by counting how many years the breeding pair produced pups, and proportion of Wisconsin breeding pairs that bred for > 1 year.